PD
539.7
G326
V. 4, NO2

POWER REACTOR TECHNOLOGY

A Quarterly Technical Progress Review

Prepared for U. S. ATOMIC ENERGY COMMISSION by GENERAL NUCLEAR ENGINEERING CORP.

ILLINOIS STATE LIBRARY
MAY 22 1961
U. S. Supt. of ... Depository

March 1961

● VOLUME 4

● NUMBER 2

TECHNICAL PROGRESS REVIEWS

To meet the needs of industry for concise summaries of current atomic developments, the Atomic Energy Commission is publishing this series, Technical Progress Reviews. Issued quarterly, each of the reviews digests and evaluates the latest findings in a specific area of nuclear technology and science.

The four journals published in this series are:

Nuclear Safety, W. B. Cottrell, editor, R. A. Charpie, advisory editor, and associates, Oak Ridge National Laboratory

Power Reactor Technology, Walter H. Zinn and associates, General Nuclear Engineering Corporation

Reactor Core Materials (covering solid material developments), R. W. Dayton, E. M. Simons, and associates, Battelle Memorial Institute

Reactor Fuel Processing, Stephen Lawroski and associates, Chemical Engineering Division, Argonne National Laboratory

Each journal may be purchased ($2.00 per year for subscription and individual issues $0.55) from the Superintendent of Documents, U. S. Government Printing Office, Washington 25, D. C. See back cover for remittance instructions and foreign postage requirements.

The views expressed in this publication do not necessarily represent those of the United States Atomic Energy Commission, its divisions or offices, or of any Commission advisory committee or contractor.

Availability of Reports Cited in This Review

Unclassified AEC reports are available for inspection at AEC depository libraries and are sold by the Office of Technical Services, Department of Commerce, Washington 25, D. C. Some of the reports cited are not available owing to their preliminary nature; however, the information contained in them will eventually be made available in formal progress or topical reports.

Unclassified reports issued by other Government agencies or private organizations should be requested from the originator.

Unclassified British and Canadian reports may be inspected at AEC depository libraries. British reports are sold by the British Information Service, 45 Rockefeller Plaza, New York, N. Y.; Canadian reports (AECL series) are sold by the Scientific Document Distribution Office, Atomic Energy of Canada, Ltd., Chalk River, Ontario, Canada.

Classified U. S. and foreign reports identified in this journal as Classified may be purchased by properly cleared Access Permit Holders from the Office of Technical Information Extension, U. S. Atomic Energy Commission, P. O. Box 1001, Oak Ridge, Tenn. Such reports may be inspected at classified AEC depository libraries.

POWER REACTOR TECHNOLOGY

A REVIEW OF RECENT DEVELOPMENTS

Prepared for U. S. ATOMIC ENERGY COMMISSION
by GENERAL NUCLEAR ENGINEERING CORP.

● MARCH 1961

● VOLUME 4

● NUMBER 2

foreword

This quarterly review of reactor development has been prepared at the request of the Office of Technical Information of the U. S. Atomic Energy Commission. Its purpose is to assist interested organizations in the task of keeping abreast of new results in reactor technology for civilian application.

Power Reactor Technology contains reviews of selected recently published reports that are judged noteworthy, in the fields of power-reactor research and development, power-reactor applications, design practice, and operating experience. It is not meant to be a comprehensive abstract of all material published during the quarter, nor is it meant to be a treatise on any part of the subject. However, related articles are often treated together to yield reviews having some breadth of scope, and from time to time background material is added to place recent developments in perspective.

The intention is to cover the various areas of reactor development from the general viewpoint of the reactor designer rather than from the more detailed points of view of specialists in the individual areas. To whatever extent the coverage of *Power Reactor Technology* may occasionally overlap the fields of the other Technical Progress Reviews, the overlaps will be motivated by this objective of viewing current progress through the eyes of the reactor designer.

A degree of critical appraisal and some interpretation of results are often necessary to define the significance of reported work. Any such appraisals or interpretations represent only the opinions of the reviewers and the editor of *Power Reactor Technology*, who are General Nuclear Engineering Corporation personnel. Readers are urged to consult the original references in order to obtain all the background of the work reported and to obtain the interpretation of the results given by the original authors.

W. H. ZINN, President
J. R. DIETRICH, Vice President and Editor
General Nuclear Engineering Corporation

Issued quarterly by the U. S. Atomic Energy Commission. Use of funds for printing this publication approved by the Director of the Bureau of the Budget on November 1, 1960.

PD
539.7
G-326
V.4, No.2

contents

Foreword

1 I FUEL RESOURCES

4 II APPLICATIONS: REMOTE MILITARY POWER

10 III REACTOR PHYSICS: CRITICAL AND EXPONENTIAL EXPERIMENTS

13 IV HEAT TRANSFER

13 Conduction
13 Forced Convection in Annular Passages
15 Boiling Heat Transfer
19 Superheated-Steam Heat Transfer
20 Short Notes
20 References

22 V CONFERENCE ON REACTOR KINETICS

22 Power Excursion Research
25 Reactor Transfer Functions
26 Thermal and Hydraulic Effects
28 Analytical Methods
30 References

31 VI CONTAINMENT

31 Condensation in a Containment Vessel
32 Pressure Suppression
33 References

34 VII SHIELDING

34 Thermal-Neutron-Capture Gamma Spectra
34 Shielding Properties at Elevated Temperatures
35 Gamma and Neutron Penetrations Through Iron Slabs
36 Thermal-Neutron Attenuation Through Boral
36 Effective Neutron Removal Cross Section of Zirconium
36 References

38 VIII FUELS: THERMAL CONDUCTIVITY OF UO_2

44 IX DESIGN AND CONSTRUCTION PRACTICE

44 Nuclear Pressure Vessels: Codes and Practice
48 Autoclave Testing of Zircaloy-2
49 Carbon Steel for Reactor Systems
50 References

52 X OPERATING EXPERIENCE

52 Refueling the Shippingport Reactor
59 Operational Tests of EBWR Vapor Recovery System
59 Sodium Pump and Auxiliary Components for Hallam
61 References

62 XI HEAVY-WATER REACTORS

62 Economic Considerations
64 Other Incentives for D_2O Reactors
64 Canadian D_2O-Cooled Reactors
65 U. S. Work at Savannah River
72 Canadian and U. S. Cost Estimates
73 Other D_2O-Cooled Reactors
73 Other Coolants
76 References

78 XII SUPERCRITICAL-WATER REACTOR

78 Direct Cycle
80 Indirect Cycle
80 Status of Supercritical-Water Technology
81 References

82 XIII ORGANIC-MODERATED REACTORS: PIQUA AUXILIARY SYSTEMS

82 Coolant Purification
83 High-Boiler Handling
84 Degasification System
87 Waste-Gas Disposal
88 References

Section I

FUEL RESOURCES

The latest report[1] on uranium and coal reserves contains analyses made at the request of the Congressional Joint Committee on Atomic Energy by members of the AEC Division of Raw Materials and the AEC Office of Operations Analysis and Forecasting. The previous analysis of nuclear fuel resources,[2] prepared at the time of the 1958 Geneva Conference, was reviewed in the June 1959 issue of *Power Reactor Technology*, Vol. 2, No. 3, pages 1 to 12. The new report gives estimates in somewhat greater detail and considers also the energy content of the reserve.

The findings given in reference 1 with regard to uranium reserves are summarized in Table I-1. It must be recognized that the estimates involve large uncertainties, especially in the cases of the higher cost reserves, which require estimates of the cost of mining and extraction as well as of quantity and which have been explored less extensively.

According to the reference, an extension of the estimates to include all reserves recoverable at an average cost in the range $24 to $30 per pound of U_3O_8 adds only about 100,000 additional tons to the U. S. estimate and 200,000 tons to the Canadian estimate, but it increases the European estimate by about 1 million tons, principally because of additional, lower grade contributions from the Swedish alum shales.

Table I-1 FREE-WORLD URANIUM RESOURCES[1]

(Short Tons of U_3O_8 Recoverable at an Average Cost of $16 to $20 per Pound)

	Recoverable at $8 to $10 per pound of U_3O_8		Recoverable at cost > $10 per pound of U_3O_8	
	Reasonably assured	Geologic estimate of possible future discoveries	Presumed available from submarginal material in presently exploited areas	Potentially recoverable from known low-grade deposits
United States	240,000	400,000	200,000	400,000*
Canada	400,000	200,000	200,000	?
Europe	40,000	100,000	?	1,000,000†
Latin America	3,000	?	?	100,000‡
Australasia	10,000	?	20,000	?
Africa	380,000	?	?	1,200,000*
Totals (rounded)	1,000,000	1,000,000 to 4,000,000	?	?

* Assumes 50 per cent availability of uranium in phosphate rock deposits. The large phosphate rock deposits contain uranium that may be recovered as a by-product in the production of phosphate fertilizers and chemicals. The rate of production depends on the quantity of rock acidulated for production of phosphate products. The cost of uranium by-product would depend on the grade of rock, the size of the plant, and other conditions. Total free-world potential by-product uranium recovery from existing phosphate plants is less than 1000 tons annually. A portion of this could be sold profitably at $8 to $10 per pound of U_3O_8, and most of it should be available if U_3O_8 prices were in the $16 to $20 range. The projected continuing expansion of the phosphate industry will increase the by-product uranium production potential. However, for many decades the by-product uranium from phosphate is not likely to be an important factor in total uranium production.

† Primarily uraniferous alum shales of Sweden (0.03 per cent U_3O_8).

‡ Primarily uranium associated with pyrochlore deposits in Brazil.

Extension of the estimates to include reserves recoverable at an average cost up to $30 to $50 per pound, however, increases the totals markedly. The reference estimates that an additional 5 to 10 million tons of U_3O_8 is available in this price range from low-grade shales having U_3O_8 content from 0.1 to 0.2 lb per ton in Sweden, the United States, and the USSR. The previous report[2] had estimated these low-grade deposits at more than 20 million tons, with 5 or 6 million tons in the United States; however, it was less specific in assigning a recovery cost for the deposits.

The report[1] also contains estimates of the amount of energy that can be extracted from the coal and uranium reserves. For uranium this quantity can vary over a wide range and is large only if plutonium and uranium are recycled through the reactor. If this recycling is done, the energy yield, or fuel utilization, depends on the average conversion ratio (or a related quantity, the regeneration ratio, defined in Table I-3) and on the losses incurred in chemical and metallurgical processing. The processing losses, which become important only when the regeneration ratio is high enough to support many recyclings of the fuel, depend on the frequency of processing, being lower for the less frequent cases that correspond to higher irradiation levels of the fuel per pass through the reactor. Table I-2 shows the effect

Table I-2 EFFECT OF IRRADIATION LEVEL, PER REACTOR PASS, ON FUEL UTILIZATION[1]

(Losses Are 1 Per Cent per Processing Cycle; Regeneration Ratio Is 1.4)

Irradiation level, Mwd/metric ton	Per cent of initial uranium burned
5,000	39
10,000	55
15,000	65
20,000	71

of irradiation level per pass on the percentage burnup of uranium (U^{235} plus U^{238}) when the loss is 1 per cent per processing cycle and the regeneration ratio is 1.4, about the practical upper limit for fast-breeder reactors.

Table I-3 shows the effect of the regeneration ratio on the fuel utilization, for losses of 1 per cent per processing and an irradiation level of 15,000 Mwd/metric ton per reactor pass. The reference states[1] that regeneration

Table I-3 HEAT ENERGY AVAILABLE FROM URANIUM[1]

	Regeneration ratio*				
	0.6	0.8	1.0	1.2	1.4
Per cent of initial U burned	0.68	0.94	1.5	62	65
Megawatt-days of heat per metric ton of initial U	6,200	8,600	14,000	565,000	590,000
Trillion (10^{12}) Btu's per short ton of initial U	0.46	0.64	1.05	42	44

*Regeneration ratio is defined here as the gross number of fissionable nuclei produced per fission, including fissions of U^{235}, U^{238}, Pu^{240}, and Pu^{241}. This regeneration ratio should be distinguished from the conversion ratio, usually defined as the gross number of fissionable nuclei produced per fissionable nucleus destroyed.

ratios are about 0.8 for converter reactors of types presently being constructed in the United States; note, however, that the energy yield of 8600 Mwd per metric ton of initial uranium is attained only with plutonium recycle.

The estimate of the total energy available from the uranium reserves available at costs up to three times present costs is given in Table I-4, along with similar estimates for energy from coal reserves. The specific energy yield used for the uranium estimates (590,000 Mwd/metric ton) is close to the theoretical upper limit, corresponding to a regeneration ratio of 1.4, a loss of 1 per cent per processing, and a fuel exposure per pass of 15,000 Mwd/metric ton.

Undoubtedly all of the uranium in the reserve will not be used at the maximum energy yield. Figure I-1 illustrates the approximate situation for lower yields. It applies to partially enriched solid-fuel reactors, in which roughly 1 ton of natural uranium is required to yield the inventory for each megawatt of electrical generating capacity. Three degrees of fuel utilization, or energy yield per ton of initial natural uranium, are considered. In each case the amount of U_3O_8 committed, as inventory supply and burnup, over a 20-year reactor life, is computed as a function of installed electrical generating capacity. At 5000 Mwd/ton, which is characteristic of current partially enriched reactors without plutonium recycle, a rather large reserve would be committed if the in-

Table I-4 HEAT ENERGY AVAILABLE FROM URANIUM AND COAL RESERVES*[1]

	At present prices		At 100 per cent increase† over present prices		At 200 per cent increase† over present prices	
	Reserves, millions of short tons	Maximum energy, 10^{18} Btu	Reserves, millions of short tons	Maximum energy, 10^{18} Btu	Reserves, millions of short tons	Maximum energy, 10^{18} Btu
Uranium:						
United States	0.20	9	0.7	31	0.8	35
Free World	0.85	37	3.4 (?)	150	4.2 (?)	180
Coal:						
United States	45,000	1.2	675,000	15	830,000	18
Free World	58,000	1.5	1,035,000	22	1,270,000	28

* Uranium reserves in terms of U_3O_8 have been multiplied by 0.85 to obtain contained uranium. Reserves of uranium and coal used here do not include geologic estimates of possible future discoveries.

† Increase in prices of uranium or coal.

stalled generating capacity were great enough to supply the present electrical consumption of the United States. At 20,000 Mwd/ton, which might be achievable with plutonium recycle plus some improvement of neutron economy, the uranium commitment is quite considerably lower; and at 590,000 Mwd/ton the uranium commitment is still lower. In the low-utilization cases the major fraction of the commitment is for fuel burnup, whereas in the high-utilization case (590,000 Mwd/ton), almost all of the commitment results from the inventory requirement. The steepest curve in Fig. I-1 shows the result of omitting the inventory requirement in the 590,000 Mwd/ton case. Since the inventory presumably would be transferable to new reactors at the end of reactor life, it is important to remember that the other curves in Fig. I-1 show fuel commitment, not fuel consumption. It should also be remembered that the inventory for expanding the installed capacity of breeder reactors can in principle be supplied by the excess fissionable isotope produced by previous breeders (if the doubling time of the breeding cycle is sufficiently short to supply the desired rate of expansion of capacity) and that the inventory requirements of thermal-neutron fluid-fuel breeders may be considerably lower than those typical of solid-fuel fast breeders, which were postulated in making Fig. I-1.

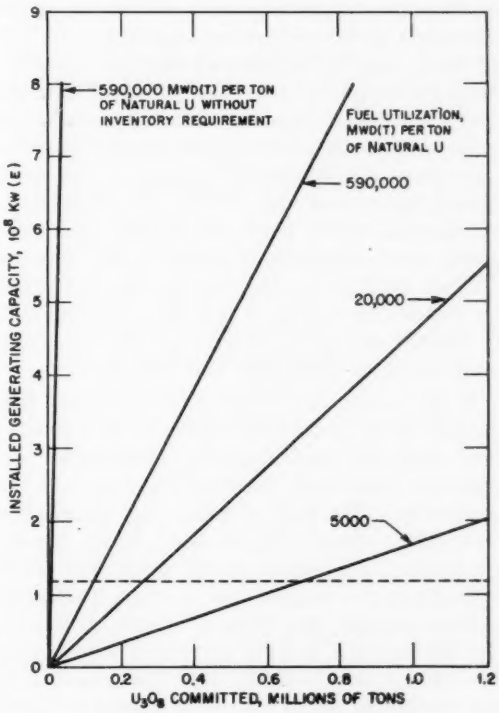

Fig. I-1 Natural U_3O_8 committed, for 20-year plant life, for various degrees of fuel utilization. The generating capacity indicated by the dashed line would, at 80 per cent plant factor, supply the present U. S. consumption of electricity.

References

1. R. D. Nininger et al., Energy from Uranium and Coal Reserves, USAEC Report TID-8207, May 1960.

2. J. C. Johnson, Resources of Nuclear Fuel for Atomic Power, *Proceedings of the Second United Nations International Conference on the Peaceful Uses of Atomic Energy, Geneva, 1958*, Vol. 2, p. 3, United Nations, New York, 1958.

Section II

APPLICATIONS: REMOTE MILITARY POWER

A study of the application of nuclear power in a number of specific military installations has recently been completed by Kaiser Engineers[1-14] for the AEC. Thirteen military sites were considered; these were designated by the AEC and the Department of Defense as installations where increased power-generating capabilities of 5 to 40 Mw(e) may be required by the U. S. Government for the period 1963 through 1970. The number of sites was reduced to 10 after preliminary consideration. In addition to the 10 specific military sites, a hypothetical site in the northeastern United States was also considered, similar to hypothetical sites used for civilian nuclear-power-cost estimates, as a datum point.[15] Studies for two additional sites having power requirements less than 5 Mw(e) have also been reported in another series of Kaiser reports[13,14] and are included in the discussion that follows.

In each case the power-generation cost was estimated for a nuclear plant and for a fossil-fuel plant of equal capacity, constructed and operated under the conditions peculiar to the application. The type of fossil-fuel plant used was either diesel or oil-fired steam turbo-generator, the choice being influenced most strongly by the required plant output. The applications studied, the types of plants chosen for the applications, and the estimated power costs are summarized in Table II-1. The ground rules for computing power cost were rather different from those generally used for commercial power plants, reflecting the differences between military and commercial operation. The major differences are summarized in the following list of ground rules for cost estimates of small reactors for military applications in remote areas.[1]

1. The power-plant designs, both nuclear and conventional, chosen for each application are to be the most economical concepts suitable to meet the particular power requirements for the site or transient application.
2. The nuclear design selected must be capable of construction and operation by 1965.
3. No interest on the initial investment is used in computing annual fixed charges.
4. A power-plant life of 20 years is assumed in computing annual fixed charges.
5. The nuclear and conventional power plants selected for each site are the plants having the lowest over-all cost.
6. Land for the plants is assumed to be available at no cost.
7. Acquisition cost for vessels from the laid-up fleet is not included.
8. Government costs, estimated to be 5 per cent of the total construction cost excluding contingency, are not included in the total project cost, nor are they included in the annual cost and unit power cost.
9. No taxes, insurance (including nuclear indemnity insurance), or interest on the cost of spare parts and fuel oil in storage are included in computing operation and maintenance costs.
10. Nuclear fuel costs exclude the nuclear fuel use charge.
11. Fuel oil costs are based on 1959 commercial rates, plus transportation by commercial carriers, and total escalation of 20 per cent over the 20-year life of the plant.
12. Operating labor costs are based on the going wage rates of the area involved or, in the case of plants to be operated by the military, on an average yearly cost per man (for military operating and maintenance personnel) of $6500 in the United States and $7500 outside the United States, plus escalation over the 20-year life of the plant.

Although only boiling-water and pressurized-water reactors appear in Table II-1, the initial Kaiser study covered other types as well. Sodium-graphite, fast-breeder, fluid-fuel, heavy-water, and gas-cooled types were eliminated as unsuitable, at least in the near future. It was judged that organic-moderated reactors would not show enough advantages over the

TABLE II-1. SUMMARY OF POWER PLANT DATA AND COSTS FOR NUCLEAR AND CONVENTIONAL POWER PLANTS[1,13,14,15]

SITE	OKINAWA RYUKYU ISLANDS	GUAM MARIANA ISLANDS	THULE GREENLAND	NORAD USA	ASMARA ERITREA	SUPER SACK JEA	NIKE ZEUS USA	INCHON KOREA	ATLANTIC BARGE	McMURDO SOUND ANTARCTICA	HYPOTHETICAL SITE	BYRD STATION ANTARCTICA	POLE STATION ANTARCTICA
POWER REQUIREMENT	40 Mw(e) in 1963 (1st inc) 80 Mw(e) in 1965	20 Mw(e) in 1963	25 Mw(e) Plus 150,000,000 Btu/hr of heat in 1963	7 Mw(e) in 1963 (4 Mw(e) firm)	5 Mw(e) in 1963	5 Mw(e) in 1963 (3.2 Mw(e) firm)	10 Mw(e) (firm)	10 Mw(e) in 1963	20 Mw(e) in 1963 (10 Mw(e) firm)	4.5 Mw(e) in 1963 (3.0 Mw(e) firm) 6 Mw(e) in 1964	40 Mw(e)	800 kw(e) by 1963	300 kw(e) by 1964
Total yearly power produced	290,000,000 kw-hr	145,000,000 kw-hr	178,000,000 kw-hr	52,600,000 kw-hr	43,800,000 kw-hr	28,000,000 kw-hr	87,600,000 kw-hr	70,000,000 kw-hr	149,000,000 kw-hr	26,300,000 kw-hr (1st INCREMENT)	293,000,000 kw-hr	7,000,000 kw-hr	4,380,000 kw-hr
Plant operating factor	80%	80%	80%	100% of average power	100% of firm power	100% of firm power	100% of firm power	80%	80%	100% of firm power	80%	100% of firm power	100% of firm power
NUCLEAR PLANT DATA													
Reactor size	150 Mw(t)	75 Mw(t)	130 Mw(t)	28 Mw(t) (SM-2)	28 Mw(t) (SM-2)	28 Mw(t) (SM-2)	28 Mw(t) (SM-2)	40 Mw(t)	83 Mw(t)	11.4 Mw(t) (PM-1)	135 Mw(t)	5.5 Mw(t) (FL-2)	3.6 Mw(t) (FL-2)
Reactor type	Direct cycle, natural circulation, boiling water	Direct cycle, natural circulation, boiling water	Direct cycle, natural circulation, boiling water	Pressurized water	Pressurized water	Pressurized water	Pressurized water	Pressurized water	Two loop, pressurized	Pressurized water	Direct cycle, natural circulation, boiling water	Direct cycle, natural circulation, boiling water	Direct cycle, natural circulation, boiling water
Number of reactors	One	One	One	Two	One	One	Two	One	One	Three	One	Two	One
Containment	120 ft dia. steel sphere	92 ft by 44 ft steel cylinder	94 ft by 50 ft steel cylinder	63 ft by 24 ft steel cylinder	63 ft by 24 ft steel cylinder	63 ft by 24 ft steel cylinder	63 ft by 24 ft steel cylinder	73 ft by 28 ft steel cylinder	48 ft diameter steel sphere	None	Pressure supression system	None	None
Size of turbine-generators	22,000 kw	22,000 kw	27,000 kw	6,000 kw	6,000 kw	6,000 kw	6,000 kw	10,820 kw	11,500 kw	1,760 kw	44,000 kw	975 kw	625 kw
Number of units	Two	One	Two	Two	One	One	Two	One	Two	Three	One	Two	One
Type of stand-by unit	260,000 lb/hr oil fired steam boiler	None	200,000 lb/hr oil fired steam boiler	None	None	1,100 kw diesel-engine generator	2,000 kw diesel-engine generator	None	160,000 lb/hr oil fired steam boiler	None	None	None	250 kw diesel-engine generators
Number of stand-by units	One		One			Four	Four		One				Three
Rated capacity of plant	41,400 kw	20,700 kw	25,400 kw	10,800 kw	5,400 kw	6,000 kw	10,800 kw	10,000 kw	20,000 kw	4,635 kw	40,000 kw	975 kw/reactor	625 kw
Net firm power	20,700 kw	0	15,000 kw	4,000 kw (6,000 kw av.)	5,000 kw	5,400 kw	10,000 kw	0	10,000 kw	3,090 kw	--	800 kw	500 kw
Type of installation	Land based	Platform barge	C3 hull	Hardened	Land based	Hardened	Land based	EC2-S-C1 hull	C3 hull	Land based	Land based	Land based	Land based
Location	Kin	Tumon Bay	Barge basin	Camp Carson	Tract "E"	(Classified)	(Classified)	Inchon Harbor	Atlantic Ocean area	Naval Air Facility	Hypothetical site	Byrd Station	Pole Station
Total project cost	$22,700,000	$16,500,000	$21,700,000	$11,100,000	$ 5,800,000	$ 8,700,000	$11,300,000	$11,100,000	$20,000,000	$10,100,000	$20,700,000	$ 9,600,000	$ 7,400,000
Average annual operating and maintenance cost	$ 360,000	$ 437,000	$ 597,000	$ 308,000	$ 239,000	$ 235,000	$ 324,000	$ 358,000	$ 384,000	$ 382,000	$ 578,000	$ 270,000	$ 215,000
Annual nuclear fuel cost	1,040,000	655,000	898,000	771,000	506,000	388,000	1,146,000	472,000	647,000	609,000	892,000	132,000	77,000
Average annual fuel oil cost	179,000	--	207,000	--	27,000	17,000	71,000	--	93,000	--	--	--	132,000
Total average annual operating, maintenance, and fuel cost	$ 1,579,000	$ 1,092,000	$ 1,702,000	$ 1,079,000	$ 852,000	$ 640,000	$ 1,541,000	$ 830,000	$ 1,124,000	$ 991,000	$ 1,470,000	$ 402,000	$ 424,000
Cost per kw-hr	5.4 mills	7.5 mills	8.2 mills (power cost only)	20.5 mills	19.4 mills	22.9 mills	17.6 mills	11.9 mills	7.6 mills	37.8 mills	5.0 mills	57.4 mills	96.8 mills
Annual fixed charges (5% of total project cost)	$ 1,135,000	$ 825,000	$ 1,085,000	$ 555,000	$ 290,000	$ 435,000	$ 565,000	$ 555,000	$ 1,000,000	$ 505,000	$ 1,035,000	$ 480,000	$ 370,000
Total average annual cost	$ 2,714,000	$ 1,917,000	$ 2,787,000	$ 1,634,000	$ 1,142,000	$ 1,075,000	$ 2,106,000	$ 1,385,000	$ 2,124,000	$ 1,496,000	$ 2,505,000	$ 882,000	$ 794,000
Cost per kw-hr	9.4 mills	13.2 mills	14.0 mills	31.1 mills	26.1 mills	38.4 mills	24.0 mills	19.7 mills	15.2 mills	56.8 mills	8.5 mills	126 mills	181 mills
CONVENTIONAL PLANT DATA													
Type	Steam turbine-generator	Steam turbine-generator	Steam turbine-generator	Diesel engine generator	Diesel engine generator	Diesel engine generator	Diesel engine generator	Diesel engine generator	Steam turbine-generator	Diesel engine generator	Coal-fired steam boiler	Diesel engine generator	Diesel engine generator
Total project cost	$10,200,000	$ 7,700,000	$11,100,000	$ 4,700,000	$ 2,915,000	$ 3,800,000	$ 5,300,000	$ 4,700,000	$ 7,100,000	$ 4,100,000	$12,600,000	$ 3,100,000	$ 2,580,000
Average annual operating and maintenance cost	$ 214,000	$ 292,000	$ 469,000	$ 163,000	$ 156,000	$ 126,000	$ 241,000	$ 272,000	$ 290,000	$ 222,000	$ 498,000	$ 221,000	$ 215,000
Average annual fuel oil cost	2,423,000	1,245,000	3,370,000	624,000	532,000	331,000	1,420,000	520,000	1,253,000	2,244,000	1,296,000	2,101,000	1,316,000
Total average annual operating, maintenance, and fuel cost	$ 2,637,000	$ 1,537,000	$ 3,839,000	$ 787,000	$ 688,000	$ 457,000	$ 1,661,000	$ 792,000	$ 1,543,000	$ 2,466,000	$ 1,794,000	$ 2,322,000	$ 1,531,000
Cost per kw-hr	9.1 mills	10.8 mills	14.1 mills (power cost only)	14.9 mills	15.8 mills	16.3 mills	19.0 mills	11.3 mills	10.4 mills	93.5 mills	6.2 mills	331.7 mills	350 mills
Annual fixed charges (5% of project cost)	$ 510,000	$ 385,000	$ 555,000	$ 235,000	$ 146,000	$ 190,000	$ 265,000	$ 235,000	$ 355,000	$ 205,000	$ 630,000	$ 155,000	$ 129,000
Total average annual cost	$ 3,147,000	$ 1,922,000	$ 4,394,000	$ 1,022,000	$ 834,000	$ 647,000	$ 1,926,000	$ 1,027,000	$ 1,898,000	$ 2,671,000	$ 2,424,000	$ 2,477,000	$ 1,660,000
Cost per kw-hr	10.9 mills	13.3 mills	17.0 mills (power cost only)	19.5 mills	19.0 mills	23.1 mills	21.9 mills	14.7 mills	13.6 mills	101.7 mills	8.4 mills	354 mills	379 mills

water reactors during the period before 1965 to justify their selection, although they were considered promising for construction in and after 1965.

In the preliminary study[12] made to select reactor types, ranges of capital costs and fuel costs for pressurized-water and boiling-water reactors were estimated on the basis of costs experienced in the past and on the basis of estimates by experienced reactor manufacturers. These cost ranges are summarized in Table II-2. In the individual site studies, the costs

Table II-2 REACTOR COST DATA[12]

Power level, kw(e)	Pressurized-water reactor		Boiling-water reactor	
	Capital cost, $/net kw	Fuel cost, mills/kw-hr	Capital cost, $/net kw	Fuel cost, mills/kw-hr
5,000	750–1100	7.5–8.5	750–1000	7.5–8.5
10,000	700–1000	5.5–8.0	650–850	5.5–8.0
20,000	500–750	4.5–6.5	500–650	4.5–6.5
40,000	400–550	3.0–4.5	350–500	3.0–4.5

were, of course, estimated for the particular reactor and the particular site; but because the estimates shown in Table II-2 did not show great differences between the two reactor types, the availability of a previously developed reactor design fitting the load requirements of the site was allowed, in some cases, to play an important part in the selection of the reactor type. Six basic design approaches were used to cover the requirements of the 13 different sites studied. The relatively high power requirements of the Okinawa, Guam, Thule, and hypothetical site installations were met with boiling-water reactor designs that were derived from the General Electric design for the Humboldt Bay plant, or by a design interpolated between those of Humboldt Bay and Vallecitos. The Atlantic Barge was supplied with a pressurized-water reactor typical of the Westinghouse designs, partly because of expected advantages of the pressurized-water approach for the barge application. The Inchon plant, also barge-mounted, used a pressurized-water design that had been previously prepared by Alco Products, Inc., as part of a survey of pressurized-water plants in the 10- to 30-Mw(e) range.[16] The NORAD, Asmara, Super Sage, and Nike-Zeus installations were supplied by SM-2 reactors, the two higher power installations using two each.* The McMurdo Sound installation was supplied with three PM-1 reactors. The Pole Station used one PL-2 reactor, whereas the Byrd station used two of the same type.

The reactor development carried out specifically by the Army Reactors Branch of the AEC up to this time has been confined to reactors of relatively low output; hence one finds, in Table II-1, that the higher capacity installations utilize reactors typical of current commercial designs, whereas the lower capacity installations use reactors of the Army series. The reactors that have been built under the Army reactors program, as either prototypes or experimental reactors, are the SM-1 (formerly APPR) producing 1855 kw(e), the SL-1 (formerly ALPR) producing 300 kw(e) and 400 kw(t) for space heating,† and the Gas-Cooled Reactor Experiment (GCRE), an experimental direct-cycle gas-cooled unit producing 2200 kw(t) and having no power-conversion equipment. Portable units based on these prototypes are under development and design by several contractors. These projects are summarized in Table II-3. In addition, the SM-2, a scaled-up and improved version of SM-1, is under design and development by Alco Products, Inc.[17] The SM-2 design has been used for several of the applications summarized in Table II-1. In making the cost estimates for the installations using SM-2 reactors, the reactor design and development costs were assumed to be nominal, inasmuch as design and development are already being done under the Alco project. The major features of

* In the Army reactor designations, the first letter refers to plant mobility as follows: S = stationary, not designed for subsequent relocation; P = portable, operates while stationary, but can be dismantled and reassembled at another location; M = mobile, can be moved intact or virtually intact. The second letter designates the design power, as follows: V = very low, less than 100 kw(e); L = low, 100 to 1000 kw(e); M = medium, 1000 to 10,000 kw(e); H = high, greater than 10,000 kw(e). The third character, a numeral, designates the order in which plant concepts having the same two initial letters were developed, and a letter after the numeral designates successive units of the same design in alphabetical order.

†On Jan. 3, 1961 (subsequent to the writing of this review), the SL-1 reactor core was wrecked by an explosion in the reactor vessel. There is no indication that the accident implies any inherent weakness in the basic reactor type—Editor's Note.

Table II-3 SUMMARY OF CHARACTERISTICS OF PORTABLE AND MOBILE NUCLEAR POWER PLANTS[13]

Designation	ML-1	PL-2	PM-1	PM-2A
Type of reactor	Gas-cooled	Boiling-water	Pressurized-water	Pressurized-water
Design contractor	Aerojet-General Nucleonics	Combustion Engineering	The Martin Co.	Alco Products
Nominal capacity	330 kw (net)	1000 kw (net) + 0.4 Mw(t) steam	1000 kw (net) + 2.0 Mw(t) steam	1560 kw (net) + 0.3 Mw(t) steam
Auxiliary power, kw(e)	70	237	250	315
Reactor thermal rating, Mw(t)	3.4	8.8	9.37	10
Core lifetime, Mw(t)-years	3.9	30.0	18.7	8.0
Design ambient air temp., °F	100	60	70	Arctic conditions
Design altitude, ft above sea level	0	6000	6500	Arctic conditions
Plant lifetime, years	6	20	20	20
No. of operating personnel per reactor	6	7	8	8
No. of shipping packages per reactor (excluding foundations and turbine building)	4	17	17	26
Shipping weight, lb per reactor (excluding foundations and turbine building)	120,000	480,000	510,000	710,000
Delivery time (FOB plant)	15 months	15 to 18 months	14 months	15 to 18 months
Status of project	Prototype operation scheduled in 1961; component tests, GCRE, and GTTF are now operating	Ref. design of PL-2 complete; stationary 300-kw prototype (SL-1) now operating; PL-2 type core to be tested at 8–10 Mw(t) starting July 1961	Design complete; operation scheduled for summer 1961 at Sundance, Wyo.	Was to be installed at Camp Century, Greenland, and was to be in operation by Sept. 1, 1960

the SM-2 design are evident in Table II-4, a summary of the power-plant data (nuclear versus conventional) for the NORAD site, which, in the nuclear version, uses two SM-2 reactors.

In Fig. II-1 the results of the economic analysis are shown for the reactors in the 5- to 40-Mw(e) range. The results show that by far the most important factor in determining the cost of nuclear power production is the electrical capacity of the station—or, in cases where multiple reactors are used, the average power production per reactor. In the case of the conventional plants, the important determining factor is, of course, the cost of fuel. The curve in Fig. II-1 shows the power output per reactor at which a nuclear plant would be competitive with a conventional plant, as a function of the conventional fuel cost. The curve is drawn as a very broad one to allow for the effects of other variables. In all regions above the curve, nuclear power costs are lower than conventional power costs; whereas in all regions below the curve, conventional power costs are lower than nuclear power costs. The various installations considered [in the 5- to 40-Mw(e) range] are plotted at the appropriate points on the figure.

It is not surprising that two of the facilities lie well above the curve and that several lie in or near the marginal zone, since the conventional fuel costs are high and the economic ground rules employed for the estimates are much more favorable for the nuclear plants than the ground rules used for commercial estimates. Also, it is reasonable to use such economic studies to show whether the general proposition of using nuclear plants at relatively remote military sites is at all attractive. There is no indication in the report of the study that a criterion of economic competitiveness would be applied to determine whether or not a nuclear plant would be built at any specific site. Indeed, since the construction and operation of each reactor yields important advances in nuclear power technology for both the nation and the military services, it would appear to be short-sighted policy to allow a difference of a few mills per kilowatt-hour, in a plant of small

Table II-4 SUMMARY OF POWER-PLANT DATA FOR THE NORAD STATION[5]

	Nuclear power plant	Conventional power plant
Over-all performance:		
Type of reactor/conventional power source	Pressurized-water reactors	Diesel-engine-driven generators
No. of reactors	2	
No. of turbine-generators/diesel-engine generators	2	6
Gross electrical capability	12,000 kw	9000 kw
Net electrical capability	10,800 kw	6000 kw (firm)
Turbine steam flow	166,000 lb/hr	
Turbine steam pressure	600 psia	
Turbine steam temperature	486°F (saturated)	
Feed-water return temperature	339°F	
Fuel assemblies (each reactor):		
Fuel material	UO_2 in stainless-steel matrix	
Initial enrichment	90+% U^{235}	
Weight of fuel in the core	36.2 kg, U^{235}	
Fuel burnup at discharge	38.8%	
Cladding material	Stainless steel	
No. of stationary fuel assemblies	38	
No. of control-rod followers	7	
No. of control rods	7	
Control material	Europium	
Reactor vessels:		
Internal diameter	41 in.	
Internal height	12 ft 5 in.	
Material	Stainless steel	
Containment structures:		
Type	Vertical steel cylinder (2 required)	
Over-all height	63 ft	
Diameter	24 ft	
Turbine-generators:		
No.	2	
Type	3600 rpm, single casing	
Gross capability (1½ in. Hg abs.)	6000 kw	
Generator coolant	Air	
Generator voltage	2400/4160 volts	
Condensers:		
No.	2	
Type	Two-pass, divided water box	
Condensing surface	9000 sq ft	
Pressure (at 100% capability and 75°F cooling water	1½ in. Hg abs.	
Standby power	Nuclear	
Diesel-engine generators:		
No.		6
Type		Heavy duty
Rating		1500 kw
Generator voltage		2400/4160 volts

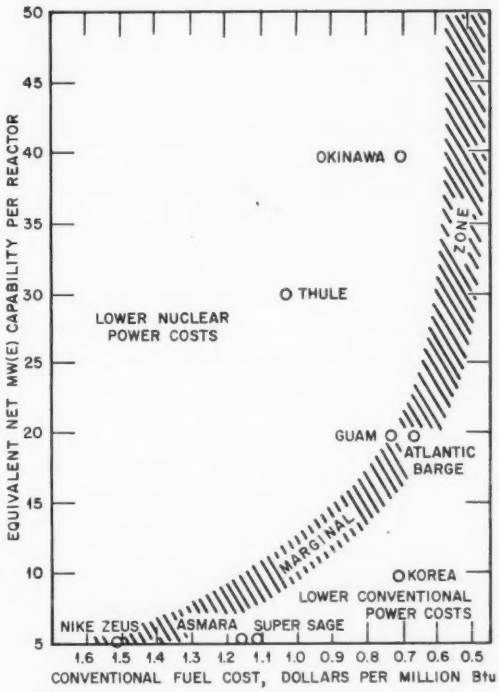

Fig. II-1 Effect of fuel cost on relative economics of nuclear and conventional power.[1]

capacity, to play a large part in determining whether the plant should be built for a military application.

References

1. Kaiser Engineers Div. of Henry J. Kaiser Co., Study of Remote Military Power Applications, Report No. 1, Summary, USAEC Report NYO-2937, January 1960 (revised July 1960).
2. Kaiser Engineers Div. of Henry J. Kaiser Co., Study of Remote Military Power Applications, Report No. 2, Okinawa, Ryukyu Islands, USAEC Report NYO-2938, January 1960 (revised July 1960).
3. Kaiser Engineers Div. of Henry J. Kaiser Co., Study of Remote Military Power Applications, Report No. 3, Guam, Mariana Islands, USAEC Report NYO-2939, January 1960 (revised July 1960).
4. Kaiser Engineers Div. of Henry J. Kaiser Co., Study of Remote Military Power Applications, Report No. 4, Thule Air Base, Greenland, USAEC Report NYO-2940, January 1960 (revised July 1960).
5. Kaiser Engineers Div. of Henry J. Kaiser Co., Study of Remote Military Power Applications, Report No. 5, North American Air Defense Command Operation Center, USAEC Report NYO-2941, January 1960 (revised July 1960).
6. Kaiser Engineers Div. of Henry J. Kaiser Co., Study of Remote Military Power Applications, Report No. 6, Fourth U. S. ASA Field Station, Asmara, Eritrea, USAEC Report NYO-2942, January 1960 (revised July 1960).
7. Kaiser Engineers Div. of Henry J. Kaiser Co., Study of Remote Military Power Applications, Report No. 7, Super Sage Rocky Mountains Area, USAEC Report NYO-2943, January 1960 (revised July 1960).
8. Kaiser Engineers Div. of Henry J. Kaiser Co., Study of Remote Military Power Applications, Report No. 8, Nike-Zeus Far Site, USAEC Report NYO-2944, January 1960 (revised July 1960).
9. Kaiser Engineers Div. of Henry J. Kaiser Co., Study of Remote Military Power Applications, Report No. 9, Inchon, Korea, USAEC Report NYO-2945, January 1960 (revised July 1960).
10. Kaiser Engineers Div. of Henry J. Kaiser Co., Study of Remote Military Power Applications, Report No. 10, Atlantic Barge, USAEC Report NYO-2946, January 1960 (revised July 1960).
11. Kaiser Engineers Div. of Henry J. Kaiser Co., Study of Remote Military Power Applications, Report No. 11, U. S. Naval Air Facility, McMurdo Sound, Antarctica, USAEC Report NYO-2947, January 1960 (revised July 1960).
12. Kaiser Engineers Div. of Henry J. Kaiser Co., Study of Remote Military Power Applications, Report No. 12, Evaluation and Selection of Applicable Reactor Concepts, USAEC Report NYO-2948, January 1960 (revised July 1960).
13. Kaiser Engineers Div. of Henry J. Kaiser Co., Study of Remote Military Power Applications, Byrd Station, Antarctica, USAEC Report NYO-9052, May 1960 (revised July 1960).
14. Kaiser Engineers Div. of Henry J. Kaiser Co., Study of Remote Military Power Applications, Pole Station, Antarctica, USAEC Report NYO-9053, May 1960 (revised July 1960).
15. Kaiser Engineers Div. of Henry J. Kaiser Co., Study of Remote Military Power Applications, Hypothetical Site, USAEC Report NYO-2978, February 1960 (revised July 1960).
16. Alco Products, Inc., Survey of PWR Power Plants, 10–30 Mw(e) Size, USAEC Report TID-8513, Oct. 10, 1959.
17. Alco Products, Inc., Conceptual Design of SM-2 12,000 Kw(e) Power Complex, Report APAE-68, May 27, 1960.

Section III

REACTOR PHYSICS: CRITICAL AND EXPONENTIAL EXPERIMENTS

The first experiments in a series of critical experiments to be performed under the Multiregion Reactor Lattice Studies Program at the Westinghouse Reactor Evaluation Center are reported in reference 1. These experiments were carried out in uniformly loaded lattices using 2.7 per cent enriched UO_2, stainless-steel-clad fuel rods and a water-to-uranium-metal volume ratio of 2.5 : 1 for both cylindrical and slab fuel configurations. The cadmium ratios in the fuel at several radial positions, the critical loading, and the flux distributions were measured in the cylindrical core. Flux distributions were measured in the slab core for a uniform core and in cores containing water slabs and slabs of aluminum, steel, and silver-indium-cadmium.

A series of experiments with boron–stainless steel septa was carried out in the Pressurized Critical Assembly (PTR) at Knolls Atomic Power Laboratory (KAPL).[2] The quantities measured in these experiments were k_{eff}, bucklings, temperature coefficients, and neutron density distributions in all three dimensions of the core. Fifteen experiments covering a wide range of temperatures and fuels were performed in an 8- by 30- by 32-in. water-reflected core having a metal-to-water ratio of 1.160 ± 0.015. Twelve of these experiments contained 0.030-in. boron–stainless steel septa which had various B^{10} weight percentages and which bisected the 8-in. dimension of the core; the remaining three experiments contained no boron–stainless steel septa. The experimental results were compared with theoretical values determined by using Deutsch cross sections and "thin region theory."

The exponential experiments performed at Atomics International in graphite-moderated lattices containing cylindrical, uranium-metal fuel elements are described in reference 3. Measurements of the material bucklings and intracell flux distributions were made for eight individual lattices constructed from combinations of three fuel enrichments (0.4962, natural, and 0.9124 at.% U^{235}) and three lattice spacings (7.0, 9.5, and 12.0 in.). The resonance escape probabilities were measured for the three lattice spacings using natural-uranium fuel. The purpose of these experiments was to provide accurate experimental data for a simplified lattice which can serve as a basis for comparison with new theoretical calculations or modifications to existing theories.

Reference 4 describes a series of critical measurements made at the University of California Lawrence Radiation Laboratory on BeO-moderated enriched-uranium-fueled systems. The critical sizes of unreflected assemblies having BeO/U^{235} molecular ratios ranging from 247 to 7660 were determined from critical-height measurements. The fuel was used in the form of uranium foils; fuel density was varied by using different foil thicknesses and different spacings between foils. Varying the fuel foil thickness for three of the ratios provided information on the effects of self-shielding and flux depression on the critical dimensions. The data[5] provided by these experiments were used in multigroup criticality calculations on homogeneous BeO-moderated U^{235}-fueled systems.

Thermal-neutron-flux distribution measurements[6] were made at the Savannah River Laboratory in the Process Development Pile (PDP) for 10 different D_2O-moderated lattices of natural-uranium tubes. Both single and double fuel tubes were used at lattice spacings of 7 and 14 in. The purpose of the experiments was to provide a detailed comparison between the measured flux distributions and the flux distri-

butions calculated by the P_3 approximation to transport theory.

In September 1959 a panel of experts on the physics of heavy-water reactors was convened in Vienna by the International Atomic Energy Agency (IAEA). The proceedings of the panel have been published (references 8 to 14 and 17 to 20) by the Agency as a volume entitled *Heavy Water Lattices*. The volume contains a discussion of the status of the physics of heavy-water lattices and an appendix consisting of technical papers that were prepared as background to the discussions by the panel. A number of the papers in the appendix contain results of critical and exponential experiments, or discussions of such results.

The results of many of the critical experiments performed in ZEEP at Chalk River are covered in reference 7. Some additional measurements were reported at the panel meeting. The buckling measurement[8] for the 9.5-in. hexagonal lattice of NPD-1 oxide rods was repeated in a critical lattice, and the accuracy was improved considerably. Some uniform temperature coefficients were measured in ZEEP and were compared with the uniform temperature coefficients given for NRU, HIPPO, and the NPD-1 oxide lattice. The over-all cadmium ratios of the U^{238} wires at the centers of the elements in the central rod cluster of each of the three NPD-1 metal-rod lattices are given in reference 9 along with an interpretation of some of the results. A set of experiments[10] was performed in ZEEP to evaluate the effect of the resonance absorption in Zircaloy-2 on the reactivity of D_2O reactors using this material. These experiments were done in a 9.5-in. hexagonal lattice of NPD-1 oxide rods. Critical height changes, due to the presence of a Zircaloy-2 tube, and to an aluminum tube, were measured for four different fuel arrangements in the central cell of the lattice. Cadmium ratios and thermal-flux distributions were also measured. An analysis of the results gave an effective resonance integral for the zirconium in the Zircaloy-2 tube and an effective cross section for the Zircaloy-2 in this tube size.

Some experiments[11] that gave a general indication of the departures of the slowing-down spectrum from dE/E dependence in various positions in a D_2O natural-uranium lattice were also performed in ZEEP. A number of experiments[12] have been done in ZEEP to measure the effect on reactivity of a loss-of-coolant accident. Central-rod experiments were done in the three 19-element uranium-metal lattices (NPD-1 metal) and in the five 19-element UO_2 lattices (NPD-1 oxide). In addition, single off-center rod experiments were done in three of the 19-element UO_2 lattices. An interpretation of the central-rod experiments in terms of the reactivity effect of loss of all coolant in a bare, uniform reactor is given, assuming no interaction between rods with respect to this effect.

Some of the quantities measured in the approach-to-critical experiments[13] in the NRU research reactor at Chalk River are critical size, uniform temperature coefficient at several powers and temperatures, power coefficient, reactivity effect of equilibrium xenon at several powers, and xenon transients after shutdown.

New buckling measurements made in the joint Swedish-Norwegian subcritical facility, ZEBRA, on clusters of UO_2 rods are reported in reference 14. Most of the earlier measurements were covered in references 15 and 16. In the case of the 19-rod clusters, the effect of changing the cooling medium from D_2O to air was studied; also, the effect of gas channels around uranium rods has been measured. Activation measurements of the temperature coefficient of the resonance integral for uranium-metal and -oxide rods as a function of surface-to-mass ratio over a wide temperature range are described in reference 17. These preliminary results are compared with other published values of the temperature coefficient of the resonance integral. A major effort has been made to develop methods for correlating ZEBRA and other integral measurements with theory.

Reference 18 describes a series of buckling measurements made for heavy-water lattices in the PDP at Savannah River. An addendum[19] to reference 18, presented at the previously mentioned IAEA panel meeting on the physics of heavy-water reactor lattices at Vienna in September 1959, contains a list of the buckling values before and after they were corrected for the "L^2 correction" indicated in reference 18. The measured buckling values cover a wide variety of lattices including clusters of natural-uranium plates and rods, natural-uranium plates in gas-filled tubes, clusters of aluminum-clad UO_2 rods, and natural-uranium tubes. A comparison[20] was made between these buckling measurements, and the results of

calculations were made in accordance with the modified Aquilon recipe.

References

1. I. H. Coen, Multi-Region Reactor Lattice Studies, Quarterly Progress Report for the Period April 1 to June 30, 1960, USAEC Report WCAP-1419, Westinghouse Electric Corp., Atomic Power Dept., July 1960.
2. G. D. Hickman et al., Water-Moderated Cores with Boron Steel Septa at Elevated Temperatures, *Nuclear Sci. and Eng.*, 8(5): 381–392 (November 1960).
3. R. W. Campbell and R. K. Paschall, Exponential Experiments with Graphite-Moderated Uranium-Metal Lattices, USAEC Report NAA-SR-5409, Atomics International, Sept. 15, 1960.
4. F. A. Kloverstrom et al., Critical Measurements on Near-Homogeneous BeO-Moderated, Enriched-Uranium Fueled Systems, *Nuclear Sci. and Eng.*, 8(3): 221 (September 1960).
5. R. E. Lingenfelter, Criticality Calculations of BeO-Moderated Enriched-Uranium Systems, *Nuclear Sci. and Eng.*, 8(3): 226 (September 1960).
6. T. B. Ponder, Neutron Flux Distributions in Natural Uranium Tubes, USAEC Report DP-467, Savannah River Laboratory, March 1960.
7. D. W. Hone et al., Natural-Uranium Heavy-Water Lattices, Experiment and Theory, *Proceedings of the Second United Nations International Conference on the Peaceful Uses of Atomic Energy, Geneva, 1958*, Vol. 12, p. 351, United Nations, New York, 1958.
8. E. C. Critoph, D_2O-Uranium Lattice Experiments by the ZEEP Group and Blanket Group, in *Heavy Water Lattices, International Atomic Energy Agency, Panel on the Physics of Heavy Water Lattices*, p. 65, Vienna, 1960.
9. E. C. Critoph, Appendix to the Preceding Paper, Interpretation of the U^{238} Wire Cadmium Ratio Results in the NPD(1) Metal Lattices, in *Heavy Water Lattices, International Atomic Energy Agency, Panel on the Physics of Heavy Water Lattices*, p. 67, Vienna, 1960.
10. D. W. Hone, ZEEP Experiment on the Effective Cross Section of Zircaloy No. 2 in Several Different Spectra, in *Heavy Water Lattices, International Atomic Energy Agency, Panel on the Physics of Heavy Water Lattices*, p. 128, Vienna, 1960.
11. C. B. Bigham, Departures of Reactor Spectra from dE/E, in *Heavy Water Lattices, International Atomic Energy Agency, Panel on the Physics of Heavy Water Lattices*, p. 131, Vienna, 1960.
12. R. E. Green et al., Reactivity Effect of Removing Coolant from Lattices of Multiple Rods, in *Heavy Water Lattices, International Atomic Energy Agency, Panel on the Physics of Heavy Water Lattices*, p. 135, Vienna, 1960.
13. E. C. Critoph, Some Information from NRU Startup and Operating Experience, in *Heavy Water Lattices, International Atomic Energy Agency, Panel on the Physics of Heavy Water Lattices*, p. 41, Vienna, 1960.
14. R. Persson, New Measurements in ZEBRA, in *Heavy Water Lattices, International Atomic Energy Agency, Panel on the Physics of Heavy Water Lattices*, p. 69, Vienna, 1960.
15. R. Persson et al., Exponential Experiments on Heavy Water Natural Uranium Metal and Oxide Lattices, *Proceedings of the Second United Nations International Conference on the Peaceful Uses of Atomic Energy, Geneva, 1958*, Vol. 12, p. 364, United Nations, New York, 1958.
16. E. Anderson and O. Aspelund, Exponential Experiments with Uranium Oxide Clusters in Heavy Water, *Proceedings of the Second United Nations International Conference on the Peaceful Uses of Atomic Energy, Geneva, 1958*, Vol. 12, p. 374, United Nations, New York, 1958.
17. P. Blomberg et al., The Temperature Coefficient of the Resonance Integral for Uranium Metal and Oxide, Report RFX-32, p. 109, 1959; and Addendum to Report RFX-32: The Temperature Coefficient of the Resonance Integral for Uranium Metal and Oxide, in *Heavy Water Lattices, International Atomic Energy Agency, Panel on the Physics of Heavy Water Lattices*, p. 126, Vienna, 1960.
18. N. P. Baumann, Process Development Pile Measurements of Lattice Parameters of Natural Uranium in Heavy Water, USAEC Report DP-407, Savannah River Laboratory, July 1959.
19. N. P. Baumann, Addendum to Report DP-407, in *Heavy Water Lattices, International Atomic Energy Agency, Panel on the Physics of Heavy Water Lattices*, p. 87, Vienna, 1960.
20. R. Naudet, Analysis of Experimental Results at Savannah River, SPM Report 570, in *Heavy Water Lattices, International Atomic Energy Agency, Panel on the Physics of Heavy Water Lattices*, p. 95, Vienna, 1960.

Section IV

HEAT TRANSFER

Conduction

The subject of heat conduction in a large, uniformly heated solid that is pierced by coolant holes distributed in an equilateral triangular array was studied several years ago by Fend et al.[1] An analysis of this system was reported at a later date in reference 2. The analysis assumed a "high-solidity" system, or one in which the holes were small in comparison to the pitch; this made it possible to assume that the variation of the coolant-passage wall temperature with azimuthal angle was zero. The Laplace equation including the heat-generation term was then solved using circular harmonics. For simplicity, only two terms of the series solution were retained, and this resulted in setting dt/dx equal to zero at two points on the boundaries of the unit cell. The assumption of small-diameter coolant passages also enabled the authors to neglect certain terms in the series expansion for temperature.

The same general problem has recently been treated in reference 3. Both square- and triangular-pitched coolant-passage distributions were studied, and up to 10 terms were retained in the series representation. Uniform coolant-passage wall temperature was assumed, and the solutions are valid for all values of the ratio of the passage radius to one-half pitch (r_0/s). Tables of the series coefficients are presented for both the square and triangular array for values of s/r_0 from 1.05 to 4.0. Equations giving the maximum solid temperature and graphs of the coolant-passage heat flux as a function of azimuthal angle are given.

The analytical technique presented in reference 1 has also been used in another recent report on the same subject.[4] The equilateral triangular spacing was utilized, but the method included the effects of finite convection coefficients and temperature differences around the boundaries of the coolant passages. The same truncated series of circular harmonics was utilized, but the boundary condition at the coolant-passage wall included the heat-transfer film coefficient. Three terms of the series were retained and are presented in tabular form for the cases where the film coefficient approaches zero or infinity. Results are presented in graphical form and in the form of equations, and the authors conclude that the effect of the convective film coefficient on thermal gradients in the solid is small for values of s/r_0 greater than about 1.8.

Forced Convection in Annular Passages

The use of annular coolant passages in power reactors is often attractive, since an annulus exhibits a small equivalent diameter and yet can give a relatively large flow area per annulus. Heat transfer in an annulus is sometimes complex since heating and cooling of the fluid can take place simultaneously. The work of a number of experimenters has been summarized in reference 5. Table IV-1 lists the experimenter or correlator, the correlation, and the applicability. The correlations of Davis, Monrad and Pelton, and Wiegand, available in many heat-transfer texts, are also cited in the reference. Figure IV-1 is a plot of the various correlations with respect to D_2/D_1, considering only the film coefficient at the inner wall. Although the Russian data apparently conflict with the others for inner-wall film coefficients, a similar graph presented in reference 5 for outer-wall film coefficients shows satisfactory agreement.

Table IV-1 ANNULAR HEAT-TRANSFER CORRELATIONS*[5]

Experimenter	Correlation	Notes
Mikheyev (1952)	$Nu_f = 0.021\ Re_f^{0.8}\ Pr_f^{0.43} \left(\frac{Pr_f}{Pr_w}\right)^{1/4}$	Heating or cooling, both walls; D_e based on wetted perimeter; $1 \le D_2/D_1 \le 5.6$
Chiprianov (1952)	$Nu_{f_1} = 0.02 \left(\frac{D_1}{D_2 + D_1}\right)^{0.2} Re_f^{0.8}$	Inner wall; D_e based on wetted perimeter; $1 \le D_2/D_1 \le 7$
Chiprianov (1952)	$Nu_{f_2} = 0.02 \left(\frac{D_2}{D_2 + D_1}\right)^{0.2} Re_f^{0.8}$	Outer wall; D_e based on wetted perimeter; $1 \le D_2/D_1 \le 7$

*Properties are evaluated at bulk fluid temperatures (subscript f) or wall temperatures (subscript w).

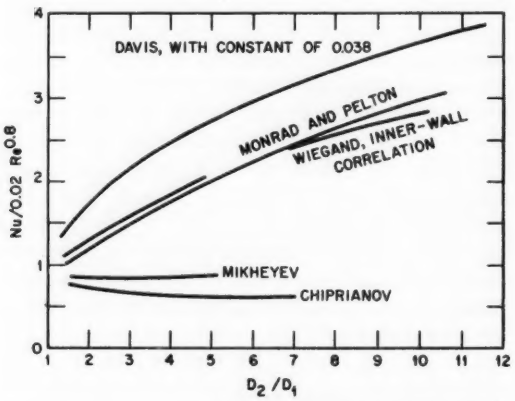

Fig. IV-1 Inner-wall film coefficient correlations.[5]

The Colburn correlation can be plotted in Fig. IV-1 as a horizontal line at an ordinate of approximately unity. Data presented in reference 6 on the flow of water through an internally heated annulus with D_2/D_1 of about 3 indicates a Nusselt number approximately between the Colburn correlation and the Wiegand correlation for the inner wall. More recent data are presented in reference 7, wherein the turbulent flow of water in internally heated annuli was studied. The data were then examined using the inner annulus wall correlations of Monrad and Pelton, Davis, and Wiegand, except that the term $(1 + CD_h/L)$ was included. The diameter ratio of the annulus was 1.593; the heated length was 2 ft, or about 60 hydraulic diameters. The correlation of Davis, even with the coefficient* reduced to 0.031 from 0.038 (to eliminate the effect of some questionable data) runs above the data, and the best correlation was determined to be that of Wiegand.

Reference 8 also treats heat transfer in an annulus. The basic purpose of the paper is to determine the effect of inner-wall surface spoilers on heat transfer and pressure drop in an annulus; however, data were taken for the smooth-tube case also. An essential difference between the apparatus in reference 7 and the apparatus in reference 8 is that the test section utilized in reference 7 was uninsulated, whereas that utilized in reference 8 was well insulated. Both test sections used water as a test fluid at pressures slightly above atmospheric and at temperatures of around 100°F. The annulus used in reference 8 had a diameter ratio of about 1.38. The smooth-tube data were correlated within ±7 per cent by an equation of the Sieder and Tate type, with a constant of 0.023. The final work to be mentioned is a progress report from the Engineering Research Laboratories of Columbia University.[9] An internally heated aluminum annulus with a diameter ratio of 1.5 was utilized; water was the heated fluid, and other parameters were as follows:

Water velocities: 2 to 10 ft/sec
Heat flux: 9000 to 90,000 Btu/(hr)(sq ft)
Water temperature: 80 to 200°F

Although the purpose of the experiments was to study an eccentric annulus, a number of runs were made with a concentric annulus. The heat-transfer coefficients calculated from the linear average tube surface temperatures, and the calculated water-bulk temperatures for both the concentric and eccentric annuli, were found to agree very well with either the Colburn or the Stein and Begell correlations. The agreement with the latter correlation was ±10 per cent.

*This is the term D in the correlation $Nu = D\,Re^m\,Pr^n$.

It cannot be said that it is clear what the detailed effect of the annulus diameter ratio is on heat transfer. For D_2/D_1 values between 1 and 2, the differences between the various correlations are almost within the experimental error. Since power-reactor coolant passages are usually designed with diameter ratios between 1 and 2, the spread in the correlations at higher D_2/D_1 ratios is of somewhat academic interest; however, the problem does appear to warrant further study.

The information contained in reference 8 on spoiler performance is of interest aside from the question of the various correlations and their applicability. The various spoilers studied are given in Table IV-2.* The integrally machined spoiler consists of a spiral thread of semicircular cross section protruding from the base diameter of the tube. The grooved spoiler is machined into a tube of the base diameter of 0.5 in. Conclusions are presented in graphical form and are compared to existing correlations. The wire type spoiler is found to be inferior to the integral spoiler design in all respects; Table IV-3 illustrates the relative advantages of the integral spoilers and grooved-tube designs.

Table IV-2 SPOILER CONFIGURATIONS TESTED[8]

Configuration	Spoiler height, in. (average)	Ratio of pitch to height (nominal)	Explanatory remarks
Smooth	0		Smooth tube
P&W 10-1	0.0046	10	Spoilers integrally machined into tube surface
P&W 20-1	0.0049	20	Spoilers integrally machined into tube surface but with a 0.0005-in. groove accidentally machined between 0.005-in. spoilers
W 10-1 w	0.0053	10	Ten-mil-diameter wire wound into 5-mil-deep groove
W 10-1 g	0.0052 (depth)	10	Five-mil-deep groove without wire

*Tables IV-2 and IV-3 are reprinted here by permission from the American Society of Mechanical Engineers.[8]

Table IV-3 COMPARISON OF SMOOTH- AND SPOILER-TUBE PERFORMANCE[8]

Configuration	Nu	Re	f	Pressure drop per foot of length, psi	Pumping power per foot of length, ft-lb/hr
Smooth tube	107	16,500	0.0075	1.22	7,590
10-1 integral spoilers	247	16,500	0.0170	2.78	17,200
Smooth tube	247	52,000	0.0057	9.24	181,000
Grooved tube	247	35,800	0.0069	5.30	71,300

Boiling Heat Transfer

The various flow regimes occurring in the cocurrent turbulent flow of a liquid and a gaseous phase through a pipe are discussed in reference 10. Because definitions of these flow regimes are somewhat qualitative in nature and overlap each other to some extent, the following quotation* from reference 10 will serve to define the regimes.

> Turbulent cocurrent flow of a liquid and a gaseous phase through a pipe or channel is characterized by several regimes. If the volumetric rate of flow of the gas is much greater than that of the liquid, the gas will flow as a continuous or a dispersed phase, depending upon the mass velocities, the pipe diameter, and the orientation of the flow axis. In horizontal flow at relatively low mass velocities, the liquid flows along the bottom of the pipe (stratified flow). As the mass velocities are increased, keeping the ratio of the volumetric flow rates constant, the interface becomes quite wavy; and eventually a portion of the liquid is entrained as droplets in the gas. If the gas mass velocity only is increased, the liquid tends to spread out into an annular film over the walls of the pipe (annular flow). On the other hand, if both mass velocities are increased, so that the liquid and gas are flowing at comparable volumetric flow rates, the gas phase becomes discontinuous, resulting in a coarse suspension of bubbles in the liquid. The bubbles are not uniformly distributed except near the critical pressure, where the densities of the phases are nearly equal, or at very high Reynolds numbers, where the turbulent stresses are very much larger than the buoyant forces. This mode of flow ("bubble flow") is especially observed in vertical pipes at void fractions less than approximately 0.8. The bubbles are, in general, not uniformly distributed

*Reprinted here by permission from the *Journal of Heat Transfer*.[10]

across the pipe cross section except when the difference in the densities of the phases is small, or when the turbulent intensity is large. In vertical flow the vapor tends to concentrate near the pipe axis. The diffusion of vapor toward the center of the pipe is due to the lift force resulting from the unequal flow of the viscous liquid around any individual bubble in the presence of the pipe wall. As the vapor content increases the bubbles tend to coalesce near the center of the pipe; at still higher concentrations of vapor the flow eventually changes to either "slug" flow (alternate slugs of liquid and vapor completely filling the pipe cross section) or annular flow, depending upon the Froude and Weber numbers. For small pipes and velocities where the surface tension forces are comparable to the inertial forces, the slug flow regime is stable. At larger pipe diameters or gas velocities annular flow results.

Reference 10 presents a model for two-phase flow called the variable density, single-fluid model. It is postulated that the mixture flows as a suspension of bubbles in the liquid, with a radial gradient existing in the concentration of bubbles. The bubbles have a maximum concentration at the pipe axis and a zero concentration at the wall. At any one radius the two phases move with the same speed; but the average slip velocity of the phases is not zero, since the bubbles are concentrated in a region of higher velocity. The exact radial bubble-distribution-frequency function is not known, but the author assumes a power-law distribution for both the velocity and the void fraction, i.e.,

$$U/U_{max} = (y/R)^{1/m}$$
$$\alpha/\alpha_{max} = (y/R)^{1/n} \qquad (1)$$

where U = velocity
α = void fraction
y = distance from wall
R = radius of tube
m,n = positive constants

A material balance around a section of the pipe results in the following expressions for the slip velocity ratio, ϕ.

$$\phi = (1 - \bar{\alpha})/(K - \bar{\alpha}) \qquad (2)$$

where $\bar{\alpha}$ = average void fraction across the cross section
$K = \alpha/(V_G/V_T)$
V_G/V_T = ratio of gas volumetric flow to total volumetric flow

Using the concept of a single fluid with position-dependent properties, the wall shear stress is formulated in the same manner as single-phase flow, and the following equation results for pipe flow:

$$\frac{\tau}{\tau_{sp}} = \left[1 - \bar{\alpha}\left(1 - \frac{\rho_G}{\rho_L}\right)\right]^{3/4} \left[1 - X\left(1 - \frac{\rho_L}{\rho_G}\right)\right]^{7/4} \qquad (3)$$

where τ = wall shear stress in two-phase flow
τ_{sp} = wall shear stress if liquid only were flowing at same mass velocity
X = quality
$\rho_{L,G}$ = liquid and vapor density

Equation 3 was compared with the Martinelli-Nelson correlation using a value of 0.89 for K over the pressure range 100 to 2500 psia with a range of mean void fractions from 0 to 0.85; agreement was found to be good. Comparison with various experimental data indicates that the model apparently predicts steam void fractions better than the momentum exchange theory, as described in the September 1960 issue of *Power Reactor Technology*, Vol. 3, No. 4, page 28. The two models predict about the same frictional pressure drop versus quality, up to a quality of about 20 per cent, above which the momentum exchange theory appears to be a better representation of the Moen and Larson data.

Further insight into the model is provided by the discussion presented in reference 11. In this technical brief, Zuber compares Eq. 2 with data taken by Armand and Kholodovski. The latter correlated all the Russian data for steam-water mixtures by Eq. 2, which he also derived. The correlation is claimed to be valid for the two-phase flow of air and water and liquid metals. The value of K as a function of pressure is given in Table IV-4,* taken from a paper of Kholodovski. Some interesting questions raised[10] by Bankoff's model are quoted† as follows:

The flow parameter assumes different forms for flow in circular pipes and for flow between two flat

*Table IV-4 is reprinted here by permission from the *Journal of Heat Transfer*, page 257 of reference 11.

†Reprinted here by permission from the *Journal of Heat Transfer*, page 271 of reference 10.

Table IV-4 THE VALUE OF K AS A FUNCTION OF PRESSURE[11]

Pressure, kg/cm²	K	Pressure, kg/cm²	K
3	0.793	81	0.808
5	0.790	110	0.827
7	0.786	115	0.830
9	0.784	140	0.850
10	0.783	145	0.856
20	0.783	180	0.904
30	0.785	185	0.911
40	0.788	200	0.938
60	0.796	210	0.975
65	0.799		

plates. The equivalent diameter concept has been justified experimentally for single-phase turbulent flows, although some deviation has been observed for narrow wedge-shaped passages in which the laminar sublayer is relatively thick. It has not been demonstrated, however, that the equivalent diameter concept is equally valid for two-phase turbulent flow.

The wall has been assumed to be wetted by a liquid so that the void fraction at the wall itself is zero [see Equation 1*]. If, however, the vapor is being generated at the walls, as in boiling channels, some fraction of the wall will be continuously in contact with bubbles. It may be expected that these bubbles will act as additional roughnesses and that therefore the pressure drop characteristics would be different than for nonboiling channels under the same flow conditions. This question is as yet unresolved.

References 12 to 14 are all devoted to reporting on natural-circulation boiling-loop experiments. The apparatus[12] of the General Electric Company's Atomic Power Equipment Department (San Jose) had a test section consisting of a heated rod enclosed in a 0.875-in.-ID stainless-steel pipe. A 0.54-in.-OD by $8\frac{1}{2}$-ft-long heater rod and a 0.375-in.-OD by 9-ft-long rod were utilized at a nominal pressure of 1000 psia. The two-phase mixture was introduced into an 8-in. steam drum about 13 ft above the top of the test section. The water was recycled to the test section through a bypass subcooler, where varying degrees of subcooling could be accomplished. A forced-circulation pump was present in a bypass since some runs were made with forced circulation. Appropriate instrumentation to measure temperatures, pressures, flow rates, etc., was provided; in addition, a "burnout detection" system was utilized to shut off the power at the point of incipient burnout to prevent destruction of the heater. In the case of the runs with the $\frac{3}{8}$-in. rod, the tests were repeated with a restriction present in the downcomer.

The data are presented in graphical and tabular form, and the effects of the following variables are discussed: power input, subcooling, heater-rod geometry, and system geometry. Also included are traces for pressure drop and flow rate as a function of time. Because of the physical limitations of the system, it was not possible to trace the flow-power curve from zero power to burnout power; in general, the condition of increased flow with increased power could not be established, and operations took place in the region where increased power resulted in decreased flow. As power only was increased, hydraulic instability became apparent and pressure and flow-rate fluctuations were noted; as stability worsened, burnout occurred. It is important to note, however, that stable operation was achieved at flows considerably less than the maximum circulation rate. The initial stability of the test loop and the rate of onset of instability were dependent on the operating variables of the system.

Decreased subcooling resulted in decreasing flow rates. In one run, low subcooling (25 to 30 Btu/lb) exhibited a stability approaching that of a forced-circulation system. When the subcooling was increased (125 Btu/lb), violent oscillations were noted that vibrated the test section and cracked the sapphire spacers maintaining the rod-channel gap. Because of the nature of the natural-circulation system, it is not possible to vary only the subcooling since increased subcooling yields higher flow rates and lower exit-steam quality.

As expected, the smaller heater rod yielded higher flow rates due to reduced pressure drop. The smaller rod exhibited less stable operation, however. Pressure oscillations of ± 10 per cent were obtained at power densities of 110 to 120 kw/liter for the smaller rod compared to 180 to 200 kw/liter for the larger rod. No runs were made with the unrestricted smaller rod that exhibited pressure-drop fluctuations of less than ± 6 per cent.

Some of the burnout data obtained with natural circulation are shown in Fig. IV-2.* For the

*The equation number has been changed to be compatible with the equation appearing in this Review.

*Figure IV-2 is reprinted here by permission from the American Society of Mechanical Engineers.[12]

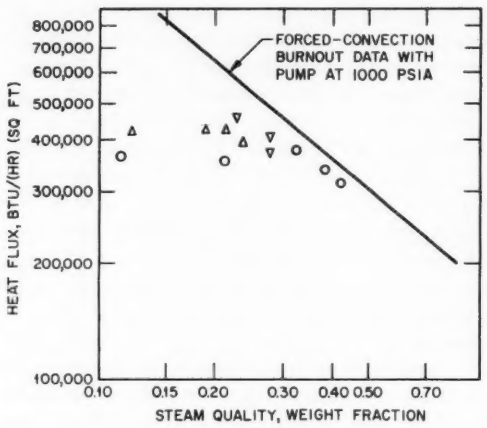

Fig. IV-2 Natural-circulation burnout data at 1000 psia.[12] ○, 0.540-in. heater rod. △, 0.375-in. heater rod, unrestricted. ▽, 0.375-in. heater rod, restricted.

same range of subcooling and power densities, the oscillations were about one-half as large with the restricted system compared to the unrestricted system. Burnout occurred at about the same heat flux, however, and the stabilizing effect of the pump can be noted in Fig. IV-2. Reference 12 concludes with a discussion of the various models presently available to describe the hydraulic behavior of natural-circulation reactors; it is concluded that none are presently adequate for a complete understanding of the problem. Reference 13 is a report on essentially the same type of experiment, but with the test section inclined to 45°. The results indicated that the performance of the inclined section could be readily determined from measurements on the vertical channel.

The Bettis natural-circulation tests with water are reported in reference 14. The experiments were performed with the following objectives: (1) to compare experimental natural-circulation loop flow rates with predicted flow rates; (2) to compare natural-circulation pressure drop, riser density, and heat-transfer burnout data with corresponding forced-circulation data; and (3) to obtain information about two-phase exit losses and steam-water slip ratios at low water velocities. With respect to the first objective, the reference contains a comprehensive discussion of the techniques of pressure-drop calculations and would be of interest to the specialist. The test-section geometry was rectangular, having a width of about 1 in. and a length of about 3 ft; the nominal channel thickness was 0.100, 0.200, and 0.250 in. The test section was connected to a 2-in.-diameter riser, 81 in. in length, by means of a 9½-in. transition section. The various runs accomplished are given in Table IV-5.* Some of the pressure-drop terms

Table IV-5 NATURAL-CIRCULATION RUNS[14]

Nominal test-section size, in.	Values of inlet subcooling (ΔT_{in}), °F			
	800 psia	1200 psia	1600 psia	2000 psia
0.100 by 1 by 27		109		
0.200 by 1 by 27	20,* 70*	20,* 70,* 109	20, 70,* 109	70, 109
0.250 by 1 by 27	20, 70, 109	20, 70, 109	20, 70	

*Duplicated with forced circulation.

were studied experimentally. The exit loss from the test section to the riser was one of these terms, and it was found that a fog-flow model adequately represented the behavior of the two-phase flow in this region. It was concluded that natural-circulation flow rates could be predicted to within 10 per cent for both single- and two-phase flow for the loop studied. Data are presented on the slip ratio at 1200 psia for water velocities from 0.1 to 0.3 ft/sec.

Fluctuating flow was also observed in the Bettis experiments. It was concluded that fluctuations increased with lower inlet subcooling and lower pressures. The effect of inlet subcooling thus appears to be in contradiction with the conclusions of reference 12; but reference 14 presents little quantitative data on the magnitude of pressure fluctuations, and it is difficult to ascertain if the effect of subcooling is being masked by other variables.

The two references[12,14] agree as to the effect of flow and pressure fluctuations on burnout:

1. Pressure drop, burnout heat flux, and riser density measured under natural-circulation conditions are no different from those measured with forced circulation at the same fluid conditions provided that no large flow fluctuations are present.
2. Flow fluctuations can occur in two-phase natural-circulation flow which are not present during forced-circulation flow at the same conditions. These flow fluctuations increase at lower inlet subcooling and system pressures. Burnout can occur prematurely as a result of flow fluctuations.

*Table IV-5 is reprinted here by permission from the American Society of Mechanical Engineers.[14]

Superheated-Steam Heat Transfer

For many years the only experimental data on the transfer of heat to superheated steam encompassing an appreciable range of temperature and pressure were those reported by McAdams et al.[15] The paper originally evaluated the data using the thermal-conductivity values of Timroth and Vargaftik, and the resulting correlation was published:

$$\frac{hD_e}{k_f} = 0.0126 \left(\frac{GD_e}{\mu_f}\right)^{0.89} \left(\frac{c_p \mu}{k}\right)_f^{1/3} \left(\frac{L}{D_e}\right)^{-0.13} \quad (4)$$

In an addendum to the paper, however, the data were reevaluated using the thermal-conductivity values of Keyes and Sandell, with the following correlation resulting:

$$\frac{hD_e}{k_f} = 0.0214 \left(\frac{GD_e}{\mu_f}\right)^{0.80} \left(\frac{c_p \mu}{k}\right)_f^{1/3} \left(1 + \frac{2.3}{L/D_e}\right) \quad (5)$$

Equation 4 correlates the data with an average deviation of 7 per cent and a maximum of 28 per cent. Equation 5 has a maximum deviation of 17 per cent.

Nowak and Grosh,[16] however, recently concluded that the Russian thermal-conductivity data "are to be preferred." With this background the new experiments reported in reference 17 are of particular importance. The objectives of the experiments were to corroborate and extend existing information to higher Reynolds numbers at intermediate pressures and to examine the effect upon the convection coefficient by a change from a circular tube to a rectangular channel of high aspect ratio. Two test sections were fabricated from type 304 stainless steel and were incorporated into a heat-transfer rig. The tubular section had an inside diameter of 0.333 in. and a heated length of 1 ft, and it was heated by alternating current. The rectangular section had dimensions of 1.25 by 0.047 by 12 in. and was chosen to simulate the BORAX-V core. Levy, Fuller, and Niemi reported that experiments performed with water flow in rectangular channels of high aspect ratio yielded convection coefficients about 40 per cent below the values for round tubes having the same equivalent diameter, and this was investigated. This latter work was reviewed in the March 1959 issue of *Power Reactor Technology*, Vol. 2, No. 4, pages 36 and 37. Other parameters are as follows: Reynolds number, 20,000 to 370,000; pressure, 300 to 1500 psia; inlet superheat, 5 to 160°F; film drop, 30 to 550°F. The Russian thermal-conductivity values are shown in Table IV-6; the values of viscosity used are given in Table IV-7.

Table IV-6 THERMAL CONDUCTIVITY, k, OF SUPERHEATED STEAM[17]

Temp., °F	Thermal conductivity, Btu/(hr)(ft)(°F), at indicated pressure			
	300 psia	600 psia	1000 psia	1500 psia
500	0.0258	0.0301		
550	0.0268	0.0300	0.0344	
600	0.0281	0.0361	0.0339	0.0396
650	0.0297	0.0317	0.0344	0.0393
700	0.0316	0.0332	0.0353	0.0398
800	0.0356	0.0370	0.0390	0.0421
900	0.0400	0.0410	0.0428	0.0450
950	0.0424	0.0431	0.0447	0.0466

Table IV-7 DYNAMIC VISCOSITY, μ, OF SUPERHEATED STEAM[17]

Temp., °F	Dynamic viscosity, lb/(ft)(sec), at indicated pressure			
	300 psia	600 psia	1000 psia	1500 psia
500	12.6	12.8		
550	13.2	13.4	13.6	
600	13.8	14.0	14.3	14.8
650	14.5	14.7	15.0	15.4
700	15.2	15.4	15.6	16.1
800	16.7	16.9	17.2	17.5
900	18.3	18.5	18.7	19.1
950	19.1	19.5	19.5	19.9

The results of the experiments are quoted[17] below:

Concerning the round channel experiments, the following conclusions may be drawn:

1. Convection coefficients may be predicted within ±10 per cent, using the following equations and the properties found in Tables [IV-6 and IV-7*].

$$\frac{hD_e}{k_f} = 0.0157 \left(\frac{GD_e}{\mu_f}\right)^{0.84} \left(\frac{c_p \mu}{k}\right)_f^{1/3} \left(\frac{L}{D_e}\right)^{-0.04}$$

for $6 < L/D_e < 60$, and

*The table numbers have been changed to be compatible with the other tables in this Review.

$$\frac{hD_e}{k_f} = 0.0133\left(\frac{GD_e}{\mu_f}\right)^{0.84}\left(\frac{c_p\mu}{k}\right)_f^{1/3}$$

for $L/D_e > 60$.

2. Particular attention should be paid to the type of unheated entrance section preceding the heated length of channel. The first of the above equations is applicable when this precedent section is 16 diameters in length. It may be safely used (with respect to limiting surface temperatures) for shorter unheated sections and should closely apply for a more fully developed velocity profile (unheated $L/D_e > 16$), because of the relatively weak influence of L/D_e.

3. Making allowances for the unheated entrance section, the data substantiate the experiments of McAdams, Kennel, and Addoms within ±5 per cent, even to a Reynolds number of 370,000.

4. The Dittus-Boelter equation,

$$\frac{hD_e}{k_f} = 0.023\left(\frac{GD_e}{\mu_f}\right)^{0.80}\left(\frac{c_p\mu}{k}\right)_f^{1/3}$$

when compared to the present study, yields values of the coefficient which are 11.5 per cent high in the lower Reynolds range (25,000) and 1.8 per cent high in the upper range (370,000). It is conjectured that this is due, in part, to the unsettled question of correct steam conductivity values.

Concerning the thin rectangular channel experiments, the following observations are made:

1. The vena contracta caused by the sharp-edged entrance condition influences the heat-transfer coefficient to a length of approximately 75 equivalent diameters, including the unheated entrance length of 13 diameters.

2. There is no observable difference between the rectangular data and the round channel correlation in the L/D_e range from 60 to 121. Even if it is postulated that the flow is not fully established in this region, there is no evidence that any serious decrease in coefficient will occur beyond this range, even according to the data of Levy, Fuller, and Niemi, whose data run to an L/D_e of approximately 180.

Short Notes

A number of ASME papers have become available which are pertinent to power-reactor heat transfer. Reference 18 is a mathematical treatment of the transient temperatures in a coaxially moving tube (coolant) and in a stationary rod (fuel element) resulting from a step change in the rate of energy generation within the rod. A variable flow resistance orifice is described in reference 19. It is suggested therein that the orifice under consideration would be adjusted throughout the lifetime of the reactor core, so as to match the element power and flow. Radiation heat-transfer problems are treated in references 20 and 21, whereas references 22 and 23 deal with natural-convection heat transfer. Fundamental studies on two-phase flow are reported in references 24 to 26.

References

1. F. A. Fend et al., An Approximate Calculation of the Temperature Distribution Surrounding Coolant Holes in a Heat-Generating Solid, USAEC Report BMI-T-42, Battelle Memorial Institute, Oct. 25, 1950.
2. P. J. Schneider, *Conduction Heat Transfer*, p. 206, Addison-Wesley Publishing Co., Inc., Reading, Mass., 1955.
3. E. M. Sparrow, Temperature Distribution in an Internally Cooled, Heat-Generating Solid, ASME Paper 60-SA-15, 1960.
4. T. R. Regenie and J. C. Rowley, Approximate Calculation of the Temperature Distribution Surrounding Coolant Holes in a Heat-Generating Solid with Finite Value of Fluid Heat Transfer Coefficient, USAEC Report LAMS-2436, Los Alamos Scientific Laboratory, June 20, 1960.
5. Wang Pu-Hsuan, On the Convective Heat Transfer for Turbulent Flow of Single-Phase Fluid Through Concentric Annuli, *Sci. Sinica*, 8(1): 98–109 (1959).
6. D. A. Dingee et al., Heat Transfer from Parallel Rods in Axial Flow, USAEC Report BMI-1026, Battelle Memorial Institute, Aug. 5, 1955.
7. Z. Rotem and I. Shai, Heat Transfer to Water in Turbulent Flow in Internally Heated Annuli, Part 1, Stationary Flow, ASME Paper 60-HT-20, 1960.
8. G. A. Kemeny and J. A. Cyphers, Heat Transfer and Pressure Drop in an Annular Gap with Surface Spoilers, ASME Paper 60-HT-15, 1960.
9. T. Diskind et al., Basic Studies in Heat Transfer and Fluid Flow, Quarterly Progress Report for Period April 1, 1960 to June 30, 1960, USAEC Report TID-6035, Engineering Research Laboratories, Columbia University, June 30, 1960.
10. S. G. Bankoff, A Variable Density Single-Fluid Model for Two-Phase Flow with Particular Reference to Steam-Water Flow, *J. Heat Transfer*, 82(4): 265 (November 1960).
11. N. Zuber, On the Variable-Density Single-Fluid Model for Two-Phase Flow, *J. Heat Transfer*, 82(3): 255 (August 1960).
12. S. Levy and E. S. Beckjord, Hydraulic Instability in a Natural Circulation Loop with Net Steam Generation at 1000 Psia, ASME Paper 60-HT-27, 1960.
13. S. Levy and C. L. Swan, Performance—Two-Phase Pressure Drop, Burnout, and Hydraulic

Oscillation of an Inclined Test Section with Net Steam Generation at 1000 Psia, USAEC Report GEAP-3228(Rev. 1), General Electric Co., Atomic Power Equipment Dept., Aug. 15, 1959.

14. O. J. Mendler et al., Natural-Circulation Tests with Water at 800 to 2000 Psia Under Nonboiling, Local Boiling, and Bulk Boiling Conditions, ASME Paper 60-HT-36, 1960.
15. W. H. McAdams et al., Heat Transfer to Superheated Steam at High Pressures, *Trans. ASME*, 72: 421 (1950).
16. E. S. Nowak and R. J. Grosh, An Investigation of Certain Thermodynamic and Transport Properties of Water and Water Vapor in the Critical Region, USAEC Report ANL-6064, Argonne National Laboratory, October 1959.
17. J. B. Heineman, An Experimental Investigation of Heat Transfer to Superheated Steam in Round and Rectangular Channels, USAEC Report ANL-6213, Argonne National Laboratory, September 1960.
18. V. S. Arpaci, Transient Conduction in Coaxial Cylinders with Relative Motion and Heat Generation, *J. Appl. Mech.*, Paper 60-APM-24, 1960.
19. J. Sherman et al., Variable Flow Resistance with Adjustable Multihole Orifice Plates in Series, *J. Basic Eng.*, 82(3): 645–653 (September 1960).
20. E. M. Sparrow et al., Radiation Heat Transfer in a Spherical Enclosure Containing a Participating, Heat-Generating Gas, ASME Paper 60-HT-9, 1960.
21. E. M. Sparrow et al., Analysis, Results, and Interpretation for Radiation Between Some Simply Arranged Gray Surfaces, ASME Paper 60-HT-4, 1960.
22. B. Gebhart, Transient Natural Convection from Vertical Elements, ASME Paper 60-HT-33, 1960.
23. J. S. McDonald and T. J. Connolly, Investigation of Natural Convection Heat Transfer in Liquid Sodium, *Nuclear Sci. and Eng.*, 8(5): 369–377 (November 1960).
24. K. Goldmann et al., Burnout in Turbulent Flow—A Droplet Diffusion Model, ASME Paper 60-HT-34, 1960.
25. P. Griffith and G. B. Wallis, Two-Phase Slug Flow, ASME Paper 60-HT-28, 1960.
26. S. T. Hsu and F. W. Schmidt, Measured Variations in Local Surface Temperatures in Pool Boiling of Water, ASME Paper 60-HT-32, 1960.

Section V

CONFERENCE ON REACTOR KINETICS

On Oct. 12 to 14, 1960, a conference on reactor kinetics was held at Sun Valley, Idaho. The proceedings of the conference will be published by Phillips Petroleum Company. The objective of the conference was to review the present state of the art and thereby to stimulate a free exchange of ideas and information. Review papers were presented, and these were followed by discussion periods. There was some discussion of the importance of research in reactor kinetics and dynamics, of the desirable objectives of such research, and of the relation of the reactor safety staff of the AEC to such research efforts and to the administration of safe reactor design and operating practices. The following résumé, however, will cover only the purely technical presentations and discussions. A substantial fraction of the material on stability and transfer functions resulted from the continuation of researches that were described at an earlier conference at Argonne National Laboratory (ANL). These researches were summarized briefly in the September 1960 issue of *Power Reactor Technology*, Vol. 3, No. 4, pages 33 to 37. The proceedings of that conference have been published[1] and will be found useful as related material.

Power Excursion Research

The present status of knowledge on the self-limiting response of reactors to step and ramp reactivity insertions was outlined at the Sun Valley conference by F. Schroeder.

The first-burst behavior of the Special Power Excursion Reactor Test No. 1 (SPERT-I) cores (four aluminum and two stainless steel) to step reactivity insertions shows striking similarities when, for example, characteristic results of the bursts, such as peak power and energy release up to the time of peak power, are plotted as functions of the initial reciprocal period, α_0. These similarities prevail over the range of initial reactor periods covered in the tests (from several seconds to 5 msec) in spite of the wide range of nuclear characteristics, e.g., the void coefficient C_v covered a range of a factor of 10 and the effective prompt-neutron lifetime l covered a range of a factor of 5. The features of the plots are related to the shape of the power burst.

For reactivities greater than prompt critical, the burst shapes (reactor power as a function of time) can be fitted by a mathematical model wherein the reactivity loss during the transient is simply related to the energy release. The general form of the coupling equation is

$$\alpha(t) = \alpha_0 - b\,[E(t-\tau)]^n$$

where $\alpha(t)$ is the reciprocal period at time t following the step insertion, τ is a delay time between the energy release and the reactivity loss, $E(t-\tau)$ is the energy release up to the time $t-\tau$, b is the reactor shutdown coefficient, and n is a positive constant. When $\tau = 0$ and $n = 1$, the coupling equation is that of the Fuchs model. For best fit to the experimental burst shapes, $\tau \gg 1/\alpha_0$ and $n = 1.5$ to 2.0. An equally good fit is then obtained for the time variation of reactivity compensation, which can be computed from the experimental power burst shapes. This model is referred to as the long-delay model ($\tau \gg 1/\alpha_0$); for the best over-all fit, it must involve a nonlinear relation between the energy release and the reactivity feedback (i.e., $n \neq 1$). For reactivities less than prompt critical, this model also fits the observed features of the power burst when the effects of the delayed neutrons are taken into account. The model predicts that peak power is proportional

to $b^{-1/n}$ where, in turn, b is proportional to the ratio C_v/l; this prediction is in reasonably good agreement with the experimental observations. From the safety point of view, it is important to note that below prompt critical the reactivity compensation required to limit a power burst is considerably less than the excess reactivity initially introduced.

The physical processes responsible for self-limiting behavior do not appear explicitly in the theory. The difficulty has been that the computation of some of the processes for conversion of energy into reactivity is extremely complicated and that the characteristics of some of the processes are not known. In the SPERT cores the decrease in water content of the core due to expansion of water upon heating, the expansion of the fuel plates, and the formation of steam void contribute strongly to the self-shutdown processes during a transient. At present the understanding of transient boiling is inadequate, and thus it is not possible to calculate reliably the steam-void growth during a power burst. The steam volumes required to terminate typical power excursions turn out to be at least an order of magnitude less than the volumes that would be calculated to form during the excursion on the basis of steady-state heat transfer. Elevation of the boiling point by transient pressures, steam blanketing of the fuel plates, and transient superheat requirements may be responsible.

Experiments are under way using fuel-bearing water-filled capsules placed in a high-flux reflector region of the SPERT core. The capsules are instrumented to provide pressure, volume, and temperature data during transient power excursions and should give valuable information on the nature of transient boiling phenomena. As a visual aid, high-speed photography has been incorporated into the in-pile capsule experiment.

W. E. Nyer presented some further remarks concerning the variety of mechanisms contributing to self-shutdown in a power excursion in a water-cooled reactor. Suppression of boiling, due, for example, to operation at elevated pressures, is not as serious as it was once thought to be. With boiling suppressed, more of the energy released in an excursion is channeled into the other self-shutdown mechanisms so that often there is no great increase in peak power or total energy release. The effect of coolant flow on self-limitation characteristics is not large; the peak fuel-element temperatures actually are less for full-flow conditions than for zero flow. The net effect should be an increase in safety, although this conclusion must be considered preliminary for the present.

Experiments performed as part of the Kinetic Experiment on Water Boilers (KEWB) program on a small aqueous homogeneous reactor ($12\frac{1}{4}$-in.-diameter sphere filled with uranyl sulfate solution and surrounded by a 56-in. cube of graphite) demonstrate its ability to withstand the transient pressures generated (up to ~600 psi) in excursion periods as low as 2 msec. The shutdown mechanisms arise from expansion of the fuel solution upon heating and from radiolytic gas formation. The temperature effect predominates except at very short periods, when radiolytic gas formation is the important contributor. The use of a simple analytical model with adjustable constants (not derivable from basic principles) gives good predictions of peak power for initial reactor periods of less than 10 msec. The model overestimates the radiolytic gas shutdown effect for periods of more than 10 msec. The major obstacles to correlation of the analytical model with the physical processes involved are insufficient knowledge of the dissociation-recombination phenomena in radiolytic gas formation and the effects of the transient pressures on the gas bubbles.

The important shutdown effect for TRIGA is the prompt negative temperature coefficient of the hydride fuel-moderator element, which arises principally from neutron-spectrum effects associated with the bound hydrogen. The prompt burst shapes obtained for reactor periods as low as 3.2 msec are in good agreement with the Fuchs model.

M. E. Remley, in describing recent progress in the KEWB program (transient tests on a cylindrical core for reactor-period values down to 0.9 msec), reported an anomaly in the burst shapes which can be ascribed to the neutron-return effects of the reflector. A plot of burst width (expressed in units of reactor period τ) versus τ reveals a maximum at $\tau = 150$ to 200 msec and a minimum at $\tau = 5$ to 7 msec, where the width is about 2 τ. The width then increases to about $3\frac{1}{2}\,\tau$ at $\tau = 1$ msec; this indicates that some phenomenon at the shorter reactor periods is preventing the very sharp cutoff of the power bursts on the trailing edge. These results have been ascribed to reflector effects, which can be interpreted as equivalent to the introduc-

tion of short-period delayed neutrons into the reactor system. On the basis of inhour calibration results, it is shown that the behavior is consistent with that produced by a seventh group of (pseudo) delayed neutrons with a mean lifetime of 2 msec and a relative abundance of 2.2 per cent.

Experiments with capsules adjacent to the core are under way in order to determine the volume change and associated reactivity compensation as a function of time during a pulse. M. E. Remley expressed the opinion that integral reactor experiments will not give a basic understanding of the inherent shutdown processes but that one must turn to more detailed experiments such as those represented by the capsule approach.

T. F. Wimett described briefly some of the more interesting neutronic characteristics of Godiva-II, which is a fast bare assembly of U^{235} metal built to produce, in a routine fashion, sharp intense bursts ($\sim$100 μsec, $\sim 10^{16}$ neutrons) of near-fission-spectrum neutrons. Effects of neutron reflections from the room walls were observed and identified as resulting in a perturbation of the burst shape and in an increase in the peak power of the burst. The neutron-return effects are again comparable to the effects expected from short-period delayed neutrons. It was found that all the characteristics of neutron reflections could be adequately reproduced if the existence of two effective groups of "delayed" neutrons is postulated (in addition to the six normal delayed-neutron groups). The startup of Godiva with no external neutron source results in a wait time between initiation of the step reactivity insertion and actual occurrence of the burst. Nevertheless, sourceless startup is used because of the sharpness and reproducibility of the bursts obtained. The wait times are due to the time-varying fluctuations in the initiation of persistent fission chains and in the growth of these chains to a significant fission rate. A theory dealing with the problem of statistical distribution of fission chains has been developed by Hansen[2] and extended by Wimett et al.[3] Measurements of wait times have been made in a series of 94 Godiva bursts to obtain a histogram of the fraction of bursts per second versus the wait time; this distribution function is fitted reasonably well with the distribution curve given by the theory. For this series of bursts, the average wait time was 3 sec.

J. F. Boland reviewed the TREAT program and the experimental results obtained to date.[4] The core of the TREAT reactor is essentially a homogeneous mixture of graphite and U^{235} and incorporates a central test hole within which a test fuel element can be placed and melted down during a fast transient. By proper adjustment of the ratio of power density to heat capacity in the test fuel element (relative to that of the reactor core), the meltdown of the test fuel element is accomplished with no damage to the reactor core itself. The shutdown mechanism observed in TREAT transients agrees well with the Fuchs model when the measured negative temperature coefficient of the fuel-moderator mixture is used as the total shutdown coefficient.[5] In transients performed to date (45-msec minimum period), a 3000-Mw peak power and a 900-Mw-sec energy release have been reached.

The TREAT program includes (1) investigation of the mechanism of melting of fast-reactor fuel elements and (2) measurements of metal-water reactions. Meltdown experiments have been performed on single fuel pins, as described in *Nuclear Safety*, Vol. 2, No. 1, September 1960 (of types considered for the EBR-II and the Enrico Fermi reactors) within an inert atmosphere. These experiments give qualitative information on the mechanism by which the melted uranium leaves the pin (or is driven out by the vapor pressure of the bonding sodium) and is deposited on the cooler surfaces outside the pin. This work will be extended to pins within stagnant and flowing sodium coolant and eventually to pin clusters. Provisions have been made for photographing the sequence of events occurring during the meltdown process. Metal-water reaction experiments (see *Power Reactor Technology*, Vol. 4, No. 1, December 1960) have been conducted on about 46 samples, which include uranium pins, both unclad and zirconium-clad; unclad aluminum-UO_2 cermet pins; and UO_2 pins clad with aluminum, stainless steel, and zirconium. For the experiments the sample is placed within an autoclave containing water at high pressure. The amount of metal-water reaction which occurs during the meltdown transient is determined by measurement of the amount of hydrogen gas evolved within the autoclave. In a uranium sample that reached a temperature of 1560°C during the transient, a 3.2 per cent metal-water reaction was measured. In another experiment, complete

melting of the zirconium-clad uranium pin occurred and resulted in amalgamation of the zirconium and uranium. Only an 0.8 per cent aluminum-water reaction was measured in an experiment on an aluminum-clad UO_2 pin; the UO_2 evolved as particles outside the cladding. This work is continuing and will be extended to higher energy inputs.

Several related items were taken up during the discussion period. The investigation of shock-wave effects in extreme short-period excursions is being considered for future work. Some work is under way using scaled-down explosions. Consideration is being given to carrying SPERT tests to destruction. The question was debated as to whether it is conceivable, in a practical sense, to have a tight accident (i.e., one in which the assembly is sufficiently confined to hamper seriously the inherent shutdown mechanisms) so as to get the reactor on a 1- to 2-msec period.

Reactor Transfer Functions

J. A. Thie presented a review paper on the measurement of reactor transfer functions and their application for detecting oscillatory tendencies. A variety of experimental techniques is available for obtaining information on the transfer function. The particular technique used generally depends on the specific objectives of the investigation, on the precision required, and on the relative convenience of performing the experiment for the specific reactor system. Dynamic experiments can be classified according to the form of the excitation introduced into the system (oscillation, step, or a more general time function) and the mechanism by which the excitation is introduced (control rod, dynamic variable such as valve setting, or self-excitation). Step tests are performed quite often with control rods [as, for example, in investigations of the Experimental Boiling Water Reactor (EBWR) and BORAX-IV dynamic characteristics]. In the Pressurized Water Reactor (PWR), a xenon spatial oscillation was excited by a "tilting" of the control-rod bank position. In nuclear-power-plant systems, a step change in a dynamic variable (movement of a valve, change in flow, etc.) is generally most convenient to accomplish. In the ZPR-3 fast critical reactor, random movement of a control rod was used; the transient variations obtained lend themselves to transfer-function analysis. Trapezoidal reactivity oscillations introduced by the movement of ganged control rods have been impressed on a large D_2O natural-uranium reactor at Savannah River; the information obtained is restricted in applicability to the low frequency range. It was convenient in an experiment on the EBWR to vary the output of the feed-water condensate-return pump in a trapezoidal manner to obtain transient data which can be analyzed for the transfer function. Reactors operated at power levels just below instability display intermittent power oscillation, the characteristics of which can give information on the transfer function. Statistical analysis of power-reactor noise has been demonstrated to yield reliable information on the dynamics of the reactor.

A. Wasserman presented a status report on the SPERT-I pile oscillator program. The immediate program objectives are (1) to determine l/β (ratio of prompt-neutron lifetime to delayed-neutron fraction) for comparison with other methods of measurement, (2) to determine the effect of reactivity amplitude on the measured transfer function, and (3) to determine to what extent the transfer function can be used to predict reactor transient behavior. For the oscillator assembly used, the reactivity wave shape, as fitted by the least-squares method, contained a second harmonic content of less than 2 per cent and a third harmonic content of less than 3 per cent.

Peak-to-peak reactivity amplitudes of from 7 to 33 cents have been used at the low reactor power levels (50 to 1000 watts) with the bulk water temperature in the 10 to 50°C range; at the high power levels (50 to 600 kw), reactivity amplitudes of from 7 to 13 cents have been used with the water temperature in the 50 to 100°C range. Near the conditions resulting in bulk boiling, the boiling noise in the raw data records made their interpretation impossible.

The measurements of l/β made for the Bulk Shielding Reactor No. 2 (BSR-II) reactor using the pulsed-neutron technique were described by E. Silver. Two separate pulsed-neutron sources were used: (1) a 300-kev accelerator and (2) the BSR-I reactor incorporating a chopper in the collimating tube between the source and the experiment reactor. A value of 3.2 ± 0.2 msec was measured for l/β of the BSR-II reactor; this compares with 2.9 msec obtained by A. H. Spano from transient data.

P. Kasten described the fuel instability difficulties encountered in operation of the Homogeneous Reactor Experiment (HRE). Under "normal conditions," power fluctuations of about 1 to 2 per cent in magnitude are obtained; with "fuel-plating-out conditions," the fluctuations increase to 3 per cent or greater. The results of a statistical noise analysis show that the shape of the autocorrelation function varies, depending on the fuel loss from the solution as determined by chemical analysis. The change in fuel content results from plating out of the fuel onto the surfaces of the circulating system and from redissolution of the fuel. Since this is a relatively slow situation and since the degree of oscillatory tendency is related to the fuel loss, a continuous display of the shape of the transfer function on a "transfer-function meter" was mentioned as a possibility to give an indication of approaching instability.

E. Beckjord briefly outlined several experiments conducted on the Dresden reactor to obtain an indication of the stability of the spatial power distribution. In the low frequency range (1 cycle/min to ~0.27 cycle/sec), a rod oscillator giving a trapezoidal input was used. At higher frequencies, reliance was placed on statistical analysis of the reactor noise. Output responses from the ion chambers located throughout the core were compared. Within the frequency range studied, there was no apparent phase shift across the core; this indicates that the core behaves radially as a single unit. A measurement was also made with very little boiling in the core and consisted simply of a change in rod position. The change was detected by all the ion chambers throughout the core, and all indicated the same percentage change. Axially, a small phase shift was detected, and it was due (presumably) to coolant flow time.

Thermal and Hydraulic Effects

N. Zuber reviewed the status of knowledge on nucleate boiling and two-phase flow and their relation to two-phase flow instability phenomena. Considerable progress is being made in this field, and, in particular, the important advances reported in the foreign literature were noted. To obtain a quantitative understanding of nucleate boiling, account must be taken of the mechanisms of bubble nucleation, growth rate, and detachment from the heated surface with consequent vapor removal from the system. Zuber indicated that, with the present theoretical and experimental knowledge, an understanding of these mechanisms of bubble dynamics is well in hand for steady-state boiling systems. The effects of system pressure on bubble dynamics are of special interest in boiling-water reactors. In accord with experiments, theoretical considerations show that, as system pressure is increased, it is much easier to nucleate a bubble, thus increasing the number of nucleating centers. Also, bubble growth is much slower, and hence the boiling process is "smoother." The net effect of increase in system pressure is an increase in nucleate-boiling heat flux. The size and distribution of the microroughness of the heated surface have an unpredictable effect on the nucleate-boiling characteristics. The number of nucleation centers is related, in a sensitive manner, to the degree of liquid superheat attained within the thin film adjacent to the heated surface; in turn, the surface characteristics determine the degree of superheat actually obtained.

It has been observed in the laboratory experiments that the phenomenon of chugging is generally associated with surfaces whose characteristics provide for poor bubble nucleation. Chugging occurs in the transition from the stable bubble-flow regime to the unstable slug-flow regime. As the system pressure is increased, there is an increased tendency for the stable bubble-flow regime to predominate.

Zuber discussed results of Russian work on the determination of the slip-velocity ratio (steam velocity divided by liquid velocity). The slip-velocity ratio is the basic quantity directly determining the heat-removal performance of boiling channels. The Russian work enables prediction of the slip-velocity ratio in stable two-phase flow systems.

The transient boiling experiments being conducted in an electrically heated heat-transfer rig at the University of California were described by V. Schrock. The primary purpose of this work is to measure the time elapsed for inception of boiling and the rate of steam-vapor volume generation from the surface of a heated ribbon following an exponential input of power to the ribbon. The work has been limited to atmospheric-pressure runs in which the aim was principally to develop the temperature-measuring instrumentation and the necessary photographic and X-ray absorption techniques

for measurements of the void volumes. Three simultaneous views of the heated ribbon were photographed with a high-speed movie camera. The system is now ready for operation at pressures of interest in water reactors, for both stagnant- and flowing-water conditions.

In the atmospheric-pressure runs, which were conducted on a horizontal ribbon in stagnant water, power pulses with periods ranging from 5 to 100 msec have been used with the water temperature at 100, 170, and 200°F. Bubble size, growth rate, and site density are photographically observed. From the information obtained, it is possible to plot ribbon temperature and steam volume as functions of time after initiation of the power pulse. Superheats (in the thin liquid film adjacent to the ribbon surface) are developed far in excess of the values attained in steady-state boiling; the degree of superheat increases with decreasing period of the power pulse. For large subcooling an initial burst of bubbles appears at the heated surface; however, these bubbles quickly collapse and are followed almost immediately by a fine distribution of small bubbles. Extremely good accuracy in the measurements is required at the inception of boiling because of the very rapid growth of the steam volumes.

E. Beckjord discussed the problem of hydrodynamic instability, particularly with respect to experimental observations of the flow pulsations observed in an electrically heated natural-circulation boiling loop. The system pressure was 1000 psi, and the observations were limited to steam exit qualities of less than 10 per cent. The amplitudes of the flow pulsations observed ranged from zero to twice the steady-state flow that existed prior to the inception of instability. It was observed that the period of the instability was related to the mean transit time of the coolant in the thermal-convection loop. The pulsations occurred over a wide range of conditions, e.g., conditions of coolant subcooling and steam exit quality. A typical behavior pattern would proceed as follows: (1) in a single sequence, oscillations would start, grow rapidly to some level, and then stop; (2) this sequence would repeat a number of times; and (3) finally a sequence would develop in which the oscillations would result in burnout. Attempts to describe the kinematics of the flow pulsations have led to the development of a transient model which is based on steady-state relations among the pertinent variables. The starting point in development of the model is to set the integral of the total pressure change (including inertia, friction, and static driving-head terms) around the loop equal to zero. The measured steady-state dependence of pressure drop through the flow channel on void fraction was used. The transient model predicts the stability limits of the loop and indicates the several methods of stabilization (as, for example, by increasing flow restriction or by increasing flow inertia in the downcomer).

D. Langmuir reported results obtained in measurements of the power-void transfer function for the steam voids produced in an electrically heated water channel simulating a SPERT-IA core channel. The work included investigation of both the static and dynamic steam-void behavior within the channel for natural-circulation water flow at atmospheric-pressure conditions (as in the SPERT-IA tests). The interpretation of the measurements to yield a lumped-parameter power-void transfer function for the SPERT-IA reactor required spatial averaging of the single-channel results over the multiplicity of channels in the reactor. The resultant power-void transfer function was coupled with the neutron kinetic equations, in the form of the zero-power transfer function; this required a determination of the effective mean void coefficient, thereby involving assumptions on the void distribution and void importance function over the core volume. The results obtained enable a prediction to be made for boiling oscillations in SPERT-IA; a resonance peak is revealed at a frequency of 1 cycle/sec, near the frequency at which divergent oscillations occurred in SPERT-IA under boiling conditions.

Hydrodynamic instability, wherein flow and void oscillations spontaneously occur at constant power input without the necessity of neutronic feedback, was observed in the simulated SPERT-IA channels. (Several channels, differing only in methods of assembly, were used in the experiments.) On the basis of the observed threshold power at which hydrodynamic instability began and on the basis of resultant frequency of oscillation, it appears that hydrodynamic instability is not involved in the oscillatory behavior of the SPERT-IA reactor.

A difficulty in interpretation of the experiments is due to the apparently important effect of surface condition of the boiling passage. Although every channel tried would oscillate at some power level, the channels differed widely

in their oscillating characteristics. It appears that the degree of hydrodynamic instability inherent in the system at a given power level depends on the steam-bubble nucleating properties of the surfaces of the channel. This structure-sensitive property is not understood: sandblasting of the surfaces of a channel to provide for possible increased nucleation centers had no effect on the hydrodynamic stability characteristics. The spatial distribution of voids within the channel (including the lateral variation across the channel) appears to be an important factor.

Measurements of frequency of natural oscillation within a single channel, in which the driving head, degree of subcooling, and power level were varied, revealed that the natural oscillation frequency was inversely proportional to the nonboiling length in the channel. This empirical relation showed surprising accuracy.

Measurements of the static distribution of voids along the boiling channel revealed some interesting simple relations for which no satisfactory quantitative explanation has been developed. The experimental curves of void fraction as a function of distance along the boiling channel are remarkably similar for the various power levels when the distance is measured relative to the position in the channel at which boiling begins.[6] The major effect of change in power level appears to be to shift the height in the channel at which boiling begins. It was found that the power-void transfer function can be calculated with very encouraging accuracy. In this calculation the void-fraction response is taken simply as a shifting of the void-fraction curve vertically up and down the channel as the point of initiation of boiling oscillates in response to the modulated power input. The implication is that the statically determined characteristics (which correspond to zero frequency) appear to hold reasonably well at the higher frequencies, at least up to the resonant frequency region.

Analytical Methods

A. F. Henry traced the development of the analytical methods used in problems of reactor kinetics. The statistical approach was first explored in the early work; with the recent emphasis on autocorrelation functions and on the problem of sourceless reactor startup, interest in the use of the statistical approach has been renewed.

When the average behavior of the statistical ensemble is considered, the result is the time-dependent transport equation which leads to the more tractable, conventional kinetic equations. Wigner[7] first introduced the use of the adjoint flux in the application of perturbation techniques to reactor physics. From the two-group adjoint equations, Nordheim derived the appropriate inhour formula, defining the reactivity and the effective neutron lifetime for a complex system. Physical interpretations of the adjoint flux have been advanced by a number of authors. Hurwitz[8] introduced the concept of iterated fission probability for a critical reactor. Ussachoff[9] derived the adjoint Boltzmann equation for the source-free time-independent case. Selengut[10] defined the adjoint for a steady-state subcritical system. Lewins[11,12] has extended this to the case of the time-dependent adjoint equations.

Analytical solutions of the space-independent kinetic equations have been given by many authors. Wallach[13] considered the case of linear ramp reactivity additions and obtained solutions in terms of a contour integral which can be numerically evaluated under certain conditions which are of interest. Wilkins[14] and Garabedian have extended this work, and Smets[15] has presented a general study of the problem. Hurwitz[16] obtained approximate solutions for several cases which represent the different phases associated with a reactor startup accident.

The question of nonlinear stability has been investigated by several authors.[17,18] The stability criteria established in these analyses are still approximate; actually the established criteria represent only sufficiency conditions for stability. It is doubtful that the criteria are applicable to the xenon spatial oscillation problem or to the boiling-water-reactor stability problems wherein the flux shape changes appreciably.

The problems of space-dependent reactor kinetics may be attacked either by the use of modal expansion techniques or by means of a nodal treatment or by a combination of both. Both methods have been applied to the problem of xenon spatial oscillations. In the modal expansion technique, the transient neutron-flux and precursor distributions in the space-time domain are represented in terms of a series of eigenfunctions of the group diffusion operator. The eigenfunctions are space-dependent functions with time-dependent coefficients. Each function is associated with a given spatial mode,

starting with the fundamental and going on to the progressively higher overtone modes. The problem then reduces to an investigation of the time behavior of each mode, as determined by the time-varying coefficients of the individual eigenfunctions. The completeness of the set of eigenfunctions used has not been established in most cases.

In the nodal treatment the reactor is divided into sections, and each section is first treated separately; the sections are then coupled together. Avery's treatment of the half-fast reactor[19] is an illustration of this type of approach.

The use of a digital computer for point-by-point calculations of transient response by the finite-difference method is handicapped by arithmetical difficulties. These difficulties arise from the fact that the time differencing must be small enough to account for prompt-neutron regeneration (lifetime $\sim 10^{-4}$ sec), but the complete problem may involve a time that is large relative to the time constants of the delayed neutrons (~10 to 50 sec). Long computer running times are inevitably involved.

Description of the transient behavior of the over-all nuclear power plant, which must include the feedback processes inherent in the entire system, is an important objective. Numerous attempts on this problem, which involve digital and analogue computers, are under way. Nonlinearities are handled in a natural way by the analogue machines. The present judgment is that an over-all plant description is possible and practical. Work is under way on the individual parts of the problem; the immediate goal is to establish the practical representations of the various dynamic processes involved.

Another important problem is the prediction of the kinetic behavior of simpler reactor systems throughout the reactor lifetime.

W. Stratton recently completed a study of the prompt-critical accidents (about 18 of them) which have occurred in this country;[20] he reported his findings on a few typical ones. The purpose of the study was to ascertain the cause of the accident and its termination and to estimate the power history and energy release during the excursion.

The May 1954 accident at Oak Ridge occurred with a uranium-solution critical assembly when a central cadmium-plated cylinder became detached at its upper connection. The reactor was just about critical when the detached rod fell to one side. The total fission yield was 10^{17}, with 5×10^{16} fissions contained in the initial spike. The scram system started drainage of the solution and terminated the chain reaction with little or no damage to the system.

The June 1958 accident at the Y-12 chemical-processing plant occurred when uranyl nitrate solution was drained from a safe geometry into a 50-gal drum in sufficient quantity to attain a critical system. The total fission yield was estimated at 1.3×10^{18}, the system possibly starting above prompt critical. The initial spike was of unknown magnitude; the startup was sourceless and from zero power. The accident was "seen" by a boron chamber 1400 ft away. After the initial spike, oscillations of much smaller amplitude occurred, probably due to steam bubbles leaving the system. The solution boiled nearly 20 min.

The August 1945 accident occurred as tungsten carbide bricks were being stacked around a plutonium-metal core. Just before the final brick was added, criticality was noticed but the final brick was accidentally dropped onto the stacking. The result was essentially a step addition of reactivity in excess of prompt critical, and the excursion was terminated by disassembly. The total yield was 10^{16} fissions with 2×10^{15} fissions in the initial spike.

The final Godiva accident occurred during an irradiation experiment on a graphite-polyethylene stacking when the stacking slumped near Godiva. The system was then 21 cents above prompt critical, and the resulting excursion, in which Godiva was badly damaged, gave a yield of 1.2×10^{17} fissions. The inertial effect was important in this accident. The estimated maximum center temperature during the excursion was about 1050°C (melting temperature of uranium is 1133°C).

An accident with the Los Alamos Scientific Laboratory (LASL) aquarium machine occurred during an experiment to measure the critical (horizontal) separation distance of two large masses of enriched uranium in water. During the scram (accomplished by vertical movement of one of the masses), an excursion was observed which resulted in a vapor cloud over the water. Two factors were responsible for the excursion during the scram: (1) the center of reactivity of one mass was normally below that of the other so that vertical displacement of the one mass increased reactivity momentarily, and (2) the Bernoulli effect resulted in shifting

of the one mass closer to the other during the vertical movement.

References

1. Argonne National Laboratory, Proceedings of the Conference on Transfer Function Measurement and Reactor Stability Analysis, USAEC Report ANL-6205, May 1960.
2. G. E. Hansen, Assembly of Fissionable Material in the Presence of a Weak Neutron Source, *Nuclear Sci. and Eng.*, 8(6): 709–719 (December 1960).
3. T. F. Wimett et al., Godiva II — An Unmoderated Pulse-Irradiation Reactor, *Nuclear Sci. and Eng.*, 8(6): 691–708 (December 1960).
4. F. Kirn et al., Reactor Physics Measurements in TREAT, USAEC Report ANL-6173, Argonne National Laboratory, October 1960.
5. D. Okrent et al., The Reactor Kinetics of the Transient Reactor Test Facility (TREAT), USAEC Report ANL-6174, Argonne National Laboratory, September 1960.
6. Ramo-Wooldridge Div., Thompson Ramo Wooldridge, Inc., Kinetic Studies of Heterogeneous Water Reactors, Annual Summary Report, 1959, USAEC Report RWD-RL-167, Feb. 29, 1960.
7. E. P. Wigner, Effects of Small Perturbations on Pile Period, USAEC Report CP-G-3048, 1945.
8. H. Hurwitz, Jr., A Note on the Theory of Danger Coefficients, USAEC Report KAPL-98, Knolls Atomic Power Laboratory, Sept. 18, 1948.
9. L. N. Ussachoff, Equation for the Importance of Neutrons, Reactor Kinetics and the Theory of Perturbations, *Proceedings of the International Conference on the Peaceful Uses of Atomic Energy, Geneva, 1955*, Vol. 5, p. 503, United Nations, New York, 1955.
10. D. S. Selengut, Variational Analysis of Multidimensional Systems, in USAEC Report HW-59126, p. 89, Hanford Atomic Products Operation, Jan. 20, 1959.
11. J. Lewins, The Time-Dependent Importance of Neutrons and Precursors, *Nuclear Sci. and Eng.*, 7(3): 268–274 (March 1960).
12. J. Lewins, Variational Representations in Reactor Physics Derived from a Physical Principle, *Nuclear Sci. and Eng.*, 8(2): 95–104 (August 1960).
13. S. Wallach, Solutions of the Pile Kinetic Equations When the Reactivity Is a Linear Function of the Time, USAEC Report WAPD-13, Westinghouse Electric Corp., Bettis Atomic Power Laboratory, Nov. 3, 1950.
14. J. E. Wilkins, Jr., The Behavior of a Reactor at Prompt Critical When the Reactivity Is a Linear Function of Time, *Nuclear Sci. and Eng.*, 5(4): 207–214 (April 1959).
15. H. B. Smets, Reactor Dynamics at Low Power, *Proceedings of the Second United Nations International Conference on the Peaceful Uses of Atomic Energy, Geneva, 1958*, Vol. 11, p. 237, United Nations, New York, 1958.
16. H. Hurwitz, Jr., Approximate Analysis of Reactor Startup Incidents, *Nuclear Sci. and Eng.*, 6(1): 11–17 (July 1959).
17. W. K. Ergen and A. M. Weinberg, Some Aspects of Nonlinear Reactor Dynamics, *Physics*, 20: 413 (1954).
18. T. A. Welton, A Stability Criterion for Reactor Systems, USAEC Report ORNL-1894, Oak Ridge National Laboratory, July 7, 1955.
19. R. Avery, Theory of Coupled Reactors, *Proceedings of the Second United Nations International Conference on the Peaceful Uses of Atomic Energy, Geneva, 1958*, Vol. 12, p. 182, United Nations, New York, 1958.
20. W. R. Stratton, A Review of Criticality Accidents, in *Progress in Nuclear Energy, Series IV: Technology, Engineering, and Safety*, Vol. 3, Pergamon Press, New York, 1960.

Section VI

CONTAINMENT

Condensation in a Containment Vessel

One type of accident commonly postulated in hazard studies on pressurized-water systems is the release of coolant into the containment vessel through a major leak or rupture in the primary system. In designing the containment structure, an estimate of the pressure buildup within the structure due to such a leak should be made, and the greatest uncertainty in the estimate usually is the effect of heat loss to the walls of the containment structure and to other surfaces. Experiments relating to this question are reported in reference 1. The experiments were made in a setup which simulated, on a reduced scale, the rapid leakage of steam into a reactor containment vessel. The objective of the experiments was to derive a correlation of the heat transfer from the steam to the containment-vessel walls during the forced-convection regime when the steam is being injected into the vessel and during the free-convection regime after injection of the steam has stopped. The test vessel, simulating a containment vessel, was a horizontal Lancashire boiler, 8 ft 3 in. in diameter by 30 ft long, with two flues 3 ft in diameter, blanked off at both ends. The vessel was unlagged but was partially insulated by an external brickwork foundation. Instrumentation was provided for measuring steam flow and for measuring the pressure within the vessel. Temperatures were measured by thermocouples at several points on the outside surface of the vessel and on the inside surfaces (i.e., those not exposed to steam) of the flues. The temperatures of the walls in contact with the steam-air mixture were derived from these by calculation. Nine tests were made, using three different orifice plates in the steam supply line to the vessel. The air pressure in the vessel prior to admission of the steam was adjustable, from zero to 40 psig, and tests were run at three different air pressures: 0, 20, and 40 psig. It was expected that the change in air pressure would simulate the effect of changing the hydraulic diameter of the vessel. The injected steam was supplied at a pressure of about 120 psig and was assumed to be 3 per cent wet.

Table VI-1 VARIABLES IN TESTS ON HEAT-TRANSFER CONDITIONS SIMULATING STEAM LEAKAGE INTO A REACTOR CONTAINMENT VESSEL[1]

Steam mass flow, lb/(sq ft)(sec)	40–160
Total pressure, atm	1–8.5
ΔT, °F*	35–102
Re	$(13–68) \times 10^6$
Steam-air ratio	0–3.1

*ΔT = temperature difference between steam-air mixture and estimated temperature of inner wall of boiler shell.

The variables studied are listed in Table VI-1, which is adapted from reference 1. The experimental procedure was to adjust the air pressure in the vessel to the desired value and then to admit steam to the vessel for 10 min at a steady rate determined by the orifice. Temperatures and pressures were measured during the steam admission and for 50 min following shutoff of the steam flow.

During the steam admission (the forced-convection period), the heat loss to the vessel walls was correlated by the following relation connecting Stanton number, Prandtl number, Reynolds number, and pressure:

$$\mathrm{St}\ \mathrm{Pr}^{0.5} = 0.0576/(\mathrm{Re}\ P)^{0.25} \qquad (1)$$

The probable error of the equation, derived from all experimental points, was +6.9 per cent, −6.3 per cent.

After cessation of the steam injection (the free-convection period), the rate of heat loss could be related only to the density of the steam-air mixture and the temperature difference between the mixture and the inner wall of the vessel

$$H/\rho = 0.0152\ \Delta T^{1.25} \qquad (2)$$

The probable errors of the relation as indicated by the experimental points were +23 per cent, −18 per cent. The symbols used in Eqs. 1 and 2 are defined as follows:

St = Stanton number = h/C_pG
Pr = Prandtl number = $C_p\mu/k$
Re = Reynolds number = $\rho vDm/\mu$
h = heat-transfer coefficient = $H/\Delta T$, Btu/(sec)(sq ft)(°F)
H = heat-transfer rate per unit area, Btu/(sec)(sq ft)
A = total surface area of boiler shell, sq ft
ΔT = temperature difference between steam-air mixture and estimated temperature of inner wall of boiler shell, °F
C_p = specific heat of steam-air mixture, Btu/(lb)(°F)
G = mass velocity of steam jet, lb/(sec)(sq ft)
μ = viscosity of steam-air mixture, lb/(sec)(ft)
k = thermal conductivity of steam-air mixture, Btu/(sec)(ft)(°F)
ρ = density of steam-air mixture, lb/cu ft
v = velocity of steam jet, ft/sec
Dm = hydraulic mean diameter of boiler shell = $4V/A$, ft
V = volume of steam-air space of boiler shell, cu ft
P = absolute pressure of steam-air mixture, atm

The reference states that Eq. 1 is applicable to heat loss to the vessel for values of (Re P) greater than $(40-50) \times 10^6$. It recommends that for values below this level the derived heat-transfer coefficient be compared with the heat-transfer coefficient corresponding to Eq. 2. The reference also states that there was no indication that the distance traveled by the steam jet before striking a cooler surface has any great influence on the heat-transfer coefficient. Tests were made at distances of 2.1 and 5.0 hydraulic diameters of the vessel (42 and 99 jet diameters). These distances were considered reasonably representative of the conditions that would apply for a broken steam main in a reactor containment vessel. It seems evident, however, that Eq. 1, in which the correlation involves the velocity of the steam jet, would begin to fail as the ratio of vessel diameter to dimensions of the steam jet becomes very large.

Pressure Suppression

One method of reducing the pressure due to the rupture of a pressurized-water system inside the containment vessel is to enclose the primary system in a more or less leaktight compartment which communicates with the surrounding containment vessel only through pipes having their discharge ends submerged in a pool of cold water. The purpose of this arrangement is to discharge any steam that may escape from the primary system into the cold water, where it will condense without producing a large pressure rise in the containment vessel. The possible application of this system in the containment design for the Humboldt Bay reactor, and tests of the concept by Sargent & Lundy, were reviewed in the June 1960 issue of *Power Reactor*

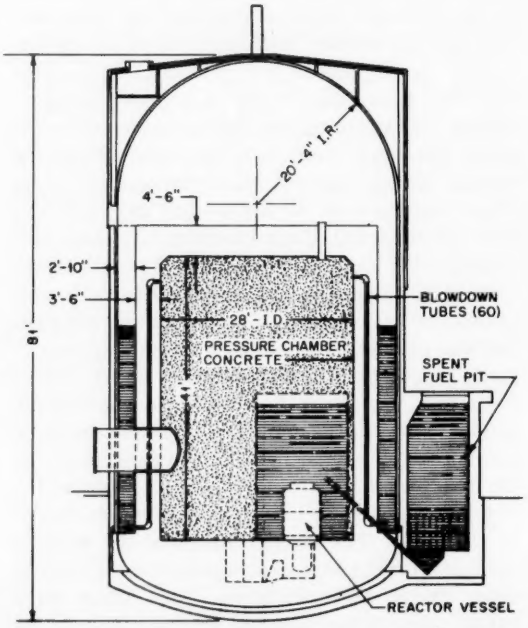

Fig. VI-1 SM-1A vapor-container energy-absorption scheme.[2]

Technology, Vol. 3, No. 3, pages 12 to 14. It has recently been called to our attention that the concept was conceived and put into use some time ago in the Stationary Medium Power Plant No. 1A (SM-1A) reactor, on which design was begun in the summer of 1956 and which is expected to go into operation in the early spring of 1961. Kenneth Kasschau, of Alco Products, Inc., designers of the reactor, has provided the diagram of the system, which is shown in Fig. VI-1. He states that analyses of the Sargent & Lundy data at Alco corroborate the initial SM-1A design. The inner containment structure, of reinforced concrete, is designed for a maximum pressure of 120 psig. The outer steel vessel is designed for 15 psig. In the event of a steam discharge into the inner structure, the pressure would be relieved through 60 vent tubes, 3 in. in diameter, which discharge into the annular, water-filled moat between the inner and outer structures.[2]

References

1. D. H. Jubb, Condensation in a Reactor Containment Vessel, *Nuclear Eng.*, 4(43): 431 – 434 (December 1959).
2. J. G. Gallagher, ed., Hazards Summary Report for SM-1A, Report APAE-13 (Suppl. 2, Rev. 1), Alco Products, Inc., October 1960.

Section VII

SHIELDING

Thermal-Neutron-Capture Gamma Spectra

The thermal-neutron-capture gamma rays born in the reactor core and in the surrounding shield are a very important, frequently controlling, part of the total gamma dose rate penetrating the biological shield of a power reactor. For this reason the capture cross sections and resulting gamma spectra are very important to the shield designer. Two compilations (one published in 1955 and the other in 1958) of the capture gamma data compiled specifically for the reactor shield designer gave the spectra in tabular form.[1,2]

A later compilation[3] (published in 1959) of capture gamma spectra contained 19 more elements and more complete spectra for many of the elements found in reference 2. This compilation contained all spectra found in the literature as of Jan. 1, 1958, as well as many investigated by the authors. Prior to this work most of the spectra had been measured with a pair spectrometer, limiting the energy measurements to the range of about 3 to 12 Mev. The Russian investigators[3] used a magnetic Compton spectrometer, thus extending the measurements to lower energies. Although the lower energy range is usually not important in determining the biological shielding required, it is important in the shield heating calculations. The information is presented in the form of curves, which are not as convenient for the shield designer as the tabular form of the earlier compilations, but this is a minor point.

Further work on tin and antimony is reported in reference 4, along with an explanation of how some of the experimental work was done in obtaining the spectra reported in reference 3.

Shielding Properties at Elevated Temperatures

In the design of concrete shields, it may often be advantageous to allow the shield to operate at some elevated temperature within the range compatible with preservation of the structural properties of the concrete. It is therefore useful to know the effects of such operation on the shielding properties of concretes.

Measurements of the effect of operating temperature on the attenuation properties of ferrophosphorus concrete have recently been reported. The measurements were made as part of a series of measurements at Hanford on high-density concretes.[5] Earlier experiments (reviewed in the September 1959 issue of *Power Reactor Technology*, Vol. 2, No. 4, pages 46 and 47) covered iron limonite, magnetite limonite, and magnetite concretes.[6,7]

The neutron-attenuation properties of unheated slabs of ferrophosphorus concrete were first measured in the 105-DR reactor bulk shield facility. The same slabs were then placed in an oven and held at the desired temperature for a minimum of three weeks. Air was allowed to circulate between the test slabs to remove evolved gases. The combined thickness of all the slabs was approximately 48 in. After the slabs were removed from the oven, they were reweighed to determine the weight loss, which, for the purpose of attenuation analysis, was attributed entirely to the loss of water. The slabs were then placed in the 105-DR reactor bulk shield facility where the neutron-flux attenuation was measured by gold foils and cadmium-covered gold and sulfur foils. The gamma dose rates were measured with a 10-cm^3 ionization chamber. The measurements were made at the interfaces of the slabs. A

further measurement, to determine the average energy of the leakage neutron flux, was made using a Lucite integrator.

The measured and calculated macroscopic fast-neutron removal cross sections are shown in Table VII-1. The difference between the two

Table VII-1 FAST-NEUTRON REMOVAL CROSS SECTIONS IN HEATED FERROPHOSPHORUS CONCRETE[5]

Temp., °C	Density, g/cm^3	$R_{measured}$, cm^{-1}	$R_{calculated}$, cm^{-1}
As-cured	4.83	0.131	0.128
As-cured	4.78	0.128	0.123
100	4.73	0.121	0.118
200	4.69	0.117	0.114
320	4.68	0.114	0.113

"as-cured" values is that one was measured as the tests were started and the other was measured at the end of the test. The loss of water initially can probably be explained by the increase in temperature of the slabs during the test, although this is not stated in the report. In the experiments on the other high-density concretes in the same facility, the concrete slabs attained a maximum temperature[6] of 91°C.

The comparison of leakage radiation through as-cured concrete and through concrete held at 320°C best describes the effect of the loss of water. This comparison is shown in terms of ratios of the leakage radiation through 48 in. of concrete in Table VII-2. Also shown for com-

Table VII-2 RELATIVE INCREASE IN RADIATION LEAKAGE THROUGH 48 IN. OF HIGH-DENSITY CONCRETE AFTER BEING HEATED[5] AT 320°C

(Ratio of Intensity After Heating to Intensity Before Heating)

Type of radiation	Ferro-phosphorus	Limonite	Magnetite limonite
Fast neutrons	8.4	45	12
Resonance neutrons	1960	1800	440
Thermal neutrons	480	580	240
Gamma	44	20	3

parison are the ratios for two other high-density concretes measured previously in the same facility.[6] In high-density concrete the attenuation of fast neutrons is to a large degree due to inelastic scattering, which reduces the neutron energy to approximately 1 Mev. The hydrogen is the important moderating agent from 1 Mev to thermal energy. With the loss of hydrogen, the intermediate-energy neutrons diffuse nearer the outside shield surface before being captured, thus increasing the capture gamma dose rate. This effect can be seen in Table VII-2. The average energy of the neutrons from the concrete slabs at all temperatures, as measured by the Lucite integrator, was less than 24 kev.

Gamma and Neutron Penetrations Through Iron Slabs

Monte Carlo calculations of the gamma and neutron penetration of iron slabs, for five incident energies and five incident angles, are reported in references 8 and 9. The gamma penetrations have been done for six thicknesses of iron, ranging from 1 to 6.9 in. The neutron penetrations have been calculated for five thicknesses of iron, ranging from 1 to 5 in.

The gamma results include the transmitted scattered dose and energy flux for 120 equal solid angles. The scattered energy flux is further broken down into energy groups. To facilitate further shield penetration calculations for regions beyond the iron slabs, the average gamma-ray energy is given for each of the solid angles. The unscattered number current and flux, as well as the energy current and flux, are also given.

The neutron results include the scattered dose transmission factors and the dose reflection factors for 120 equal solid angles, as well as the average energy of the transmitted and reflected neutrons for each solid angle. The unscattered current, flux, and dose rate are also given. For a later calculation of the gamma dose rate due to inelastic scattering of neutrons, the distribution of the gamma rays through the slab has been determined. The maximum neutron energy considered in these calculations was 4 Mev. The program, with appropriate modifications to account for higher energy inelastic scattering and for (n,p) and $(n,2n)$ reactions, can be extended to higher energies.

In using the individual solid-angle scattered transmission factors for either gammas or neutrons, care should be taken to reduce the error in the individual solid angles. This can usually be done by plotting the information of interest, dose rate or flux, as a function of the cosine of the emergent polar angle, and then drawing a smooth curve through the points.

Thermal-Neutron Attenuation Through Boral

Boral is commonly used as a thermal-neutron shield, but its effective attenuation is uncertain. This is because it is a nonuniform mixture of chunks of B_4C in B_4C-Al melt. If the boron is assumed to be uniformly distributed, the attenuation is calculated to be several factors better than that found experimentally. For a $\frac{1}{8}$-in.-thick boral shield, the transmission of thermal neutrons measured experimentally was a factor of 40 higher than the calculated transmission. Some typical experimental transmission values for $\frac{1}{8}$-in. thicknesses of boral for different incident angular distributions and for different boral samples are shown in Table VII-3. The measurements were made with a $1/v$ detector.

Table VII-3 TRANSMISSION OF THERMAL NEUTRONS THROUGH BORAL[10]

Angular distribution	Sample	Transmission factors
$1 + \sqrt{3} \cos \phi$	Brooks and Perkins	0.070
$1 + \sqrt{3} \cos \phi$	ORNL	0.094
Normal	Alcoa	0.065
Normal	Alcoa	0.070

The difference between the value calculated on the homogeneous assumption and the experimental value is due to channeling between the chunks of boron in the aluminum matrix. In reference 10 a method is derived for computing the transmission of radiation through a heterogeneous material, and the method is used to make a comparison with the experimentally measured transmission factors in boral. The agreement is within the uncertainty in the input parameters required by the theory on such things as size of chunks, angular distribution of incident neutrons, etc. The theory is intended for use on any heterogeneous material in which the channeling effect is important.

Effective Neutron Removal Cross Section of Zirconium

The measurement of the neutron removal cross section of zirconium is of particular interest in that it helps fill the gap between atomic numbers 29 and 74, the upper and lower limits of the elements previously measured.[11] The removal cross sections between $Z = 29$ and $Z = 74$ were previously obtained by interpolation, and although this seemed to be a good assumption, the addition of $Z = 40$ adds confidence. The resulting microscopic removal cross section is 2.36 ± 0.12 barns. This results in a mass attenuation coefficient, Σ_R/ρ, of $1.56 \pm 0.08 \times 10^{-2}$ cm^2/g. The mass attenuation coefficient was found to fit on the published curve of the removal cross section as a function of the atomic weight.[12]

References

1. P. S. Mittelman and R. A. Liedtke, Gamma Rays from Thermal-Neutron Capture, *Nucleonics*, 13 (5): 50 (May 1955).
2. F. E. Deloume, Gamma Ray Energy Spectra from Thermal Neutron Capture, USAEC Report APEX-407, General Electric Co., Aircraft Nuclear Propulsion Dept., August 1958.
3. L. V. Groshev et al., *Atlas of γ-Ray Spectra from Radiative Capture of Thermal Neutrons*, Pergamon Press, New York, London, Paris, and Los Angeles, 1959.
4. L. V. Groshev et al., Thermal Neutron Capture γ-Rays, *J. Nuclear Energy: Pt. A, Reactor Sci.*, 12(1/2): (May 1960).
5. E. G. Peterson, Shielding Properties of Ferrophosphorus Concrete as a Function of Temperature, USAEC Report HW-64774, Hanford Atomic Products Operation, July 15, 1960.
6. W. L. Bunch, Attenuation Properties of High Density Portland Cement Concretes as a Function of Temperature, USAEC Report HW-54656, Hanford Atomic Products Operation, Jan. 22, 1958.
7. D. E. Wood, The Effect of Temperature on the Neutron Attenuation of Magnetite Concrete, USAEC Report HW-58497, Hanford Atomic Products Operation, Dec. 11, 1958.
8. M. O. Burrell and D. L. Cribbs, A Monte Carlo Calculation of Gamma Ray Penetrations Through Iron Slabs, Report NR-82 (Vol. II), Lockheed Aircraft Corp., Georgia Div., January 1960.
9. M. O. Burrell and D. L. Cribbs, A Monte Carlo Calculation of Neutron Penetrations Through Iron Slabs, Report NR-82(Vol. III), Lockheed Aircraft Corp., Georgia Div., May 1960.
10. W. R. Burrus, Radiation Transmission Through Boral and Similar Heterogeneous Materials Consisting of Randomly Distributed Absorbing Chunks, USAEC Report ORNL-2528, Oak Ridge National Laboratory, Jan. 18, 1960.
11. J. M. Miller, Effective Neutron Removal Cross

Section of Zirconium, in Papers from Seventh Semiannual Shielding Information Meeting, October 14–15, 1959, USAEC Report TID-6302.

12. E. P. Blizard, The Shielding of Nuclear Reactors, *Proceedings of the Second United Nations International Conference on the Peaceful Uses of Atomic Energy, Geneva, 1958*, Vol. 13, pp. 3–20, United Nations, New York, 1958.

Section VIII

FUELS: THERMAL CONDUCTIVITY OF UO_2

Although the practical usefulness of UO_2 as a fuel material is by now well established, much remains to be learned before the design of UO_2 fuel elements for a given service can be described as a precise technique. It may be that certain characteristics of the material and of the application preclude the possibility of great precision in meeting design goals. Certainly some of these characteristics make the problem of gathering precise and pertinent information very difficult. Among them are the following:

1. The UO_2 normally cracks in service; therefore the experimenter is working with a poorly defined system.
2. Since fuel-element life is the quantity of direct concern, the experimenter must either use very long experimental exposures or must extrapolate his results by a large factor.
3. Optimum UO_2 behavior appears to depend strongly on attaining and maintaining a composition close to the stoichiometric.
4. The measurement of temperature of the oxide during irradiation is difficult because of the properties of the material, the high values of the temperature which are of interest, and the general complications of in-pile measurements.

Two types of processes (other than those, such as external corrosion, which affect only the fuel-element jacket) may be visualized as limiting the fuel-element life: mechanical and thermal effects involving the UO_2 itself, such as swelling and shifting; and the buildup of pressure due to gaseous and volatile fission products. The relative importance of these considerations may vary widely from one design to another according to the design characteristics and to the proposed application, but in most cases the power rating of the element is limited by some consideration of a maximum permissible central temperature, such as the melting temperature, the grain-growth temperature, or some temperature thought to correspond to the tolerable limit of the rate of fission-gas release. Hence the effective thermal conductivity of the oxide is a question of primary importance. A previous discussion of UO_2 conductivity appears in the March 1960 issue of *Power Reactor Technology*, Vol. 3, No. 2, pages 44 to 50.

Since it is impractical to measure internal temperatures for large numbers of experimental fuel elements and since the effective thermal conductivity of UO_2 cannot be considered a constant of the material as it is used in fuel elements, an alternate specification of the thermal duty—the conductivity integral—has been introduced by the Canadian workers. In any thermal conductor heated by a uniform volume source of heat, h, and cooled at its surface, and having a conductivity $k(\theta)$, which is a function of the temperature θ, the integral $\int_{T_s}^{T_0} k(\theta)\, d\theta$ is determined only by the geometry of the sample and by the magnitude of h. The limits of the integral, T_S and T_0, are the surface temperature and the temperature of the hottest point, respectively. Thus, for example, the integral for an infinite cylinder of radius r is

$$\int_{T_s}^{T_0} k(\theta)\, d\theta = \frac{hr^2}{4} \qquad (1)$$

and for an infinite slab of half-thickness a, it is

$$\int_{T_s}^{T_0} k(\theta)\, d\theta = \frac{ha^2}{2} \qquad (2)$$

Thermally then, the irradiation of a slab of a given half-thickness a is equivalent to the irradiation, at the same power density, of a cylinder having a radius $\sqrt{2}a$. If both samples contain the same material and if both surface temperatures

are held the same, then T_0 will be the same for both, regardless of the form of $k(\theta)$.

Evidently, if k is known as a function of temperature, a curve can be constructed for $\int_{T_1}^{T_2} k(\theta)\, d\theta$ as a function of $T_2 - T_1$, and irradiation results that are expressed in terms of the integral can be converted to central fuel temperatures. These temperatures, of course, will be subject to whatever uncertainties there are in the conductivity values and in their applicability to the sample in question. Reference 1 gives a curve of $\int_0^T k(\theta)\, d\theta$ derived from the (unirradiated) conductivity data of Hedge and Fieldhouse.[2] This curve is reproduced here in Fig. VIII-1.

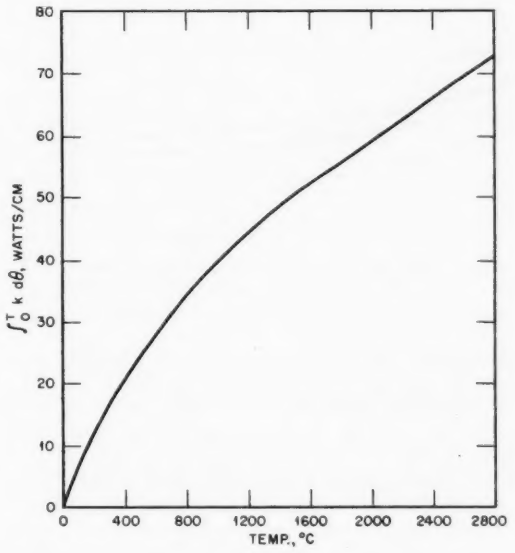

Fig. VIII-1 Conductivity integral for UO_2 as a function of upper temperature limit.[1] Derived from thermal-conductivity data of Hedge and Fieldhouse,[2] corrected to 95 per cent of the UO_2 theoretical density.

Reference 1 also gives derivations of the expressions for the conductivity integral in samples of more complex shape and extends the concept to take into account the variation in power density caused by the neutron-flux depression in the sample.

When it is recalled that the conductivity integral, for a given fuel element, is directly proportional to the power output of the element, the shape of the curve (Fig. VIII-1) gains significance. As the power output of the element is increased, the central temperature increases at an increasing rate. For example, if a UO_2 element is operating at a surface temperature of 400°C and if its power output is increased by 25 per cent, say from that corresponding to a conductivity integral of 40 watts/cm to that corresponding to 50 watts/cm, the center temperature will increase from 2090 to 2670°C, an increase of 34 per cent in the center-to-surface temperature drop.

In reference 3, Robertson et al. have reported a curve of $\int_0^T k(\theta)\, d\theta$ versus T for UO_2 pellets operating in-pile. The center temperatures were measured by thermocouples up to the temperature of 1400°C, and higher temperature points were obtained by observing the onset of grain growth and melting at the center. The plot shows considerably less curvature than Fig. VIII-1, falling below Fig. VIII-1 at temperatures below about 2000°C, and reaching a higher value, of about 80 watts/cm, at 2800°C. The curve would be consistent with a thermal conductivity which dropped gradually from about 0.039 watt/(cm)(°C) [2.3 Btu/(hr)(ft)(°F)] at 0°C to about 0.028 watt/(cm)(°C) [1.6 Btu/(hr)(ft)(°F)] at 700°C and remained constant at higher temperatures.

Although the use of the conductivity integral allows consistent irradiation experiments to be made without direct reference to a thermal conductivity, the thermal conductivity remains as the determining factor on fuel-element temperatures. Therefore the determinations of conductivities and effective conductivities hold great interest and importance for the reactor designer.

Figure VIII-2, from reference 4, is the latest collection of thermal-conductivity data. The data, which were measured on samples of various densities, were adjusted (in reference 4) to a 95 per cent density on the assumption that conductivity is directly proportional to density. The reference mentions a number of possible reasons for the spread in the data. Among them are differences in method of measurement, differences in method of fabricating the samples, possible deviations from the stoichiometric composition, and effects of cracking. The correspondence between the curve derived from the conductivity integral curve in reference 1 (Fig. VIII-1) and the Hedge and Fieldhouse curve is to be expected, for reference 1 states that the conductivity integral curve itself was derived from the Hedge and Fieldhouse data.

The data in Fig. VIII-2 are all for unirradiated UO_2. Irradiation, of course, produces

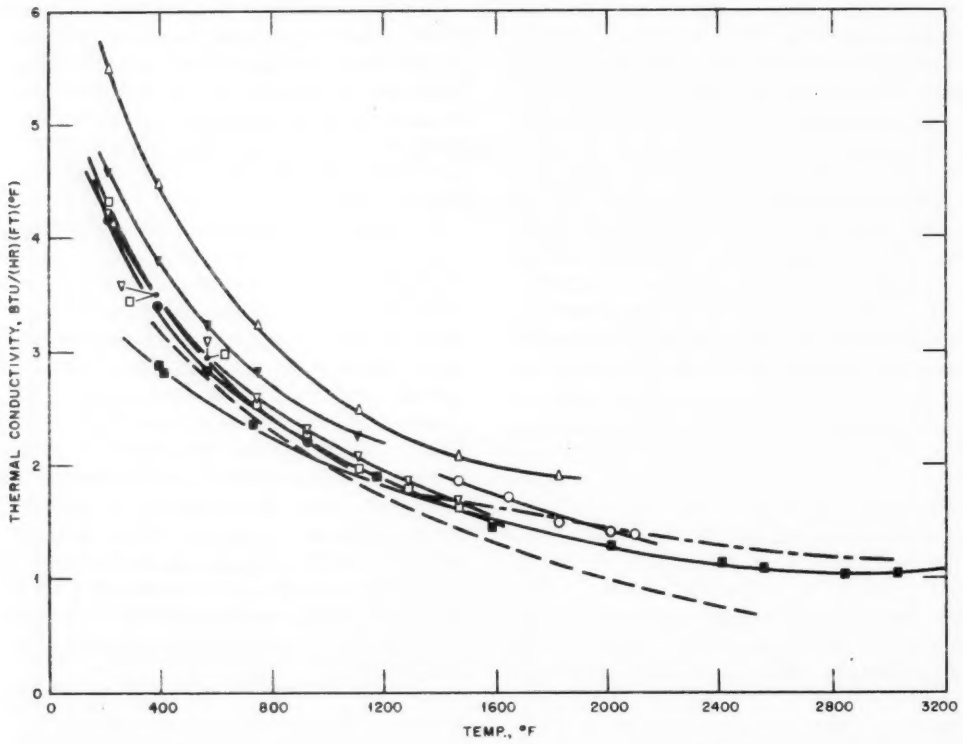

Fig. VIII-2 Thermal conductivity data of several investigators for 95 per cent dense UO_2. Conductivity at measured densities adjusted to conductivity for 95 per cent material on a linear basis.[4] △, W. D. Kingery et al., *J. Am. Ceram. Soc.*, 37(2): 107 (February 1954). ■, J. C. Hedge and I. B. Fieldhouse, USAEC Report AECU-3381, September 1956. ○, R. Scott, British Report AERE-M/R-2526, March 1958. □, ▼, ▽, and ●, BMI-HAPO Samples 70, 1000, 65, and 68, respectively, USAEC Report BMI-1315, p. 7, Feb. 1, 1959, and USAEC Report HW-59235, p. 5.14, Jan. 15, 1959 (Classified). ——, R. W. Nichols, *Nuclear Eng.*, August 1958. – – –, J. A. L. Robertson, Canadian Report CRFD-835(AECL-807), April 1959.

changes in the effective conductivity, but it is not clear how much of the change is a true radiation effect and how much is due to mechanical and thermal effects such as cracking and recrystallization. Reference 5 is a later report giving the results of a rather extensive program of in-pile effective conductivity measurements. The program encompassed an investigation of the effects of (1) diametral clearance between fuel and cladding, (2) the gap-filling gas atmosphere, and (3) the central temperature of the fuel. The experiments were conducted by means of an in-pile loop containing an instrumented capsule. Within the capsule was contained a column of 15 cold-pressed and sintered UO_2 pellets; a 67-mil hole was drilled through the pellets to contain a pair of Pt–10 Rh thermocouples to measure the center temperature of the UO_2. The capsule, made of type 304 stainless steel, had a nominal outside diameter of 1.125 in., and the fuel-containing hole was about 0.36 in. in diameter. Additional thermocouples were drilled into the capsule wall to measure heat transferred through the wall of the capsule. The experimental conditions for each of the several runs accomplished during the program are given in Table VIII-1. The data are reported in terms of the "effective" thermal conductivity, defined as follows:

$$k' = \frac{\int_{T_s}^{T_c} k\, d\theta}{\Delta T} = \frac{q}{2\Delta T}\left(\frac{r_0^2 - r_1^2}{2} - r_1^2 \ln \frac{r_0}{r_1}\right) \quad (3)$$

where

Table VIII-1 WAPD-22 EXPERIMENT: ASSEMBLY AND IRRADIATION DATA[5]

Experiment No.	As-assembled diametral clearance, in.	% of theoretical density	Gas-filling atmosphere	Type of UO_2	No. of days irradiated	MTR position	Estimated total exposure, nvt thermal	Total burnup, fissions/cm^3
22-1	0.0035	94	Helium	Production	15	A-28-NE	0.8×10^{20}	6.5×10^{18}
22-2	0.008	93.5	Vacuum	Production	1	A-31-SE	0.19×10^{18}	1.6×10^{16}
22-3	0.008	92.6	Helium	Production	15	A-28-NE	0.67×10^{20}	5.3×10^{18}
22-4	0.0015	93.7	Helium	Production	1	A-31-SE	0.43×10^{18}	3.6×10^{16}
22-5	0.0015	94.1	Helium	Laboratory	38	A-31-SE	0.50×10^{21}	3.6×10^{19}
22-6	0	96.7	1 Kr + 3 Xe	Laboratory $UO_{2.15}$	15	A-31-SE	0.19×10^{21}	1.5×10^{19}
22-7	0.013	95.0	1 Kr + 3 Xe	Production	15	A-31-SE	0.19×10^{21}	1.5×10^{19}
22-9	0.008	93.8	1 Kr + 3 Xe	Production	1	A-31-SE	0.46×10^{18}	3.8×10^{16}
22-11	0	94.9	1 Kr + 3 Xe	Production	45	A-31-SE	0.57×10^{21}	4.1×10^{19}
22-14	0.0025	94.1	1 Kr + 3 Xe	Production	30	A-31-SE	0.32×10^{21}	2.4×10^{19}
22-15	0.0035	96.3	1 Kr + 3 Xe	Laboratory (enriched to 1.02%)	15	A-31-SE	0.14×10^{21}	1.6×10^{14}

k' = effective thermal conductivity, watts/(cm)(°C)
k = UO_2 thermal conductivity, watts/(cm)(°C)
$\Delta T = T_c - T_i$, °C
T_i = bore temperature of capsule, °C
T_c = centerline temperature of UO_2, °C
T_s = surface temperature of UO_2, °C
q = volumetric heat-generation rate, watts/cm^3
r_0 = outer radius of fuel, cm
r_1 = inner radius of thermocouple well, cm

Figure VIII-3 is a plot of the effective thermal conductivity of PWR grade UO_2 as a function of central fuel temperature, with clearance (at assembly) as a parameter. Although individual data points have not been included in the reproduction of the figure, the original data from runs 22-2, 22-3, and 22-9 led the authors to conclude that "the initial atmosphere within the sheath has no apparent effect."

In Fig. VIII-3 the curve of effective conductivity for the "zero-clearance" specimen, at temperatures above 400°C, is nearly as high as the Kingery curve for unirradiated UO_2 and would be above the other unirradiated measurements (Fig. VIII-2), even though the effective conductivity of the specimen should define the lower limit of UO_2 conductivity. For this reason the Kingery curve was assumed to hold for the UO_2 in all specimens, and was used to calculate the temperature drop in the UO_2, and thus to make possible an evaluation of the effective thermal conductance of the fuel-cladding gap or interface. Figure VIII-4 is a plot of this conductance as a function of contact pressure and number of reactor startups. These data are for run 22-11 and are therefore for zero assembled clearance. The contact pressures are those calculated from the dimensions at assembly and from the relative thermal expansions of fuel and sheath corresponding to the measured temperatures; the changes with subsequent startups

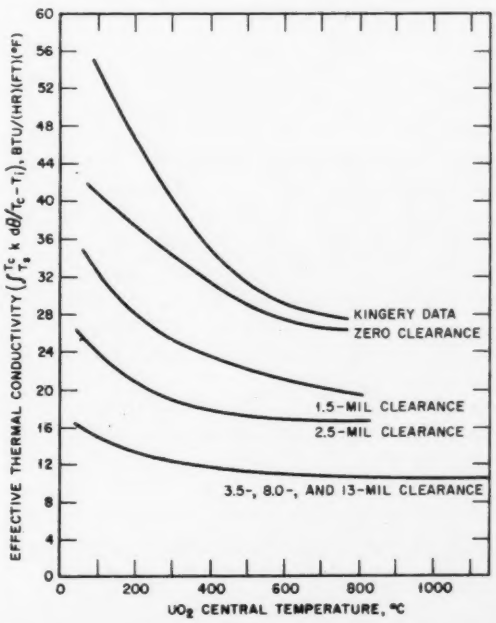

Fig. VIII-3 Effective thermal conductivity[5] of PWR production UO_2.

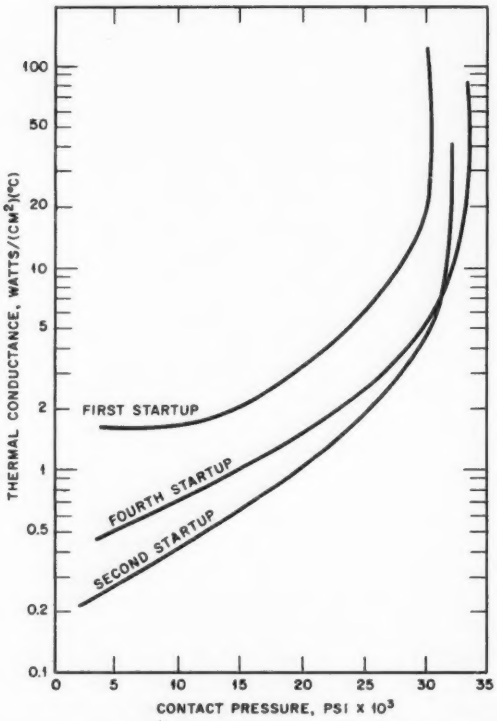

Fig. VIII-4 Effect of contact pressure on thermal conductance, WAPD 22-11 experiment.[5]

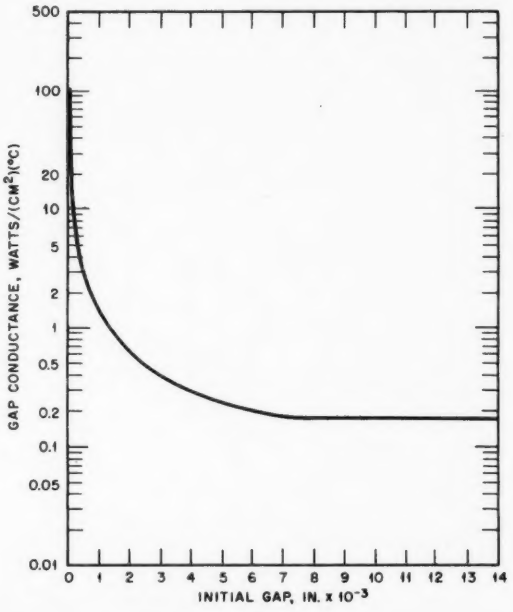

Fig. VIII-5 Effect of initial diametral gap on gap thermal conductance.[5]

were attributed to a possible plastic deformation of the stainless-steel capsule during the initial startup or to a change in UO_2 thermal conductivity due to cracking or irradiation. It should be noted that the ability to achieve the high contact pressure and high gap conductance displayed in run 22-11 depends on the particular capsule design used. For typical power-reactor fuel elements having "thin" cladding, for example, the contact pressure would be restricted to values below 5000 psi since the cladding would deform before higher pressures could be attained.

Figure VIII-5 is a plot of the thermal conductance of the fuel-cladding gap, as a function of the clearance at assembly. In the presentation of such a plot the implication is that the conductance of the gap is independent of the power density in the fuel pellets, and this was found to be very nearly the case over the range of power densities represented in the data of Figs. VIII-3 and VIII-5. The range of power density was, however, relatively low, being limited to that corresponding to maximum center temperatures of about 800°C for the gap clearances up to 3.5 mils. In the case of the 3.5-mil clearance, for example, the maximum power density investigated corresponded to a heat flux of about 90,000 Btu/(hr)(sq ft) at the surface of the fuel pellet. The reference states that in none of the experiments assembled with initial clearances did the fuel temperature rise high enough to reduce the gap to zero by expansion of the fuel.

The Canadian investigations[3,6] of the effect of gap clearance have covered power densities and pellet sizes that give considerably higher center temperatures and have led to a rather different picture of the fuel-cladding gap behavior. Reference 3 states that representative specimens, when run at values of $T_0 - T_s$ of about 2000°C, show diametral expansions of more than 1.9 per cent if the expansion is unrestrained, and that under such conditions significantly higher center temperatures are observed at a given power density for those specimens assembled with clearances greater than about 2 per cent of the pellet diameter. This expansion of about 2 per cent in the diameter of the oxide seems to indicate either a surprisingly high effective oxide temperature (about 1700°C) or an unexpectedly high value of the thermal expansion coefficient at high temperature. A diametral expansion of

2 per cent, in the case of the WAPD pellets, would amount to a diameter increase of about 7 mils.

References

1. J. A. L. Robertson, $\int k\, d\theta$ in Fuel Irradiations, Canadian Report CRFD-835(AECL-807), April 1959.
2. J. C. Hedge and I. B. Fieldhouse, Measurement of Thermal Conductivity of Uranium Oxide, USAEC Report AECU-3381, Sept. 20, 1956.
3. J. A. L. Robertson et al., Irradiation Behavior of UO_2 Fuel Elements, *Am. Inst. Mining Met. Engrs., Inst. Metals Div., Spec. Publ. 9*, pp. 45–70 (November 1959).
4. W. B. Cottrell et al., Fission-Product Release from UO_2, USAEC Report ORNL-2935, Oak Ridge National Laboratory, Sept. 13, 1960.
5. I. Cohen et al., Measurement of the Thermal Conductivity of Metal-Clad Uranium Oxide Rods During Irradiation, USAEC Report WAPD-228, Westinghouse Electric Corp., Bettis Atomic Power Laboratory, August 1960.
6. O. J. C. Runnalls, Uranium Dioxide Fuel Elements, Canadian Report CRL-55(AECL-754), May 1959.

Section IX

DESIGN AND CONSTRUCTION PRACTICE

As more and more nuclear power plants are built, the subjects relating to nuclear-power-plant design and construction practice, with emphasis on how things are actually done in the building of a nuclear plant rather than on the development or theory underlying the practices, will increase in importance; and it is hoped that more and more information of this kind will be published. The new section, Design and Construction Practice, will appear in *Power Reactor Technology* whenever suitable material is available for review and will cover whatever is new in the practices of nuclear-power-plant design and construction. In addition, this new section will attempt to take note of the actions of regulatory or advisory bodies from the point of view of their effects on design and construction practice. *Power Reactor Technology* will not, however, undertake to call attention to all regulatory and advisory actions of a technical nature, since such a function falls more naturally into the purview of the Technical Progress Review *Nuclear Safety*.

Nuclear Pressure Vessels: Codes and Practice

During the nineteenth century, the use of pressure containers became increasingly more common as James Watt's steam engine came into use for ship propulsion and for stationary power. In those early days the design and operation requirements of pressure vessels were not understood, and many boiler failures resulted in the loss of both lives and property. In an effort to protect the public, states and cities began enacting laws relative to boiler design and construction. Moreover, boiler insurance and inspection companies were formed, and they also established certain basic rules to be followed in this regard.

As a consequence of the chaotic situation created by the multitude of boiler construction laws and rules, the American Society of Mechanical Engineers (ASME) appointed a committee, early in the twentieth century, to formulate standard specifications for the design and construction of boilers and other pressure vessels. This committee produced the first issue of the ASME *Boiler and Pressure Vessel Code*. The Code is kept current by periodic revisions, normally made every third year. In addition to this function the present ASME committee, through its special subcommittees, also considers questions pertinent to the Code and requests for Code interpretations. These questions and requests are answered in the form of letters, interpretations, special rulings, or revisions to the Code. When interpretations or special rulings—also called cases—are approved by the ASME board on codes and standards, they are published in the journal *Mechanical Engineering*. Code revisions are made every six months and are published as addenda to the Code.

The designer of nuclear pressure vessels must be familiar with the *Boiler and Pressure Vessel Code*[1–4] and all applicable Code Cases,[5] particularly the "N" or Nuclear Code Cases. These nuclear cases apply for vessels in contact with fluids that have received primary nuclear radiation and, in general, are more stringent and conservative than those for vessels having other purposes. In addition, the designer must be aware of the laws of the state in which a plant will be constructed, since all states do not accept the recommendations of the ASME *Boiler and Pressure Vessel Code* committee. Finally, he must also know what is not provided

for by the Boiler Codes in order to prepare the necessary supplemental design information.

Illustrative of the latter function is the role played by the U. S. Navy's Bureau of Ships in the design and development of pressure vessels for nuclear applications. Since the Navy was the first major purchaser of fabricated vessels for reactor systems, the Bureau had to set standards that would result in the maintenance-free and ultrasafe construction considered necessary for the intended shipboard use. For this purpose, specialists in the various fields were assembled to establish the design, fabrication, and inspection requirements that would result in the most satisfactory construction based on the existing technology and techniques. These requirements are now being written into the Boiler Code Nuclear Cases. Furthermore, when the Boiler Codes do not supply information relative to the design, fabrication, or inspection of a specific assembly or part, the Navy practices are generally relied upon. Obviously, the requirements for shipboard use are not always applicable for central-station design. For example, naval propulsion units must be designed to withstand severe shock and acceleration forces that will never be experienced by land-based vessels except, perhaps, in quite special earthquake-sensitive locations. Consequently, to avoid excessive conservatism and unwarranted expense, judgment is needed in determining which provisions of the Code are appropriate to the intended application.

In general, the ASME *Boiler and Pressure Vessel Code* is used to establish minimum material thicknesses required to resist the expected pressure forces. Several existing situations are not covered adequately by the present Code equations. Specifically, these are the thicknesses required for heat-exchanger tube sheets and the reinforcement required for spherical, elliptical, or flat heads when penetrated by multiple openings. The accepted method in the past for determining the thickness of these parts has been photoelastic analysis. An analytical analysis using the method of Howay,[6,7] or similar solutions, would also appear to be acceptable for these determinations.

The Nuclear Code Cases (1270N, 1271N, 1272N, 1273N, 1274N, and their addenda) are pertinent to nuclear vessels only. However, the paragraphs relating to vessels containing lethal fluids (paragraphs UW-2 and UCI-2 of Section VIII) also apply. The following list contains the most important restrictions imposed by the nuclear cases:

1. The pressure boundary welds of all vessels containing, or which can contain, the primary coolant must be of the double butt-welded type and must be fully radiographed.
2. Vessels fabricated of ferritic steel shall be stress relieved.
3. Safety devices are not required on reactor vessels provided that the primary system contains two safety or relief valves. These valves must have a capacity sufficient to prevent the primary system pressure from rising more than 10 per cent above the design pressure.
4. The combination of membrane stress, as determined by Code rules, and thermal stresses, resulting from temperature distributions caused by steady-state operation, shall not exceed $1\frac{1}{2}$ times the Code "S" value.
5. All openings or penetrations of the vessel shall be reinforced regardless of the diameter. Any compensation for openings shall be integral with the vessel or nozzle or both.
6. All welds, including those associated with nozzles or other openings, shall be full-penetration welds except where impossible or impractical. Welds other than the full-penetration type shall be permitted only if they are of sufficient size to develop the full strength of the members.
7. The cladding shall not be included when computing the required wall thickness of vessels. The inside diameter of the vessel shall be taken as the nominal inside diameter to the cladding plus twice the nominal cladding thickness.

The following quotation* taken from the Code [paragraph (7) of Code Case 1273N] is a good illustration of the kind of judgment which must be exercised by the nuclear vessel designer.

> The Code rules are intended to provide minimum safety requirements for new construction, and not to cover deterioration which may occur in service as a result of corrosion, erosion, radiation effects, instability of the material, or operating conditions such as transient thermal stress or mechanical shock and vibratory loading; nevertheless, particular consideration shall be given to these effects with a view to obtaining the desired life of the vessel.

Thus the questions not covered by the Code rules may be more troublesome than those which

*Reprinted here by permission from the American Society of Mechanical Engineers.

are, and those not covered may have a large effect on the construction cost. The designer must have sufficient background to evaluate all these questions in the light of the intended vessel usage and to provide assurance that the design will meet the applicable requirements.

Since the Boiler Code does not consider the effects of transient loadings, their calculation becomes a part of the supplementary design task. Included are transient thermal stresses, vibration, and mechanical shock. A typical evaluation of these items involves determinations of the actual stress for each individual loading and the use of a cumulative damage theory to combine the effect of individual loadings as they relate to the total life of the part. The equation normally used is

$$CD = \sum_{i=1}^{i=k} \frac{n_i}{N_i}$$

where

CD = cumulative damage factor
n_i = number of cycles of a particular loading which can occur during life of vessel (the subscript indicates which loading condition)
k = total number of loading conditions which will occur during life of vessel
N_i = number of cycles which must occur of each particular loading condition, i, before failure occurs (this is determined from the stress fatigue curve)

The theory indicates that, when the value of CD equals or exceeds 1, the design will fail prior to the end of the design life. A maximum value of between 0.6 and 0.8 is usually allowed. N_i, the number of cycles in which a particular loading, i, must be imposed before failure occurs, is determined through involved and detailed stress and thermal analysis. The stress problem is usually solved by the method of superposition. The thermal problem involves an iteration process in which computers may be used to good advantage.

The Bureau of Ships document[8] entitled Tentative Structural Design Basis for Reactor Pressure Vessels and Directly Associated Components (Pressurized, Water Cooled Systems) is recommended as a reference and guide for studying these transient problems. This document has been used extensively by naval vessel designers and is generally accepted as the most authoritative for this type of work. It does not, however, discuss the problem of creep which may occur at temperatures above 800° F. Therefore the designer must consider creep strains in addition to those treated in the reference when high temperatures are encountered.

Fast-neutron irradiation has been observed to have a profound effect on the ductile properties of the commonly used ferrous materials. These changes have been manifested by increased embrittlement and consequent loss of impact strength. The September 1960 issue of *Power Reactor Technology* presents a detailed discussion of the available information relative to this subject.

Present practice is to specify the minimum impact values for ferritic materials so as to minimize the effects of irradiation and to preclude the possibility of brittle failures when testing at lower temperatures. In the past, the minimum average Charpy V-notch impact value for carbon-silicon steel has been specified as 15 ft-lb at +10° F. Plate, bar, pipe, forgings, castings, and weld metal have been manufactured to meet this requirement. Manganese-molybdenum steel and bolting materials have been manufactured to an impact value of 30 ft-lb and 35 ft-lb, respectively, at +10° F. Three impact tests are usually required, and no value is allowed to fall more than 5 ft-lb below the minimum average. Moreover, only one value can fall below the minimum average.[9] Since austenitic steels do not demonstrate as sharp a loss of ductility as do the ferritic steels, minimum impact values for these materials are not normally specified.

In addition to the special effects of irradiation, the designer must also be able to predict the behavior of the construction materials at the pressures and temperatures to be encountered during operation. Since instability varies with the material, complete data for each material must be available and must be studied with regard to changes in its properties — creep effects, loss of ductility at certain temperatures, etc. This requirement often limits the use of proprietary materials when adequate data on the physical or chemical properties of the materials are not available.

The construction materials and methods used in the manufacture of nuclear vessels can, with certain exceptions and/or improvements, be characterized as the best of present standard practice. The quality control of materials dur-

ing manufacture is usually closer than that imposed on materials for conventional uses. Fine-grain heat-treatments are specified, the chemical composition is held to closer tolerances, and high-cross-section materials are sometimes limited to smaller amounts. The production of castings and forgings to be used in nuclear vessels is also subject to close quality controls. The primary tool used in these examinations is the X-ray inspection, and, normally, 100 per cent investigation is required. The standard for interpretation and acceptance of these X rays is specified in the ASME *Boiler and Pressure Vessel Code*. Quite often the forgings, pipes, and plates have been inspected ultrasonically. The maximum defect allowed is about 2 per cent of the wall thickness for thick-walled vessels. However, where large-grained material is encountered, a loss of signal often occurs and gives misleading results; consequently, fabricators are reluctant to make this inspection the sole basis of acceptance. The material composition and physical properties are examined using the standards of the American Society for Testing Materials (ASTM)[10,11] to be certain that the specifications are complied with and that the results, together with those of tests on the chemical and physical properties, are supplied to the purchaser.

Material received by the fabricator is again given various inspections to ensure that the purchase specifications have been met. Usually these inspections consist of a magneflux inspection for ferritic materials, a dye penetrant inspection for austenitic and other materials, and, occasionally, an ultrasonic inspection.

Code compliance requires that adequate in-process quality-control inspections be used during fabrication. In this regard, visual inspection is a most important tool and should be part of each workman's duty. Dimensional checks of small parts and assemblies should be made whenever practical, and the machining setup for larger and more expensive parts should be inspected prior to the start of machining. The tools required are the same as those normally encountered except where very large dimensions are involved. In this case, optical telescopes are often used. It should be noted that the effect of temperature variations is critical when measuring these large dimensions.

X- or gamma-ray inspection of all pressure-containing welds is required by the Boiler Code. The inspection acceptance standard is also specified by the Boiler Code. Radiographs are normally taken upon completion of the weld, after any repairs, and after final stress relief. Other welds, such as those used for the attachment of supports, may be inspected by magnetic particle methods when ferritic materials are used and by dye penetrant methods when austenitic material is used.

Stress relieving is required of all completed vessels containing primary fluid, with certain exceptions. During stress relief a chart of the furnace temperature is kept, and from this chart the maximum temperature, time at that temperature, and rates of heating and cooling may be determined. Helium or argon atmospheres have been used to protect critical or inaccessible areas. Machining is usually accomplished after stress relieving to ensure that the material remains dimensionally stable.

Upon completion of stress relief, the vessel is rough machined and then, if practical, hydrostatically tested prior to final machining. The hydrostatic test is required by the Boiler Code and must be witnessed by a Boiler Code Inspector. During this test the vessel is pressurized to $1\frac{1}{2}$ times the design pressure multiplied by the ratio of the Code allowable S value, at operating or design temperature, to the S value at the test temperature. The Code S values may be found in Tables UCS-23 and UHA-23 of Section VIII and in Table P-7 of Section I of the ASME *Boiler and Pressure Vessel Code*.

Helium leak tests, if required, are made following the final dimensional inspections. The maximum leak rate allowed for this test in the past has been 0.01 μcu ft/hr or 1.04×10^{-7} cm^3 at atmospheric pressure. Because of (1) the large volume of expensive gas involved, (2) the difficulty of sealing openings, and (3) the small chance of leaks in thick members and heavy welds, this test should be specified only when absolutely necessary.

To reiterate, nuclear vessel construction involves the best of present standard practice. As is often the case when "the best" is specified, the costs tend to be high. Much of the extra care, close quality control, and careful inspection are fully justified by those considerations of safety and vessel life which are the substance of the *Boiler and Pressure Vessel Code*, particularly when it is remembered that the design life of the vessel must be achieved, in most cases, without the possibility of direct inspection of the vessel after it goes into service.

However, there are design decisions, particularly those involving mechanical tolerances, which may have little to do with safety or vessel life but which still have important effects on the difficulty and cost of vessel manufacture. It seems reasonable to hope that potentialities exist for reducing the costs of nuclear vessels without in any way compromising their safety.

Autoclave Testing of Zircaloy-2

Zirconium and its alloys have gained wide acceptance as structural and cladding materials in water-cooled reactors. The principal reasons for their selection are low thermal-neutron cross section, good corrosion resistance, and reasonably good high-temperature strength. Zirconium, however, is a very reactive metal in that it combines readily with most gases, including hydrogen, oxygen, and nitrogen, at elevated temperatures. The excellent corrosion resistance, therefore, is maintained only by reason of the rapid formation of a thin adherent oxide film that protects it from further corrosion. The properties of this film and the procedures used to control its formation are the subjects of reference 12.

The intentional formation of the oxide film on Zircaloy-2 reactor components in test autoclaves has been widely accepted in industrial practice and has a twofold advantage: (1) the oxide film is formed under closely controlled conditions and is not left to occur under variable conditions in the reactor, and (2) the appearance of the film serves as a quality-control check on the acceptability of the material in the finished part. Poor-quality Zircaloy-2, i.e., material containing contaminants such as iron, copper, and uranium, will show up gray or white after an autoclave corrosion test, whereas good material will have a lustrous black surface. Visual inspection is the primary method of determining acceptability of corrosion-tested zirconium components, although coupon tests are also performed using the material weight gain as a measure of acceptability.

Zircaloy autoclave tests may be performed in either pressurized water or superheated steam. The superheated-steam test is the more severe and is performed more rapidly. However, it is not so sensitive as the water test to certain types of contamination such as iron, tungsten, and copper. For the steam test the specimens are generally exposed to superheated steam at 750°F and 1500 psia; for the water test a temperature of 650 or 680°F has been used. The lower the test temperature, the longer the test must last to provide a meaningful corrosion result. The effect of pressure on the rate of zirconium oxide film formation is not very pronounced when observed by visual inspection alone. According to reference 12, when careful weight measurements were taken, a greater rate of oxide formation was observed at 100 psi than at 1500 psi.

Zircaloy-2 usually exhibits a low initial rate of corrosion and a more rapid final rate. The point at which the final rate begins has been termed breakaway and occurs in about 110 days in 680°F water; however, only about 28 days are required in 750°F steam. Tests lasting 3 and 14 days in superheated steam are generally sufficient to characterize a particular lot of material; these can be confirmed by longer tests when desired. If contamination of the Zircaloy with iron, tungsten, or copper is expected, a water test is preferable to the steam. A dual-cycle test starting with 680°F water for one day followed by two days in 750°F steam is reported capable of detecting surface contamination, although such a test still gives an overall weight gain nearly equal to that of a three-day test in 750°F superheated steam.

Problems associated with the autoclave testing of Zircaloy include those involving interpretations of the results as well as those associated with autoclave operation. In this regard the cleanliness and finish of the surface are important in achieving representative autoclave films. For example, surface contamination may be incurred as a result of machining or of other metal-working operations performed on the material. The standard procedure employed to remove this contamination is an acid etchant treatment sufficient to remove a 1- to 2-mil depth of the surface metal. However, etchant stains on the Zircaloy, caused by improper rinsing and consequent acid contamination, will also give the white or gray indications of high corrosion rate normally associated with contaminated or poor-quality material. This is a practical consideration around crevices or in the presence of poor surface finishes where the etchant can become trapped and is not subsequently rinsed away. In the case of acid con-

tamination, if the base material is of good quality, the rate will return to normal after corrosion has penetrated beneath the contaminated surface.

At high temperature, Zircaloy readily combines with hydrogen to form zirconium hydride. Concentrations of hydrogen in Zircaloy as small as 10 to 50 ppm adversely affect notch sensitivity. In hydrogen concentrations over 2000 ppm, Zircaloy becomes more and more brittle and eventually crumbles to a powder. Autoclaving under static conditions or in large low-flow-rate autoclaves yields hydrogen concentrations in the range of 20 to 40 ppm. Therefore it is recommended that an adequate flow of heated deionized water be provided for autoclaves used in the corrosion testing of Zircaloy.

Autoclave tests have also been used for the detection of defects in the Zircaloy cladding of fuel elements. Fuel elements having metallic uranium cores and defective cladding will normally rupture under the pressure caused by the buildup of hydrogen gas and by uranium oxide formation as a result of the uranium corrosion. Defective fuel elements with uranium oxide cores can be detected by means of a helium leak test after autoclaving. A pressure of at least 1000 psi is recommended in autoclave tests intended to detect defective elements.

The primary indication of defectively clad metallic uranium elements is the presence of hydrogen in the autoclave. The corrosion of uranium produces inflammable hydrogen and a pyrophoric powder of uranium hydride; therefore it is desirable to ascertain the presence of hydrogen and/or a ruptured element prior to opening the autoclave. A method of detecting hydrogen using a palladium valve is described in the report.

Cycles of startup and operation are described for both a pressurized-water test and for a superheated-steam test. Both the methods of displacing the fluid as heatup progresses and the required operating instrumentation are described. In addition, some information is given on the design of racks to hold corrosion-test coupons. The importance of rack design in obtaining meaningful corrosion data is emphasized. Information relative to detailed design, construction materials, flow diagrams, and costs of autoclaves purchased at HAPO are also given in reference 12.

Carbon Steel for Reactor Systems

The possibility of successfully substituting carbon steel for the more expensive stainless steels commonly used in reactors has intrigued reactor designers for years. In almost all cases carbon steel offers major advantages with respect to cost, availability, construction time, ease of fabrication, etc.[13] However, in spite of the encouraging results of early efforts[14] to establish quantitative corrosion data for carbon steel in high-purity water, this material has not been widely adopted for use in power reactors. One of the few plants to attempt its large-scale use is the New Production Reactor (NPR), which was described in the September 1960 issue of *Power Reactor Technology*, Vol. 3, No. 4, pages 75 to 77, and is currently being constructed at Hanford, Wash. Carbon steel is also being used in the Navy's A1W prototype plant and in the Heavy-Water Components Test Reactor (HWCTR) being constructed at Savannah River.

Prior to the final adoption of carbon steel for the NPR, studies were made at Hanford[15] regarding the technical limitations associated with the use of carbon steel. The principal areas of concern were as follows:

1. Decontamination of carbon-steel systems to remove fuel failure products or accumulated "crud" is expected to be more difficult than for a stainless-steel system. This is due to two factors. First, carbon steel is generally less chemical resistant than stainless steel and is therefore milder; consequently, less active decontamination solutions must be used. (At present this means that the decontamination procedures for carbon steel are considerably less effective than those for stainless steel. Second, in most carbon-steel systems there are also present appreciable quantities of stainless steel. Because these two different materials require dissimilar chemical treatment for best decontamination and because the decontamination solutions for one material may attack the other material, mixed systems are not easy to treat.

2. Activity induced in corrosion products and deposited throughout the system is also an area of concern. Carbon steel is expected to corrode at an average rate of approximately 0.1 to 0.2 mil/year. Corrosion rates for stainless can be held as low as 0.03 mil/year. Also, the Hanford group concluded that the cobalt content of carbon steel could not be controlled so readily as that of stainless and, although stainless steel

can readily be obtained with a cobalt content of 0.05 per cent or less, the cobalt content of carbon steel may range from zero to 0.2 per cent. The potential seriousness of the crud problem has been amply demonstrated by experiences with the naval S1W reactor where, in a mixed steel system, active crud deposited preferentially in the carbon-steel steam generator tubes caused localized radiation levels up to 12 r/hr. It should be noted that in this case the activity was believed to have come from wearing of the stellite valve faces and bearings and not from corrosion of the carbon steel.

3. The relatively high corrosion rate mentioned in item 2 may also lead to fouling of heat-transfer surfaces and of mechanical devices such as valves and pump seals. For example, in the KER-1 loop of the Hanford Coolant Testing Semiworks (an in-pile carbon-steel test facility), operation of dump valves and pump check valves has been impaired by accumulated crud. Similar loops of stainless steel were operated without any crud problems.

4. Although basic welding techniques are simpler for carbon steel than for stainless steel, postwelding heat-treatment of carbon steel tends to produce oxide scale, which is a nuisance when one is attempting to maintain reactor cleanliness standards.

5. Carbon steel requires considerably greater care in use and during storage to prevent either gross corrosion or pitting attack. The "lay-up" procedures for maintaining a carbon-steel system in standby condition are more complicated, and increased care must be exercised both in shipping and in storage to prevent rusting.

6. Because of its reduced resistance to chemical attack, more carbon steel is lost per decontamination cycle than in the case of stainless steel. With present procedures, carbon steel would probably lose 0.5 to 1.0 mil per decontamination cycle, whereas stainless steel would lose approximately 0.05. If fuel failures made it necessary to decontaminate the system very frequently, the loss of wall thickness in carbon-steel heat-exchanger tubes could become serious; however, such frequent decontamination seems unlikely.

In spite of the problems associated with carbon steel, the cost advantages are large enough to encourage continued efforts to develop the technology needed to make it useful for reactor plants, and, with the test plants currently being constructed, this technology should advance rapidly. In conclusion it should be noted that at present the use of carbon steel will be restricted to pressurized-water systems because it is necessary to have oxygen-free water in contact with the steel to avoid excessive corrosion. This can be accomplished in a pressurized-water system by maintaining an adequate hydrogen overpressure; however, in a direct-cycle boiling-water system, the addition of enough hydrogen to suppress oxygen formation is not considered to be feasible.

References

1. *Boiler and Pressure Vessel Code:* Section I, Power Boilers, American Society of Mechanical Engineers, New York, 1959.
2. *Boiler and Pressure Vessel Code:* Section II, Material Specifications, American Society of Mechanical Engineers, New York, 1959.
3. *Boiler and Pressure Vessel Code:* Section VIII, Unfired Pressure Vessels, American Society of Mechanical Engineers, New York, 1959.
4. *Boiler and Pressure Vessel Code:* Section IX, Welding Qualifications, American Society of Mechanical Engineers, New York, 1959.
5. The ASME Boiler and Pressure Vessel Code, *Mech. Eng.*, 81(7): 56–59, 91–93 (July 1959); 82(1): 120 (January 1960); 82(4): 121, 144–147 (April 1960); 82(8): 97 (August 1960); 82(10): 102–105 (October 1960); 82(12): 120–121 (December 1960).
6. G. Horvay, Bonding of Honeycombs and of Perforated Plates, *J. Appl. Mech.*, 19: 122–123 (March 1952); and discussion of this paper, *J. Appl. Mech.*, 19: 405–407 (September 1952).
7. G. Horvay, The Plane Stress Problem of Perforated Plates, *J. Appl. Mech.*, 19: 355–360 (September 1952).
8. Tentative Structural Design Basis for Reactor Pressure Vessels and Directly Associated Components (Pressurized, Water Cooled Systems), Report PB-151987, Department of the Navy, Bureau of Ships, February 1959.
9. Westinghouse Electric Corp., Bettis Atomic Power Laboratory, Supplemental Requirements Applicable to the Materials, Fabrication, and Testing of Carbon on Low Alloy Steel Pressure Vessels, USAEC Report WAPD-CTA(MP)-39(Rev. 3), Jan. 29, 1957.
10. *ASTM Standards, Part 1, Ferrous Metals*, American Society for Testing Materials, Philadelphia, 1958.
11. *ASTM Standards, Part 3, Metals Test Methods (Except Chemical Analysis)*, American Society for Testing Materials, Philadelphia, 1958.
12. R. A. Thiede, Autoclave Testing of Zircaloy-2,

USAEC Report HW-65350, Hanford Atomic Products Operation, June 1, 1960.

13. C. F. Bullinger and J. M. Harrer, Cost Study of a 100-Mw(e) Direct-Cycle Boiling Water Reactor Plant, USAEC Report ANL-6178, p. 24, Argonne National Laboratory, July 1960.
14. R. U. Blaser and J. J. Owens, Special Corrosion Study of Carbon and Low-Alloy Steels, *ASTM Spec. Tech. Publ. No. 179*, Symposium on High-Purity Water Corrosion, p. 37, 1956.
15. W. D. Gilbert et al., Carbon Steel for the Hanford New Production Reactor, USAEC Report HW-58299(Rev.), Hanford Atomic Products Operation, Nov. 26, 1958.

Section X

OPERATING EXPERIENCE

Design practice and operating experience are the foundation stones of "know-how" in any engineering field. Unfortunately the formal reporting of operating experience is often inadequate, but this deficiency should only emphasize the importance of using fully what information is reported. Future issues of *Power Reactor Technology* will include this new section, Operating Experience, whenever suitable articles are available for review. It will cover (1) the operating results of nuclear plants and plant components and (2) the proof tests of isolated components.

Refueling the Shippingport Reactor

The first refueling of the Shippingport Atomic Power Station (PWR) was conducted from Nov. 2, 1959, to May 7, 1960. During this time, 32 seed fuel assemblies and two blanket fuel assemblies were removed and replaced. In addition, modifications to some equipment and instrumentation were made, and inspections of reactor components, such as control rods, control-rod drives, and fuel, were conducted. Reference 1 contains a description of the work done, the difficulties encountered, and the remedial measures recommended or taken to alleviate these difficulties during future refueling operations. The report also contains a comprehensive treatment of the radiation problems that developed and their effect upon the refueling and modification tasks. As a prelude to discussions of these topics, a brief description of the components and facilities involved in the refueling operations is given in the following paragraphs.

The PWR core is composed of 32 highly enriched plate type seed fuel assemblies and 113 natural-uranium dioxide blanket fuel assemblies. The 32 seed fuel assemblies are arranged in a ring located at about the mid-point of the core radius. The two central regions lying within this ring and the two outer regions surrounding the ring contain the blanket fuel assemblies.

The reactor is controlled by 32 cruciform hafnium rods mounted integrally within the seed fuel assemblies. The required rod motion is obtained by ball-nut-driven lead screws which operate through nozzles welded to the top closure head of the pressure vessel. The drive motors are contained in tubes which are welded to the nozzles and which project upward to a height of about 6 ft above the vessel head.

The principal core instrumentation consists of 36 flow-measuring nozzles or venturis, 113 failed-fuel-element detectors, and 107 thermocouples. The flow-measurement and Failed Element Detection and Location (FEDAL) piping leaves the vessel through four 4-in.-diameter nozzles welded into the top head. The thermocouple leads are taken out of the vessel through 3 of the 10 fuel removal ports also welded into the top head.

The flow-measurement piping terminates in 36 differential pressure cells mounted on a support structure (trellis) attached to the top head. The FEDAL piping terminates in a multiport valve located atop one of the 4-in. piping exit nozzles. The thermocouple leads terminate in junction boxes that are also attached to the trellis. Wiring or piping, as appropriate, connects these terminal points to the reactor instrumentation system.

The reactor vessel is housed within a domed containment shell only slightly larger than the vessel (Figs. X-1 and X-2).[2] The dome of the shell projects above the floor of the reactor pit and encloses the upper vessel head and its associated equipment. The dome is removable to

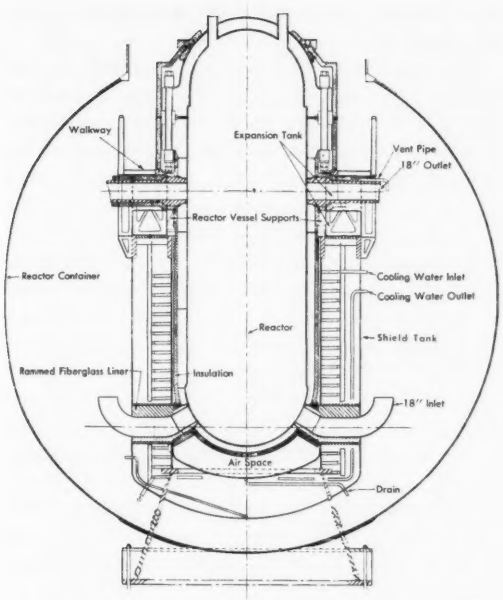

Fig. X-1 Reactor vessel, water shield tank, and containment shell.[2]

tions, each of which is provided with a watertight door to permit isolation and drainage of the individual sections.

During reactor operation the reactor pit section of the canal is drained and maintained in the dry condition. The reactor chamber, beneath the reactor pit, is normally not flooded; when the dome of the containment shell is removed, an annular seal plate must be installed to prevent flooding of the reactor chamber before water is let into the reactor pit. The center section of the canal is 45 ft deep and is used as a transfer area when carrying fuel between the reactor pit and the fuel storage pit. The fuel storage pit forms the south end of the canal and is 32 ft deep. Fuel storage and handling equipment is located in both the fuel storage pit and the transfer area.

The PWR is designed to permit the removal of fuel from the reactor without removing the upper vessel head. This is accomplished by providing the vessel head with 10 fuel removal ports through which the fuel assemblies may be withdrawn. The fuel-extraction tool used in

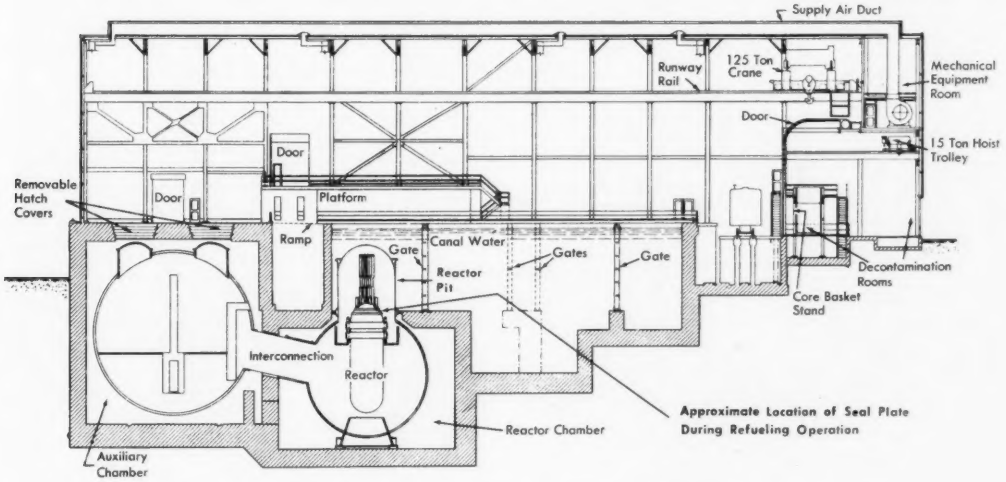

Fig. X-2 Elevation of Shippingport plant and fuel-handling facilities.[2]

permit access to the head for equipment maintenance and refueling operations.

Refueling of the PWR is accomplished using the underwater or "wet" method. The 26-ft-deep reactor pit forms one end of a canal having a total length of 109 ft and a width of 22 ft (see Fig. X-2). The canal is divided into four sec-

conjunction with port refueling is capable of retrieving fuel that is offset as much as 18.74 in. from the center line of the fuel removal port. The details of the design of this tool are not given in the report.[1]

The first refueling of the PWR required 134 three-shift working days. Of this total, 65 per

cent, or about 87 days, was spent in removing structures, components, and instrumentation preparatory to actual fuel removal and reinstallation following refueling. Replacement of the fuel proper consumed only 15 per cent or about 20 days. The remaining 20 per cent of the time, or about 27 days, was expended in modifying the core temperature-monitoring system and other equipment. Both a detailed breakdown of the operations and the times required for operations performance are contained in Fig. X-3.

Although the features of wet refueling and a ported head have been included as a means of minimizing fuel-handling problems, other facets of the design have combined to yield an exceedingly complex refueling situation. The principal causes of this complexity are (1) the utilization of the upper vessel head as a mounting point for control-rod drives and as the terminus for core performance instrumentation, (2) the requirement that all penetrations of the primary system be closed by seal welds, and (3) the mounting of control rods within the seed fuel assemblies proper.

The complexity above, and adjacent to, the vessel head resulting from item 1 may be seen in Fig. X-4. This complexity, coupled with fuel-assembly mounting of control rods, requires the dismantling of the complete control-rod-drive system as well as a significant fraction of the core performance instrumentation before actual fuel removal can begin. This equipment must, of course, be reinstalled following replacement of the fuel assemblies with the attendant additional time expenditure. Specifically, the equipment to be disassembled, and subsequently reassembled, is as follows: (1) all wiring and piping which connect head-mounted instrumentation to the reactor instrumentation system, and the associated support structures; (2) all control-rod-drive mechanisms, including motor tubes, motor assemblies, shrouds, etc.; and (3) all core temperature-monitoring instrumentation.

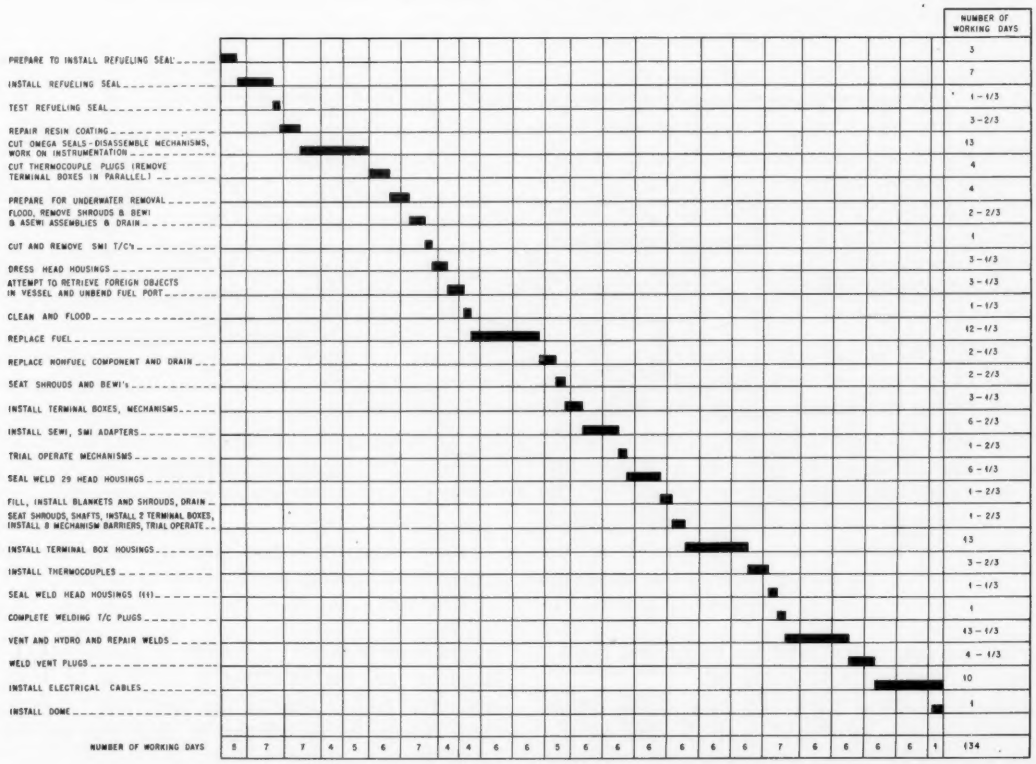

Fig. X-3 Actual seed 1 weekly refueling schedule.[1]

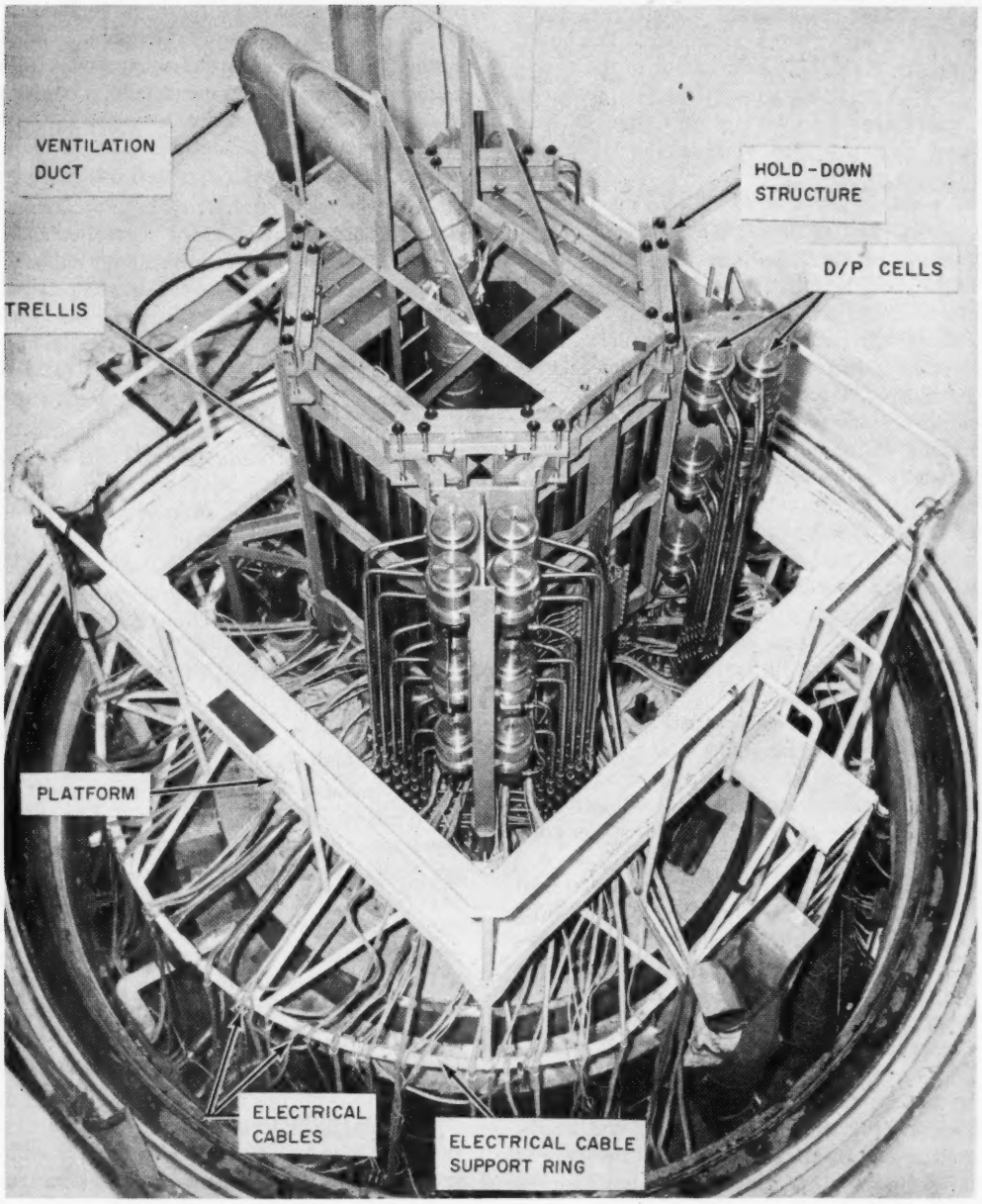

Fig. X-4 Reactor vessel head following removal of the reactor chamber dome.[1]

The disassembly requires the cutting of a considerable number of "omega" type seal welds. Because of the restricted space available at the head, specially designed welding machines and air-motor-driven rotary cutting tools must be used. After disassembly the instrument lines and the containment shell surrounding the reactor vessel must be sealed to prevent the leakage of shield water into these components when the reactor pit is flooded for underwater fuel and equipment handling. As mentioned above, leakage is excluded from the containment shell by a

seal plate which replaces the containment-shell dome during underwater operations. The outer edge of the plate bolts to the floor of the reactor pit. The inner edge is clamped to the top of the vessel head by this bolting action. Sealing surfaces are provided at both the inner and outer edges.

Two methods are used to prevent inleakage to the instrumentation lines; these are air pressurization and seal welding. The differential pressure cell terminal boxes are fitted with gasketed cover plates and are bolted closed. Air, under sufficient pressure to exclude a head of water 26 ft deep, is introduced into the terminal boxes and, through the connecting conduit, to the differential pressure cells proper. Thermocouples and thermocouple wells are disconnected and seal-welded closed.

According to the report,[1] the time involved in the actual transfer of spent fuel from the reactor, and its replacement with new fuel, consumed only a small fraction of the total time. In general, the work progressed without significant incident, although the time required exceeded the estimated time. This is attributed to delays imposed by the inspections required for seed 1 core components (control rods, mechanisms, instrumentation, etc.) which were to be reinstalled in the seed 2 core. An additional delay was incurred in an unsuccessful attempt to remove a foreign object lodged in the core support structure.

The report[1] discusses difficulties encountered in the seed 1 core refueling under the following headings: (1) preparations for refueling, (2) reactor design for refueling, and (3) radioactivity and its effect upon refueling operations.

The major criticisms falling under the first heading concern the procurement and availability of materials and equipment necessary to the refueling, the preparation of detailed procedures to accomplish the refueling, and the organization and training of personnel involved in refueling. Exemplary of the first criticism is the fact that serious equipment interferences were encountered during the actual operations at the vessel head. These involved both the cutting and welding machines, as well as the fuel-extraction tool. According to the report,[1] these interferences were not discovered during the full-scale mockup trials of the subject equipment because the effects of component "tolerance buildups" were neglected in the design of the mockup facility. The report recommends that the "worst case" tolerances be used in future trial operations of equipment. Another method of ensuring that the equipment will perform as required is to conduct trial operations of all fuel-handling equipment upon the appropriate reactor components as part of the precritical reactor tests.

As a cure for deficiencies in procedures, the report recommends a more careful consideration of the refueling requirements and a more thorough preparation for their accomplishment. In this regard, mockup facilities can also be used to quite good advantage. Considering the complexity associated with the PWR refueling, these approaches seem to be the most fruitful.

The report[1] cites the fact that originally there were two responsible individuals in charge of the refueling preparations. When the operations were placed under the control of a single individual, an improvement in the conduct of the work ensued. Consequently, the report recommends that future refueling operations be carried out under the direction of a single supervisor who would also be responsible for all preparations preliminary to the actual refueling. The report also recommends more intensive training of the entire refueling staff prior to the start of refueling.

One wonders whether a "streamlining" of the staff might have been desirable at the working level as well as at the supervisory level. From the radiation control records given in the report, the number of men working in significant radiation fields varied between 39 and 94 men per week. Even with allowance for shift work, it is hard to see how the 94 men could work effectively in the rather small area subjected to radiation, unless the radiation levels were so high as to require a frequent replacement of workers.

The major criticism of the reactor design, from the standpoint of refueling, is the employment of the vessel head as the terminus of reactor-core performance instrumentation. The following quotation is taken from reference 1:

> Difficulties encountered as a result of the limited personnel access afforded by the instrumentation supports (trellis) on the reactor vessel head, and the close spacing of the mechanism housings, caused delays throughout refueling. Future PWR core designs should minimize the amount of instrumentation and instrumentation supports on the reactor vessel head and [should] provide the maximum pos-

sible space between head penetrations consistent with functional requirements.

The initial actions taken in this direction consisted of modifying the core temperature-monitoring thermocouples to eliminate seal welding after disassembly. This was motivated by the damage sustained to the thermocouples during postdisassembly seal welding, primarily, and by the inability to replace inoperative seed-assembly performance thermocouples after installation of the fuel assemblies. Welding damage was eliminated by using thermocouples with shop-assembled Amphenol connectors and with shop-applied thermosetting insulating materials to encase the exposed leads. Replacement of seed-assembly thermocouples has been made possible by providing pilot tubes in the thermal barrier through which the couples may be drawn and by eliminating the permanent attachment of couples to the seed assemblies. Other modifications to core components include changes to control-rod-drive motor tube design and materials and to thermocouple materials.

In relation to the admonition that[1] "... primary emphasis should be placed on reducing the number of reactor parts that must be removed in order to get at fuel," the effect of the fuel-assembly-mounted control-rod provision is worth attention. It appears that a significant simplification in the refueling operation could be achieved if the control rods could be mounted in more permanent core structure. Although this may not be feasible in the seed-blanket core arrangement, the point may be valid for other reactor types.

Perhaps the most serious disadvantage of the present design, as it affects refueling, is the high radiation field in which the refueling crew must work. The report[1] mentions levels as high as 1.5 r/hr in the immediate vessel-head work area. These levels resulted mainly from the deposition of radioactive corrosion products in the control-rod-drive mechanisms and instrumentation ports at the underside of the vessel head.

The average weekly dose received by the refueling crew as a result of the radiation fields existing during the PWR refueling is given in Fig. X-5. The size of the crew receiving this average dosage is also included in Fig. X-5. The

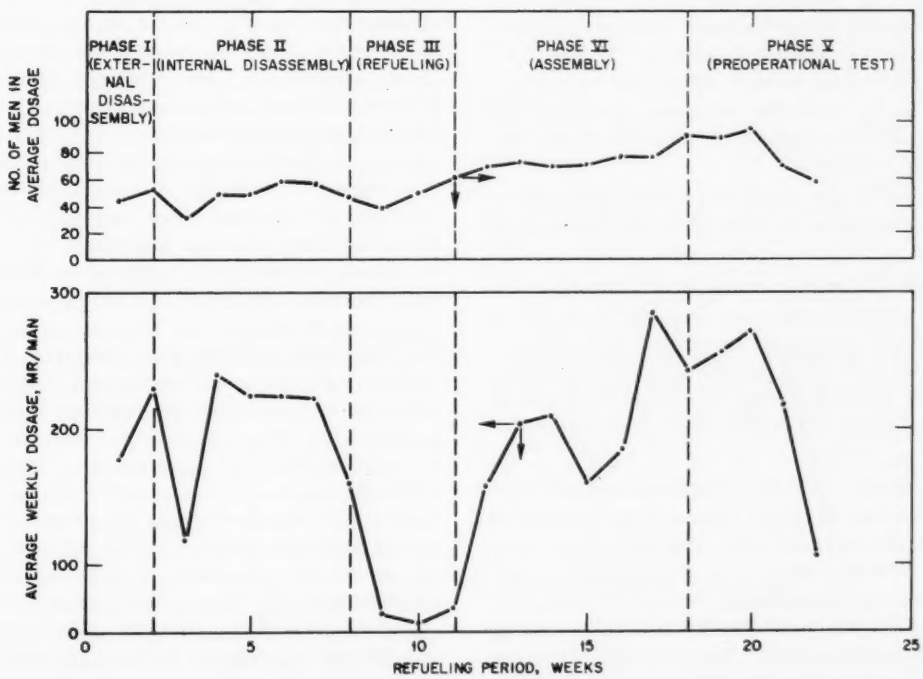

Fig. X-5 Radiation dosages incurred during refueling.[1]

maximum average weekly dose given in the report[1] is 283 mr/week; however, some members of the crew received considerably more irradiation than this average over some weekly periods. The report states that one man received a one-week dose of 860 mr, and three men received a three-month dose in excess of 2.9 r, although there was no overexposure in terms of the tolerance levels in effect at the time. The recent lowering of tolerance levels (reviewed in the December 1960 issue of *Power Reactor Technology*, Vol. 4, No. 1) may intensify the radiation problem in future reloadings unless design improvements are made.

The modifications already made to the core temperature-monitoring system and the recommendations relative to the simplification of nonfuel-handling operations made in the report, if followed, should do much to reduce the overall refueling time. In this regard the report estimates that the seed 2 refueling should require only about 60 days. This is less than one-half of the seed 1 refueling time. In addition to these steps, the report recommends that the following actions be taken, in future PWR designs, to reduce the high radiation levels exhibited by Shippingport: (1) minimize the number of crevices in the vicinity of the top head in which radioactive particles may be entrapped, (2) use low-activation cross-section materials in component wearing surfaces wherever possible, and (3) provide for flushing of areas in which entrapment occurs.

In view of the amount of effort expended on the investigation of wearing materials suitable for use in nuclear reactor cores, there appears to be little prospect of completely satisfying the second recommendation. The replacement of high-cobalt-containing materials, such as stellite, will have some beneficial effect; however, the best hope of solving this problem seems to lie in following the first and third recommendations.

Experience with the EBWR has indicated the effectiveness of these approaches in avoiding the buildup of radioactive deposits. This reactor is provided with a top shield plug mounted in the vessel, immediately beneath the top head, to protect the head from irradiation during planned D_2O operation. The underside of the plug is smooth and has few crevices in which radioactive material can collect. The radiation level observed on the underside of this plug was only 1 to 2 mr/hr after some six months of power operation, although this situation is not strictly comparable to the PWR because of the decontamination factor afforded by the steam-generation mechanism. However, during the 100-Mw modification performed recently on the EBWR, workmen were able to enter and work within the pressure vessel, in close proximity to surfaces that were continually washed by reactor coolant during power operation, without exceeding permissible dosages.

The experience with flushing has been encouraging also. To date, the major criticism of control-rod drives mounted in the bottom head of reactor vessels has been the collection of active corrosion products in the seal assemblies. In the case of the EBWR, levels in the roentgen range were observed. Periodic flushing of these seal assemblies with clean water has reduced the radiation levels by as much as several orders of magnitude.

In addition to the discussions of the refueling and other directly related operations, reference 1 also contains information regarding criticality aspects and the performance of some of the seed 1 reactor components. This information includes the results of inspections and examinations made to control-rod-drive mechanisms, structural items, and fuel assemblies. In view of the recent concern relative to hydrogen precipitation failure of Zircaloy-2 fuel jackets, it is noteworthy that deficiencies of this type were not observed in any of the blanket assemblies examined. The hydrogen content in the irradiated jacketing was found to be about the same as that usually existing in Zircaloy-2 that had been double-arc-melted in an inert atmosphere. Consequently, the report concludes that the extent of hydrogen pickup during irradiation was slight or nonexistent. Other conclusions reached and observations made, regarding the UO_2 blanket fuel performance, are as follows: (1) there were no significant radiation-induced dimensional changes in the fuel rod; (2) radial cracking occurred; however, center melting or grain growth did not occur; (3) the annular and axial spaces between the fuel and the jacketing were still in existence at the end of this irradiation period; and (4) the fission-gas release was about 0.11 per cent of that generated during the estimated fissioning of 1.77×10^{20} uranium atoms/cm^3.

Operational Tests of EBWR Vapor Recovery System

Although the EBWR uses H_2O as moderator and coolant, provisions were made in its original design for the possibility of converting to D_2O at some later date. Since the reactor employs the direct steam cycle, these provisions included a vapor-recovery and air-drying system on the steam components, to reduce both the net loss of D_2O and the inleakage of H_2O vapor.

As a result of recent D_2O reactor studies,[3,4] tests have been conducted for operational evaluation of the EBWR vapor-recovery system.[5] Although primary fluid losses and air inleakages have been calculated for this system,[6] measurements of the actual vapor-recovery-system operating pressures, temperatures, moisture content, air flows, and steam flows were desirable for determining the validity of the calculations.

The test apparatus, used in operational evaluation of the EBWR vapor-recovery system, is designed for measurement of the primary fluid collected from the high- and low-pressure turbine glands, turbine horizontal flange, reactor feed-pump seals, and all major steam-control-valve glands. Primary fluid is also collected from the air-ejector aftercooler and control-rod-thimble seals. Leakage from the turbine and reactor feed-pump seals comprises the major percentage of the total potential D_2O loss.

The vapor-recovery system consists of two main sections. One section dries atmospheric makeup air that is necessary for replacing the seal air that leaks to the atmosphere; the other section separates and recovers the working fluid (D_2O) and sealing air. Dried air is used for sealing the outboard section of glands, rather than atmospheric air, in order to reduce the addition of H_2O into the D_2O system. Both drying sections have two alumina dryers in parallel, permitting one dryer to be reactivated while the other is operating in the system. Reactivation of the alumina in the recovery section is accomplished by circulating heated air through the bed to be reactivated and then condensing the hot air in a reactivating condenser. The condensate is returned to the main condenser. The makeup air alumina beds are reactivated by circulating heated atmospheric air across them and then venting this air to the atmosphere. D_2O collected from the various seals is introduced into the vapor-recovery system through a vent condenser from which the vapor is circulated to the recovery dryers. The condensate from the vent condenser is pumped to the main condenser. Dry recovered air and makeup air are combined and pumped back to the seals.

Design seal pressures are a positive 6 in. of water at the dry gland and a negative 6 in. of water at the recovery gland. Under these conditions, 58.4 per cent of the dry seal air was recovered during the evaluation tests, and 41.6 per cent was lost. Average operating seal pressures ran slightly higher and reduced the percentage of recovered air to 56.3.

From the measurements taken during the tests, D_2O leakage and H_2O inleakage rates were calculated. Seal air flow, based on flow measurements at the average operating pressures, was 11.7 standard cubic feet per minute (scfm) recovered, 9.1 scfm lost, and 9.1 scfm makeup. With the alumina dryers in operation, there were 14.1 ppm by volume of D_2O in the dried air to the seals, which amounts to 0.27 lb D_2O/month leakage to the containment shell. There were 134 ppm by volume of H_2O in the dried air to the seals, which amounts to 5.5 lb H_2O/month contaminating the D_2O. It was concluded during the tests that contamination of the D_2O with H_2O can be reduced by introducing an alumina reactivation system in the EBWR air makeup section which is as effective as that in the recovery section. H_2O contamination could then be reduced to 11.5 ppm by volume or 0.29 lb H_2O/month.

For increased efficiency in air drying of D_2O recovery systems, a "heatless" type recovery system was recommended at the conclusion of the EBWR tests. The operating alumina chambers are pressurized in the heatless system while the standby chambers are at atmospheric pressure. Reactivation is accomplished by expanding a small portion of the dry air through the standby bed which is at atmospheric pressure. With this type of system, it was estimated that leakage could be reduced to the order of 1 lb D_2O/year from major equipment seals. Two half-capacity units were also recommended for large plants to afford maintenance and operational versatility.

Sodium Pump and Auxiliary Components for Hallam

Two centrifugal diffuser pumps, of different design, have recently been tested to demonstrate

their performance under simulated operating conditions of the Hallam Nuclear Power Facility (HNPF) reactor. The HNPF reactor is a sodium-cooled, graphite-moderated, thermal reactor designed by Atomics International for Nebraska Public Power Corp. and is being constructed near Hallam, Nebr. These pumps operate in the primary and secondary system and are capable of pumping 0 to 7200 gal of 270 to 950°F sodium per minute against a 150-ft head. The two pumps differ basically only in the design of the internal sodium seal, one being of the freeze-seal type and the other of the free-surface type.

Freeze-Seal Sodium Pump

The basic design for the freeze-seal type pump,[7] and its associated shaft freeze seal, was evolved from a series of developmental tests on smaller pumps as well as from experience gained in use of both primary and secondary pumps at the Sodium Reactor Experiment (SRE). The design includes an 18-ft vertical shaft required to space the motor from radiation emanating from the primary sodium system. Another feature of this pump is the removable internal assembly supported from the heavy flange of the pump casing at the reactor floor elevation. This internal assembly is composed of two principal parts. The upper portion serves as a radiation shield which fits within the pump casing and which surrounds the pump shaft. Suspended from the shield is the bearing housing for the pump shaft radial and thrust bearings. Immediately below the bearing housing is the thermal barrier. This thermal barrier supports the shaft freeze seal, forming a part of the case freeze seal, and locates the inner diffuser ring within the inner casing. The lower section of the pump shaft passes through the bearing housing into the thermal barrier and shaft freeze seal. Connection of the impeller is made below the freeze seal.

The principal developmental item within the pump is the shaft freeze seal. The purpose of the seal is to prevent leakage of sodium up the shaft and to keep the cover gas out of the sodium system. Experience with the freeze seals, installed in the SRE pumps, indicated a potential difficulty if the same design were used in the HNPF. Consequently, an improved seal was developed, based on data from a previous advanced SGR freeze-seal-pump program. The improved shaft freeze seal used in this pump was of the two-coolant-region, coil type designed to operate under the following conditions: (1) bulk sodium temperatures of from 350 to 945°F; (2) a sodium pressure of 10 psia; (3) shaft speeds from 0 to 850 rpm; and (4) an inert gas pressure in the pump case of 5 psig.

Three prototype, two-coolant-region shaft seals were tested under simulated reactor-service conditions to determine their operating characteristics. Information obtained from these tests included (1) the ability of the seal to retain sodium under all conditions of pump operation, (2) the heating load on seal coolant at various shaft speeds and bulk sodium temperatures, and (3) the temperature distribution along the length of the seal under several different combinations of conditions.

Satisfactory operation of the two-region freeze seal was obtained for 1100 hr of testing under controlled conditions in which the temperature was maintained at 95°F in the upper region of the seal and in the range of 240 to 285°F in the lower region. When the temperature was held uniformly at 95°F, as specified for HNPF, excessive cooling resulted in improper formation of the seal or in seizure of the shaft when rotating at low speed.

Free-Surface Sodium Pump

The free-surface type pump[8] is similar in many respects to the freeze-seal pump except that it has no shaft or casing freeze seal to contain the pumped fluid. This design has a mechanical seal consisting of wear rings which allow a small amount of sodium leakage to occur. This leakage is collected in a pool in the pump case and is then returned to the pump by way of an overflow system. Another feature of interest is the hydrodynamic type bearing which replaces the conventional radial bearing near the impeller end of the pump shaft.

The hydraulic bearing is formed from a ring containing four pressure-pad chambers mounted to the diffuser casting with the journals cast into the eye of the impeller. Sodium is supplied to the hydraulic bearing from the impeller discharge and provides a self-centering action during pumping. This self-centering action results because a radial displacement of the journal causes an increase in pressure in the pad toward which the journal moves and a decrease in the opposite pad. The bearing and journal were faced with stellite to resist the wearing

action when the pump was started, stopped, or run slowly, since the self-centering action does not exist when the inlet and discharge pressures are equal.

Initial performance testing of the free-surface type pump was hampered by seizure of the pump shaft and by entrainment of the cover gas into the pump suction line. The shaft seizure was eliminated by removal of the aluminum-bronze bushing at the bottom of the radiation barrier. Gas entrainment was caused by erratic sodium overflow. Satisfactorily stable flow was achieved by filling the loop expansion tank and pump casing to an elevation which ensured submersion of the overflow line.

After these modifications, hydraulic tests were run, under simulated operating conditions of the HNPF reactor, for about 800 hr. Overflow rate, which never exceeded 185 gal/min, was steady under loop flow rates as high as 9000 gal/min. The hydraulic bearing, the principal developmental item in this pump, proved to be trouble free. The results are interpreted to indicate that this pump should operate very satisfactorily in the Hallam plant with only slight modifications to facilitate disassembly and cleaning.[8] (Later information[9] shows that the free-surface sodium pump has been selected for the HNPF.)

References

1. H. Feinroth and T. D. Sutter, Jr., The First Refueling of the Shippingport Atomic Power Station, USAEC Report WAPD-233, Westinghouse Electric Corp., Bettis Atomic Power Laboratory, July 1960.
2. Personnel of the Naval Reactors Branch, Division of Reactor Development, USAEC; Westinghouse Electric Corp., Bettis Plant; and Duquesne Light Company, *The Shippingport Pressurized Water Reactor*, Addison-Wesley Publishing Co., Inc., Reading, Mass., 1958.
3. D. F. Babcock et al., Heavy-Water-Moderated Power Reactors, USAEC Report DP-480, E. I. du Pont de Nemours & Co., Nuclear Development Corp. of America, and Sargent & Lundy Engineers, March 1960.
4. E. I. du Pont de Nemours & Co., Engineering Dept., Heavy-Water-Moderated Power Reactors Engineering and Economic Evaluations, Volume I. Summary Report, USAEC Report DP-510, June 1960.
5. R. J. Gariboldi and D. R. Jacobson, Operational Tests of EBWR Vapor Recovery System, USAEC Report ANL-6189, Argonne National Laboratory, August 1960.
6. Argonne National Laboratory, The EBWR Experimental Boiling Water Reactor, USAEC Report ANL-5607, May 1957.
7. R. W. Atz, Testing of HNPF Freeze-Seal Pump, USAEC Report NAA-SR-4387, Atomics International, Nov. 1, 1960.
8. R. W. Atz, Performance of HNPF Prototype Free-Surface Sodium Pump, USAEC Report NAA-SR-4336, Atomics International, June 30, 1960.
9. Atomics International, Annual Progress Report—AEC Unclassified Programs for Fiscal Year 1960, USAEC Report NAA-SR-5350, August 1960.

Section XI

*HEAVY-WATER REACTORS**

The D_2O-moderated reactor is unique among current types in that it appears to be capable of extracting relatively high energy yields, in the range 8000 to 10,000 Mwd/metric ton, from natural-uranium fuel elements. The graphite-moderated reactors also operate with natural uranium, but achievable burnups appear to be considerably lower, for neutron-physics and metallurgical reasons. Much of the interest in D_2O-moderated reactors stems from the possibility of economic operation on natural uranium. This may be an overriding consideration in countries that have only a limited supply of enriched uranium, and in these countries there is a very strong incentive for the development of D_2O reactors. In the United States the use of natural uranium for reactor operation is not a strong incentive per se: it is an incentive only in so far as it can be shown to yield net economic benefits either now or in the future; similarly, interest in D_2O reactors is not limited to those using natural uranium. Opinion is not unanimous as to the economic consequences of natural-uranium operation. The Canadian work seems to indicate, for example, that natural-uranium reactors now can produce electricity at lower cost than enriched reactors. However, most studies in the United States have indicated that the power costs from D_2O-moderated reactors are somewhat higher than those from H_2O-moderated reactors and that, even for the D_2O-moderated reactors, the cheapest power results when slightly enriched fuel is used.

Reports have become available within the last few months on the various D_2O-moderated reactors under development or construction in the United States, and the Canadian effort has been reviewed in considerable detail in a recent issue of *Nucleonics*.[1] The purpose of the following discussion is to consider briefly the various factors affecting the economic prognosis for the D_2O reactor and to consider the basic incentives for D_2O-reactor development. Heavy-water reactors have been reviewed previously in the September 1958 issue of *Power Reactor Technology*, Vol. 1, No. 4, pages 59 to 63, and in the March 1960 issue, Vol. 3, No. 2, pages 52 to 58.

Economic Considerations

In the United States it is customary to make estimates and projections of the economic performances of various reactor types according to a set of more or less standard ground rules. Some of the past studies have shown the power cost estimates for D_2O reactors to be generally higher than those for a number of other types, as, for example, those for the H_2O-moderated and the organic-moderated reactors. In the face of these estimates, one may well ask what justi-

*Note added in proof: A significant new report on the economic potential of D_2O reactors has just been issued by Du Pont (L. Isakoff, Economic Potential for D_2O Power Reactors, USAEC Report DP-570, February 1961). It throws additional light on many of the economic questions discussed in this review, and discusses recent developments and analyses that have led to substantial reductions in the power cost estimates for D_2O reactors. It estimates that a total energy cost of 8.3 mills/kw-hr appears attainable in the first generation of a 300-Mw(e) base-load power reactor that is financed, built, and operated in accordance with private utility practice, that later plants of the type may produce electricity for 6.8 mills/kw-hr, and that further power cost reductions would result if a plutonium credit were accepted. It concludes that the economic potential of heavy-water power reactors appears to be as good as, or better than, that of other nuclear power plants. This report should be read in conjunction with the above review for the latest information on the subject, and for its relation to past work.

fication there is for a U. S. interest in D_2O reactors. To answer the question, the significance and validity of the estimates must be examined, and the possibility of incentives other than immediate economic ones must also be considered.

The higher power costs estimated for D_2O reactors can usually be attributed to higher estimated capital costs, which influence the power cost very strongly because rather high rates of charge against capital investment are assumed. Although these rates are set as part of the ground rules for the studies, they are probably realistic for power plants built and operated in this country by private enterprise. In addition, the large, expensive, D_2O inventory is usually considered a nondepreciable item and capital charges are assessed. So long as the construction and inventory costs of D_2O reactors are estimated to be higher than those for H_2O reactors — and this prediction seems to result consistently from all the U. S. studies — this disadvantage must be overcome by a lower fuel cost if the D_2O reactor is to compete economically. Hence the fuel cost for the D_2O plants is a key consideration; therefore, unless the fuel cost can be quite low, the reactor type does not appear to have a good chance of competing in the economic atmosphere of the United States. The Canadian workers arrive at a similar conclusion by a somewhat different route. They look directly at the question of economic competition between nuclear- and fossil-fuel plants. Since it is evident that the capital costs of nuclear plants must be considerably higher, they conclude that only nuclear plants capable of very low fuel costs have a chance of competing successfully. Again, fuel cost is a key consideration.

In the United States it is the fuel costs in the power cost estimates that are affected most strongly by government regulations. In cost estimates for the immediate future, these regulations are existing factors; when the same regulations are used to project costs far into the future, they can be considered only as "ground rules" for the study in question. These ground rules become very important when fuel costs for a low-enrichment or natural-uranium D_2O reactor are compared with those for an H_2O reactor of considerably higher enrichment. Few, if any, ground rules are necessary for the natural-uranium case. Natural uranium can be bought on the open market. Its price is set by the usual economic forces, and inventory expenses correspond to the usual expenses for working capital. For the case in which the spent natural-uranium fuel is not processed chemically for its plutonium content, no ground rules are really necessary. The fuel purchase price and interest rates are determined by the existing economic situation, and the remainder of the fuel cost estimate involves only estimates of a technical nature: fuel lifetime, fabrication costs, storage costs, etc.

In the case of partially enriched fuel, the net fuel cost contains four important components that can be considered to be based on ground rules because these components are not determined by the normal day-to-day interplay of economic forces: the uranium price, the rate of the inventory charge (or use charge), the plutonium buy-back price, and the chemical processing costs. These four items plus the fuel fabrication cost, when applied to the reactor fuel cycle, determine the net fuel cost. Although fabrication cost is a major contributor to fuel costs for current reactors, the indications are that the fabrication cost will be reduced substantially in future reactors, partly by reductions in unit costs but also, in enriched reactors, by increases in fuel lifetime. For example, even with the relatively conservative estimate of $70 per kilogram of uranium for a future fabrication cost, the contribution to total fuel cost will amount to only 0.5 mill/kw-hr if the fuel can be exposed to an average 20,000 Mwd/metric ton. This is a relatively minor contribution to a total cost between 2 and 3 mills/kw-hr. Thus in the future the fuel cost for enriched reactors will be determined largely by those cost components which involve the ground rules very strongly, whereas the fuel cost for natural-uranium reactors will depend (as it does now) on normal economic and technical factors.

Basic to all fuel costs is the cost of extracting uranium from the ground. Currently the extraction cost is decreasing, and the cost of U_3O_8 is expected by Lewis[2] to reach a minimum of about $6 per pound or less. However, if estimates of uranium reserves are at all reliable, the cost of U_3O_8 will increase as reactors begin to generate a major fraction of the power used in the United States (see Section I of this issue). The contribution of the basic cost of U_3O_8 to fuel costs (through burnup and inventory costs) appears to be less than 0.5 mill/kw-hr for the natural-uranium D_2O reactors. An increase by a factor of 2 would then amount to an increase

of less than 0.5 mill/kw-hr and could probably be tolerated by natural-uranium reactors as time goes on. To predict the effect on fuel costs of H_2O reactors, one would have to know what the appropriate ground rules are. Questions of this sort are very important for future estimates, even though they may affect only relatively small fractions of the total power cost. According to present estimates, fuel costs in the 1- to 1.5-mill range, determined strongly by fabrication costs, can be predicted for D_2O reactors. Fuel costs in the 2- to 3-mill range, determined largely by ground rules, can be predicted for H_2O reactors. Thus there appears to be about a 1 mill/kw-hr difference in favor of the D_2O reactor. Out of this advantage the D_2O reactor must make up whatever other economic deficiencies it has, such as higher capital costs and costs associated with the use of D_2O. If the fuel cost difference is really 2 or 3 mills, rather than 1 mill, then the relative economic positions of the two reactor types may be quite different.

One of the advantages claimed by the Canadian workers for natural-uranium fuel over enriched fuel is a lower unit fabrication cost because of the absence of criticality hazards and accountability requirements. These do appear to be important factors, but it is questionable whether they can be taken into account fully in economic studies that are based on fabrication quotations from existing U. S. fuel fabricators, who are in the business of handling enriched fuel. If the natural uranium is fabricated in a plant that normally handles enriched fuel, then at least part of the cost penalties of criticality hazards and accountability routines are probably built into the plant, and their cost will probably be shared by the natural-uranium process.

Finally it must be recognized that the design limitations on natural-uranium reactors are very much more rigid than those on enriched-uranium reactors. The simultaneous attainment of high thermal performance, long reactivity lifetime, and low construction cost in a natural-uranium reactor calls for the most skillful design and for the meticulous attention to detail which can usually be applied only in the stage of detailed design. Although much work has been done in the United States on D_2O reactors, much of it has been rather general research and development. The economic evaluations have, in general, been based on conceptual designs which have been made by Du Pont, Sargent & Lundy, and Nuclear Development Corporation of America at various times since early 1958. The Canadian work, however, has culminated in a rather definite design for a large reactor, optimized (for the Canadian economy) with respect to a number of design variables, and worked out in considerable detail.

Other Incentives for D_2O Reactors

Among the heterogeneous thermal reactors, those moderated by D_2O appear to have the highest potential neutron economy and are probably capable of the highest fuel utilization (i.e., extraction of the greatest amount of energy from each pound of uranium mined) on any given fuel cycle. In addition this advantage should be accentuated if plutonium is recycled, because the neutron temperature can be kept low in "cold moderator" designs to minimize the effects of the low η of Pu^{239} in the region of its 0.3-ev resonance. The relatively small (absolute) effect of uranium price on fuel costs for natural-uranium D_2O reactors has been mentioned above. If plutonium is recycled, the sensitivity to uranium cost is reduced further; it seems probable that, if plutonium recycle were developed to the point of economic feasibility, D_2O reactors could afford to use the relatively expensive uranium that constitutes the major portion of the U. S. reserve. So the good neutron economy of the D_2O reactor may be regarded as a long-term advantage in either of two ways: as one means, short of breeding, of conserving and extending our usable uranium resources, or as a characteristic which can guarantee the D_2O reactor an economic fuel supply long after the fuel for reactors of lower neutron economy has become prohibitively expensive. Although these two statements are more or less equivalent, they may inspire different courses of action. If conservation is considered important enough, a strong development effort on D_2O reactors may be supported for this reason alone; if not, the development of D_2O reactors in the United States may be slow until shortages of low-cost uranium are imminent.

Canadian D_2O-Cooled Reactors

The Canadian concept for D_2O-cooled power reactors is embodied in a 20-Mw(e) prototype plant,[3] NPD-2 (under construction and scheduled

to begin operating in 1961), and in plans for a full-scale plant, CANDU[2] (currently under design). Among the characteristic features of the concept are horizontal pressure tubes operating at a temperature near the coolant temperature, with the cool D_2O moderator contained in a low-pressure calandria tank and with the gas spaces between calandria tubes and pressure tubes serving as thermal insulation. The D_2O coolant does not boil. Fuel consists of UO_2 pellets in Zircaloy tubes, the tubes being clustered in bundles, typically of 19 tubes in a bundle, spaced by spiral Zircaloy wires welded to the Zircaloy jackets. Close approximation to uniformly graded fuel irradiation is achieved by on-power, bidirectional, push-through refueling. New fuel bundles are pushed in, as needed, at the charging ends of the pressure tubes, displacing spent bundles, which are removed from the opposite ends of the tubes. Adjacent pressure tubes in the reactor lattice have their charge-discharge ends inverted so the fuel bundles progress through the reactor core in opposite directions in adjacent tubes. This requires a charge-discharge machine at each end of the reactor. The coolant flow is also bidirectional, being in each tube in the direction opposite to that of fuel flow.[4]

The continuous refueling scheme eliminates the need for all but a minor amount of reactivity control capacity in the reactor during equilibrium operation. Absorbing rods are used for shimming, enriched-uranium "booster" rods are used to overcome xenon transients, moderator dump is used as a rapid shutdown mechanism, and soluble poison ($CdSO_4$) is added temporarily to the moderator as extra shutdown capacity for cold startup.

Careful attention has been given in the CANDU design to optimization and to the minimization of neutron losses. As a result an average fuel exposure of 9750 Mwd/metric ton is predicted with confidence for the equilibrium reactor. The system has also been designed for rather high thermal efficiency within the limitations of the pressurized-water concept. A steam throttle temperature of 482°F is used, from which the power conversion system, employing a reheat cycle, attains a steam-cycle efficiency of 33.34 per cent, for an over-all station efficiency of 29.1 per cent. The major characteristics of the CANDU plant are summarized in Table XI-1.

U. S. Work at Savannah River

In the United States the AEC-sponsored program on heavy-water reactors is directed by the Savannah River Operations Office, and an important portion of it is carried out by Du Pont at the Savannah River Laboratory. This program is still a rather general one, and although the Heavy-Water Components Test Reactor (HWCTR) (reviewed in the March 1960 issue of *Power Reactor Technology*, Vol. 3, No. 2, pages 54 and 55) is under construction as part of the program and is scheduled for operation in 1961, it is not a power-reactor prototype but a high-temperature nuclear test facility, which incorporates many of the features typical of D_2O reactors and provides a means of testing reactor components and fuel elements. The fuel program connected with this effort has given much attention to metallic fuels, and particularly to tubular elements of uranium containing a small percentage of zirconium, clad with Zircaloy. The hope for a low fabrication cost stems from the possibility of forming clad tubular elements of full reactor length by coextrusion, thus minimizing the fabrication work per pound of fuel. This approach is in striking contrast to the Canadian approach, in which the relatively short length of the oxide fuel-element bundles is given credit for reducing fabrication costs by minimizing the size of the required fabrication plant.[6] The relatively short metallurgical lifetime of the metallic fuel is, of course, a disadvantage, and oxide elements made by a combination of vibratory compaction and swaging are also under development at Savannah River Laboratory.

A number of design studies and power cost estimates have been made for various types of D_2O-moderated reactors. Reference 7 is a comprehensive study by Du Pont but is limited in its current applicability since it is rather outdated. Three of these reactor concepts were evaluated in more detail by Sargent & Lundy, and the power cost estimates are contained in references 8 and 9. The three concepts evaluated are for:

1. A boiling-D_2O-cooled, direct-cycle, pressure-tube, cold-moderator reactor.
2. A liquid-D_2O-cooled, pressure-vessel, hot-moderator reactor.
3. A liquid-D_2O-cooled, pressure-tube, cold-moderator reactor.

Table XI-1 PLANT CHARACTERISTICS OF D_2O-MODERATED POWER REACTORS FUELED WITH NATURAL URANIUM

	CANDU[1]	Direct-cycle[5] boiling D_2O
	General	
Net electrical output, Mw	203	224
Coolant	Liquid D_2O	Boiling D_2O
Reactor type	Pressure tube, cold moderator	Pressure tube, cold moderator
Fuel enrichment	Natural U	Natural U
Core inventory, tons* of U	45.8	65.6
D_2O inventory, tons*	198	294
Over-all thermal efficiency, %	29.1†	28.4
	Reactor	
Orientation	Horizontal	Vertical
Gross thermal power, Mw	698	790
Fuel configuration	19-rod bundles	37-rod bundles
Number of fuel assemblies	12 in each of 306 pressure tubes	2 in each of 268 fueled pressure tubes
Lattice spacing, in.	9, square	11.1, triangular
Core diameter, ft	~14.8	16.4
Core height, ft	~16.4	17.7
Average moderator temp., °C	Cool	68
Reactor power to moderator, %		7
Maximum heat flux, Btu/(hr)(sq ft)	333,000	325,000
Average specific power, Mw/ton* of U	15.2	12.0
Hot excess k (operating)	Small	0.032
Average fuel exposure, Mwd/ton* of U	8870	6820
Steam quality (reactor exit), %		14
Inlet pressure, psig	1473	825
Diameter, ft	19.67 (OD)	18.4 (ID)
	Fuel Assembly	
Calandria tube material	Zircaloy-2	Al
Calandria tube ID, in.	4.20 (tentative)	5.72.
Calandria tube OD, in.	4.30 (tentative)	5.84
Pressure tube material	Zircaloy-4	Zircaloy-2
Pressure tube ID, in.	3.25	4.65
Pressure tube OD, in.	3.564 (tentative)	4.97
Fuel material	UO_2	UO_2
Fuel pellet diameter, in.		0.50
Fuel cladding material	Zircaloy-4	Zircaloy-2
Fuel cladding thickness, in.	0.025 or less[6]	0.025
Fuel rod OD, in.	0.60 (reference 6)	
	Primary Cooling System	
Flow to reactor, gal/min	55,800	23.4×10^6 lb/hr = 60,000 gal/min
Number of cooling loops	8	2
Temp. entering reactor, °C	249	259
Temp. leaving reactor, °C	293	268
Over-all pressure drop, psi	163 (reactor only)	
Area of steam generators, sq ft	74,500 (boiling) 11,050 (preheating)	
Construction material, cooling system	Carbon-steel main piping, Monel boiler tubes	Steam piping, 1¼% Cr–½% Mo grade P-11 carbon steel; recirculating piping, type 304 stainless steel
	Electrical Generation Plant	
Steam to turbine throttle, lb/hr	2.56×10^6	3.27×10^6
Turbine throttle pressure, psig	565 (saturated)	750
No. of turbines	1	1
Gross steam-cycle efficiency, %	33.34	
Gross electrical output, Mw	220	
Steam cycle	Reheat	Direct, D_2O steam
Reheat pressure, psig	53	
Reheat temp., °C	221	
Condenser backpressure, in. Hg	1	1.5

*One ton = 2000 lb.

†Including effect of heat losses to cold moderator.

The concept of using full-reactor-length fuel elements leads to further differences between the U. S. and Canadian approaches. In particular, on-power fueling is less attractive with the full-length design, both because the potential benefits are less and because the difficulties are greater. The U. S. designs do not include on-power fueling, although reference 8 indicates that it is by no means ruled out as a future possibility.

Another striking difference between the two approaches is the use, in the Du Pont indirect-cycle designs, of relatively low steam pressures and consequently relatively low thermal efficiencies. For example, in the nonboiling pressure-tube designs, the steam pressure at the turbine throttle ranges from 170 to 262 psig, saturated in all cases, and the gross steam-cycle efficiency ranges from 24.8 to 26.8 per cent. These quantities can be compared with the Canadian throttle pressure of 580 psia and with the Canadian gross steam-cycle efficiency of 33.34 per cent. This difference can be traced further back into the system in terms of differences in primary coolant pressure, the Du Pont pressures lying in the 800-psi range and the Canadian pressures lying in the 1400-psi range. In the direct-cycle boiling-D_2O design, which was judged in reference 8 to be economically the most promising, the turbine throttle pressure was, of course, relatively high, 780 psig, nearly equal to the pressure in the reactor. The gross steam-cycle efficiency for this case was 30.0 per cent. The concept of the direct-cycle system does not appear to invite such cycle refinements as the reheat used in the Canadian design, although a study reported in reference 9 indicated that a net decrease in power cost of 0.042 mill/kw-hr resulted from the use of two-stage reheat with moisture removal, due to a decrease in turbine cost.

The large pressure-tube designs described in reference 7 do not employ calandria tanks for the moderator. They use the "cold-tube" design, with the pressure tubes in direct contact with the cool moderator. Heat loss from the coolant D_2O to the pressure tubes is retarded by thin Zircaloy liner tubes which provide layers of nearly stagnant D_2O adjacent to the internal pressure-tube walls. The axes of the reactors are vertical rather than horizontal. The nonboiling systems use upper (inlet) and lower (outlet) plenum chambers for distribution and collection of the coolant, to and from the pressure tubes, whereas the boiling systems (at least in the larger sizes) utilize individual feeder and collector tubes to distribute the coolant from bottom headers to the pressure tubes and to collect the steam-water mixture into headers from the tops of the pressure tubes. Refueling is from above, and vertical control rods are also driven from above.

The concept of full-reactor-length fuel elements extends to the work on swaged oxide elements, as well as to the metallic elements, although the possibility of half-length elements, which can be inverted during their exposure lifetime to distribute the exposure more uniformly over the length, is also considered. In the metallic-element development effort, more than 50 of the tubular elements (2.06 in. in outside diameter, 1.47 in. in inside diameter, and 10 ft long) have been manufactured, by the co-extrusion process, by Nuclear Metals. These tubes are typical of those which might be used in combination with others of larger and smaller diameter to give complete fuel assemblies consisting of from two to four coaxial tubular elements. So far as the manufacture of such elements is concerned, the fundamentals of the process are considered to have been adequately demonstrated, but additional development is needed to improve production yield and quality.[8] In-pile testing of the elements under power-reactor conditions has been very limited, and the need for such tests is one of the major reasons for construction of the HWCTR.

The cost of fabricating the metallic fuel elements will, of course, depend strongly on the production rate. It is estimated[8] that the cost of an initial lot of 400 tubes, which would constitute one charge for a 100-Mw(e) reactor, might be about $70 per kilogram of uranium, excluding the uranium cost but including the cost of zirconium and of material losses. The cost of subsequent lots of the same magnitude is estimated at $20 to $45 per kilogram, and substantially higher production rates—of the order of 2000 tubes per year—might reduce the cost to about $15 per kilogram.

In the oxide development effort, the emphasis is again on tubular elements, with the objective of reducing the number of individual fabrication operations to a minimum. The method under development is that of vibratory-compacting and cold-swaging a tubular assembly of oxide, jack-

eted with Zircaloy, to produce the desired oxide density. The reference element for the development is a tube 2.06 in. in outside diameter, 1.47 in. in inside diameter, and 14.7 ft long, with 0.025 in. of Zircaloy-2 as the jacket. Estimates of the cost of producing such elements, from reference 8, are tabulated in Table XI-2, along with estimated costs for swaged rod type elements and costs for rod type elements produced by the conventional method of canning sintered UO_2 pellets in Zircaloy tubes. The estimates were derived from fabrication experiments at Savannah River Laboratory and from cost data supplied by prospective fabricators and by power-reactor operators, as of the time of preparation of reference 8—late 1959 or early 1960. They were considered to be representative of commercial prices for completely assembled fuel elements in lots of 20 to 50 tons.

On the basis of such estimates, the metallic elements appear to be considerably cheaper than the oxide elements, per pound of uranium; but this advantage could be nullified if the permissible exposure of the metal elements were limited to a sufficiently low value by metallurgical considerations. Figure XI-1 illustrates the situation. The plotted points represent possible combinations of fabrication cost and fuel exposure for metallic and oxide elements, the exposure limit being set for the metallic elements by metallurgical and fission-damage considerations, and the limit for the oxide element being set by reactivity lifetime in a natural-uranium reactor. It is evident that the permissible exposure is as important as the fabrication cost in determining the most desirable element type. However, since reactivity considerations set a limit of something less than 10,000 Mwd/ton on the oxide elements, it is also evident that metallic elements have a much better chance of competing in natural-uranium reactors than in enriched reactors.

Although the fuel costs indicated in Fig. XI-1 are for natural-uranium fuel, they assume processing of the spent fuel for its plutonium content, which is estimated to yield a net saving in fuel cost of about 0.5 mill/kw-hr. They are based also on the AEC price of $40.50 per kilogram for natural uranium, whereas the free market price for natural uranium is said to be about $30.10 per kilogram. The difference between these two uranium prices represents a difference of about 0.2 mill/kw-hr in fuel cost.

The total power costs, as estimated in reference 8, for three reactor types* are summarized in Table XI-3. These estimates, like the previous NDA–Sargent & Lundy study,† show a clear-cut economic advantage for the direct-cycle boiling-D_2O pressure-tube reactor. There are, of course, technical uncertainties that could affect the estimates. The most important of these probably are the problems of preventing excessive D_2O losses in the steam system and the question of the power coefficient of reactivity in a boiling-D_2O reactor. The results of the tests on the EBWR vapor-recovery system (reviewed in Section X of this issue of *Power Reactor Technology*) are encouraging with respect to the leakage problem, and more recent Savannah River Laboratory studies[5] indicate also that the problem will not be a difficult one. Theoretical analyses indicate that both oxide-fueled and metal-fueled reactors will have small but positive steam coefficients of reactivity for steam formed within the pressure tubes. In the case of oxide fuel, the indications are that this positive coefficient will be overridden, by a wide margin, by the negative fuel temperature coefficient of reactivity (Doppler effect) to give a net negative power coefficient of reactivity. The case for the metal-fueled reactor is not so favorable and is still considered to represent an uncertainty in the feasibility of the concept.

Although, in the liquid-cooled class, the pressure-vessel reactor shows a slightly lower power cost than the pressure-tube reactor, the footnote in Table XI-3 indicates that design changes would be necessary to satisfy reactivity requirements and that these changes would increase the cost. Although the table indicates that vessel size may be a feasibility problem in

*Reference 7 states that the designs used for the cost estimates in reference 8 were, in general, compatible with the Du Pont designs in reference 7. The details of the designs upon which the cost estimates are based are contained in a Sargent & Lundy report,[9] TID-8530. The major qualitative departures from the Du Pont designs are the use of a calandria ("hot-pressure tube" design) and the use of fuel elements which consist of 37-rod bundles. The elements of the bundle are Zircaloy-2 tubes containing UO_2 pellets of 0.50-in. diameter.

†One of a series of studies made in 1958 as authorized by Public Law 85-590; the results of this study were published as TID-8503. This series of studies was reviewed in the September 1959 issue of this journal (Vol. 2, No. 4, pp. 1 to 30).

Table XI-2 DU PONT ESTIMATES OF FABRICATION COSTS FOR URANIUM OXIDE[8]

Bases: All Costs Are in Dollars Per Kilogram of Uranium, Excluding Fabrication Losses and Shipping Costs
Rod Dimensions: 0.55 In. in Outside Diameter, 0.025-In. Zircaloy-2 Cladding, 14.7 Ft Long (One-Segment Rod)
Tube Dimensions: 2.06 In. in Outside Diameter, 1.47 In. in Inside Diameter, 0.025-In. Zircaloy-2 Cladding, 14.7 Ft Long

	One-segment swaged tubes (90% density)	One-segment swaged rods†‡ (90% density)	Two-segment swaged rods†‡ (90% density)	Two-segment sintered rods‡ (95% density)
Oxide preparation*	4.50	4.50	4.50	
Primary fabrication	1.00– 1.50	2.50– 3.00	2.50– 3.00	9.00– 11.00
Welding, machining, etc.	1.00– 1.25	2.00– 2.50	4.00– 5.00	4.00– 5.00
Cleaning, handling, etc.	1.75– 2.25	5.50– 6.50	5.50– 6.50	5.50– 6.50
Autoclaving	3.00– 4.00	3.50– 5.00	3.50– 5.00	3.50– 5.00
Inspection	2.25– 3.25	4.50– 6.50	6.50– 10.00	6.50– 10.00
Total fabrication	13.50–16.75	22.50–28.00	26.50– 34.00	28.50– 37.50
Zircaloy cladding and end plugs§	11.00–18.75	10.75–14.50	11.75– 16.50	11.75– 16.50
Other hardware (spacers, end fittings, etc.)	2.75	7.00	10.00	10.00
Total cost, excluding uranium	27.25–38.25	40.25–49.50	48.25– 60.50	50.25– 64.00
Uranium*	40.50	40.50	40.50	40.50
Total cost, including uranium	67.75–78.75	80.75–90.00	88.75–101.00	90.75–104.50

*It is assumed that uranium is available from government facilities at the AEC "ground-rule" price of $40.50 per kilogram of uranium and that this price includes those processing steps which can be carried out at such facilities.

†Costs for vibratory compaction are expected to be essentially the same as those tabulated for swaging.

‡Fabrication costs for oxide rods increase as the diameter of the rod decreases. The cost of an oxide rod 0.3 in. in diameter is estimated to be 1.5 to 1.8 times that of a 0.5-in. rod, on a unit-weight basis.

§Zircaloy sheathing is expected to cost $30 to $50 per pound in the large size required for oxide tubes and $30 to $45 for oxide rods.

Table XI-3 SUMMARY OF CAPITAL AND OPERATING COSTS FOR 300-Mw(e) D_2O-MODERATED AND -COOLED REACTOR PLANTS (AS OF DECEMBER 1959)[8]

	Costs,* mills/kw-hr				
	Plant capital	D_2O inventory	Total fuel	Operation, maintenance, and insurance	Total power
Boiling-D_2O-cooled, pressure-tube, direct-cycle, cold-moderator reactor:					
Oxide fuel	5.0	1.4	2.0	1.1	9.5
Metal fuel	5.0	1.1	1.7	1.1	8.9
Liquid-D_2O-cooled, pressure-vessel, indirect-cycle, hot-moderator reactor:					
Oxide fuel	5.7	1.5	2.1	1.2	10.5†
Metal fuel	5.1	1.1	2.4	1.1	9.7
Liquid-D_2O-cooled, pressure-tube, indirect-cycle, cold-moderator reactor:					
Oxide fuel	5.7	1.5	2.3	1.1	10.6
Metal fuel	5.4	1.2	2.1	1.1	9.8

*Cost data for metal-fueled plants are on the basis of an average fuel exposure of 3300 to 5100 Mwd per metric ton of uranium, which corresponds with 100 per cent batch discharge. Cost data for oxide-fueled plants are on the basis of an average fuel exposure of 7800 to 8800 Mwd per metric ton of uranium, which requires a multizone fuel discharge.

†For illustrative purposes only. Design changes to satisfy reactivity requirements would increase this cost. Vessel size may be a feasibility problem.

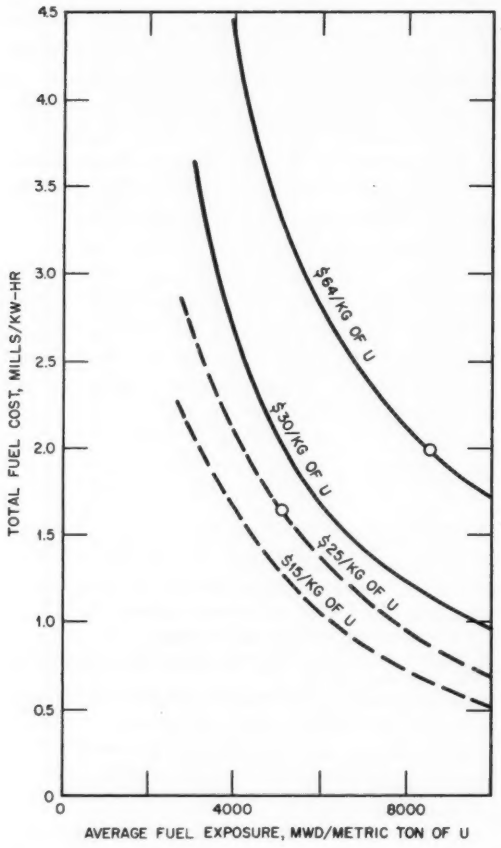

Fig. XI-1 Effect of type of fuel and exposure on total fuel cost for a boiling-D_2O 300-Mw(e) direct-cycle plant.[8] O, bases for power cost estimates. ——, UO_2. ---, metallic U. The fabrication cost appears on each curve.

the 300-Mw(e) power range, the studies reported in reference 7 show that there is some possibility of extending the pressure-vessel concept up to the 400-Mw(e) range without exceeding the capabilities of existing vessel fabrication equipment. It is stated that at least one manufacturer can shop-anneal a vessel with a maximum outside diameter of 19 ft. A possible vessel of this size, with a reactor core to furnish heat for a 400-Mw(e) plant, is shown in Fig. XI-2. The design pressure is relatively low (900 psi), and a very high power density, which may involve feasibility questions, is required to yield the necessary output.

Sargent & Lundy and NDA have continued the development of design studies and cost estimates for the Commission and have issued the reports listed as references 5 and 10, which contain the most recent and up-to-date U. S. estimates on large D_2O-cooled reactors. Reference 5 presents revised cost estimates for direct-cycle boiling-D_2O plants in the 200- and 300-Mw(e) sizes, including the effects of design improvements that evolved initially for a reactor of smaller (prototype) size. The improvements include changes in the header system for the pressure tubes, changes in the handling of the feed water to decrease the D_2O inventory and to increase the cycle efficiency, and rearrangements of equipment to decrease building sizes. The reference[5] also describes investigations that have been carried out by Sargent & Lundy on the leakage of D_2O from equipment components, on construction materials for D_2O reactor plants, and on plant arrangements.

In reference 10 an indirect-cycle boiling-D_2O reactor of 200-Mw(e) output is considered, and its estimated power cost is compared with that of the direct-cycle plant. Although the indirect cycle reduces the D_2O inventory, reduces the number of potential points of D_2O leakage, and reduces the amount of steam drying equipment needed, these advantages are offset by the costs resulting from the addition of steam generators and by the lower pressure and temperature of the steam generated. The net effect on the power cost estimates was a difference of about 0.1 mill/kw-hr in favor of the direct-cycle plant. This difference was considered to be less than the uncertainty of the estimates.

The reactors considered in references 5 and 10 are of the calandria type, with vertical axes, employing UO_2 fuel elements in the form of 37-rod bundles of half core height. The refueling scheme is a four-zone radial shift program, with axial inversion of the fuel bundles to flatten the axial burnup distribution. The major characteristics of the direct-cycle reactor are listed in Table XI-1, along with the corresponding values for the CANDU reactor. The reactor characteristics are the same for the indirect-cycle design, but a single D_2O steam separation drum is used instead of two drums as in the direct-cycle case. The D_2O steam flows at a rate of 3.34×10^6 lb/hr to the tube side of the secondary steam generators, where it is condensed and subcooled to 485°F. The recirculating coolant is subcooled to 500°F in the secondary feed-water preheater, after which it is mixed with the D_2O condensate at the suction of the recirculation pumps. The pumps discharge

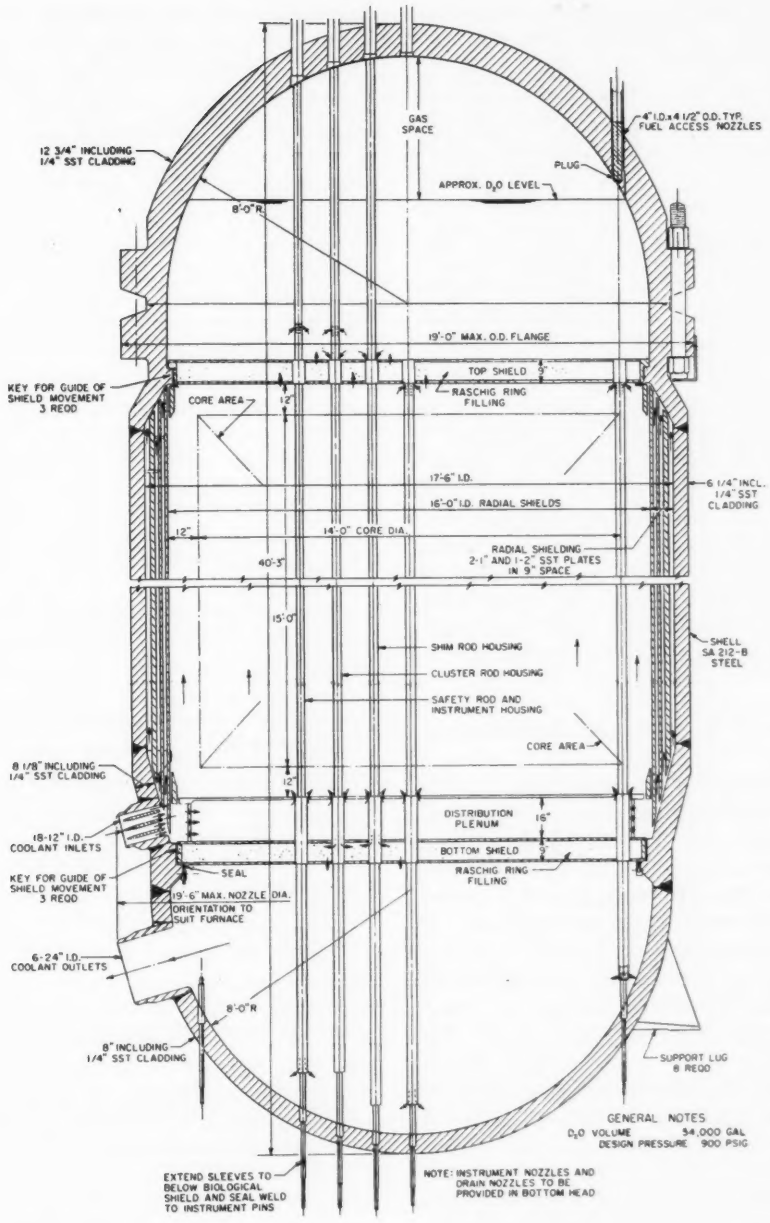
GAS SPACE
4" I.D.x4 1/2" O.D. TYP. FUEL ACCESS NOZZLES
12 3/4" INCLUDING 1/4" SST CLADDING
PLUG
APPROX. D2O LEVEL
8'-0"R
19'-0" MAX. O.D. FLANGE
TOP SHIELD 9"
KEY FOR GUIDE OF SHIELD MOVEMENT 3 REQD
CORE AREA 12"
RASCHIG RING FILLING
17'-6" I.D.
6 1/4" INCL. 1/4" SST CLADDING
16'-0" I.D. RADIAL SHIELDS
12"
14'-0" CORE DIA.
40'-3"
RADIAL SHIELDING 2-1" AND 1-2" SST PLATES IN 9" SPACE
15'-0"
SHIM ROD HOUSING
SHELL SA 212-B STEEL
CLUSTER ROD HOUSING
SAFETY ROD AND INSTRUMENT HOUSING
CORE AREA
8 1/8" INCLUDING 1/4" SST CLADDING
12"
DISTRIBUTION PLENUM 16"
18-12" I.D. COOLANT INLETS
BOTTOM SHIELD 9"
SEAL
KEY FOR GUIDE OF SHIELD MOVEMENT 3 REQD
RASCHIG RING FILLING
19'-6" MAX. NOZZLE DIA. ORIENTATION TO SUIT FURNACE
6-24" I.D. COOLANT OUTLETS
8'-0"R
8" INCLUDING 1/4" SST CLADDING
SUPPORT LUG 8 REQD
GENERAL NOTES
D2O VOLUME 54,000 GAL
DESIGN PRESSURE 900 PSIG
EXTEND SLEEVES TO BELOW BIOLOGICAL SHIELD AND SEAL WELD TO INSTRUMENT PINS
NOTE: INSTRUMENT NOZZLES AND DRAIN NOZZLES TO BE PROVIDED IN BOTTOM HEAD

Fig. XI-2 Nineteen-foot pressure vessel with core outline for 400-Mw(e) reactor.[7]

the coolant to the reactor inlet header at a temperature of 498°F and a flow rate of 23.4×10^6 lb/hr. The secondary steam has throttle conditions of 480°F and 566 psia. The net plant output is 223.6 Mw(e), giving a net plant efficiency of 28.3 per cent. One of the reasons for the smallness of difference between this efficiency and that of the direct-cycle plant (Table XI-1)

Table XI-4 SUMMARY OF CAPITAL AND OPERATING COSTS FOR BOILING-D_2O PRESSURE-TUBE REACTOR PLANTS OF 200-Mw(e) CAPACITY[10]

	Direct cycle			Indirect cycle		
	Investment, $10^6	Annual cost, $10^6/year	Power cost, mills/kw-hr	Investment, $10^6	Annual cost, $10^6/year	Power cost, mills/kw-hr
Plant	57.141	8.000	5.097	62.050	8.686	5.547
D_2O	16.500	2.060	1.310	12.970	1.621	1.034
Fuel		3.336	2.124		3.336	2.133
Operation and maintenance		1.492	0.947		1.369	0.873
Insurance		0.490	0.312		0.490	0.313
	73.641	15.378	9.790	75.020	15.502	9.900

is that the latter has been arbitrarily reduced by 1 per cent as a contingency because of lack of experience with the direct-cycle D_2O system.

The estimated power costs for the direct-cycle and indirect-cycle plants are given in Table XI-4. These are "current economic status" estimates (they were intended to be applicable for reactors that could be in operation in 1963). Reference 10 contains also an estimate for a 300-Mw(e) direct-cycle plant. The total power cost is estimated as 8.8 mills/kw-hr.

Canadian and U. S. Cost Estimates

Although the power cost estimates of Table XI-4 are encouraging, they appear inconsistent with the Canadian estimates that D_2O reactors can compete with fossil-fuel plants in the near future. Much of this difference is said to be due to differences in nontechnical economic factors between the United States and Canada. Reference 8 states that, if the U. S. cost estimates for a 200-Mw(e) oxide-fueled boiling-D_2O reactor are converted to the Canadian basis, the following changes in power cost result: capital investment decreases 20 per cent; operating and materials costs decrease 36 per cent; and the power cost decreases 48 per cent. In Table XI-5 the bases for computing power costs in the United States and in Canada, as given in reference 8, are tabulated. It is obvious that the differences are large. A further illustration of these differences is given in Table XI-6 from reference 8. This table summarizes the results of converting the cost data from an earlier boiling-D_2O design study (reference 11) to the Canadian cost base. The total power cost as estimated in reference 11, on the U. S. cost base, was 11.6 mills/kw-hr. As a reference point, Table XI-6 includes also an estimate of the

Table XI-5 COMPARISON OF BASES FOR COMPUTING POWER COSTS IN THE UNITED STATES AND CANADA[8]

	United States (S&L-NDA)	Canada (AECL-CANDU)
Plant load factor	0.8	0.8
Fixed charges:		
Reactor and auxiliaries, %/year	14.0	9.31
Buildings and plant services, %/year	14.0	6.13
D_2O, %/year	12.5	5.43
Fuel inventory charge for fabrication cost and nonnuclear material, %/year	12.0	4.0
Fuel inventory charge for fissionable material, %/year	4.0	4.0
D_2O cost, $/lb	28.00	28.00
Fuel-element costs, $/kg of U (both for natural UO_2):		
Uranium cost	40.50	30.10
Pelletizing	12.50	8.80
Zircaloy-2 and fabrication	48.75	30.10
Losses and shipping	7.80	
Total fuel replacement cost, $/kg of U	109.55	69.00

Table XI-6 SUMMARY OF ESTIMATED COSTS OF 200-Mw(e) PLANTS BUILT IN CANADA[8]

	Estimated costs, mills/kw-hr	
	U. S.-designed boiling-D_2O plant*	CANDU plant
Plant capital cost	2.5	2.6
D_2O inventory	0.7	0.5
Fuel cost	1.6	1.1
Operation, maintenance, and supplies	1.0	1.4
Total power cost	5.8	5.6

*Built and operated in Canada.

power cost for the CANDU reactor. The latter appears to be reasonably consistent with more recent Canadian estimates for the same plant.[2]

To sum up, it can be said that U. S. estimates of the capabilities and costs of D_2O-cooled reactors do not appear to be inconsistent with the Canadian estimates when basic economic differences between the two countries are taken into account. This does not mean that the conceptual designs on which the U. S. estimates are based are necessarily the economic equivalents of the Canadian design. But the elimination of the possibility that there is a large discrepancy between Canadian and U. S. estimates of the basic technological potentialities of the D_2O reactor should be an important step toward a sound evaluation of the reactor type for the U. S. program.

Other D_2O-Cooled Reactors

The other U. S. effort aimed specifically toward development of a D_2O-cooled power reactor is that of Carolinas-Virginia Nuclear Power Associates, Inc.[12] This group is having a prototype reactor built at the Parr, S. C., station of the South Carolina Electric and Gas Company. The reactor [called the Carolinas-Virginia Tube Reactor (CVTR)] is financed by the AEC, and the research and development for it are being carried out by the Westinghouse Atomic Power Department, which is also designing the prototype reactor. The Stone & Webster Engineering Corporation is providing architect-engineer services.

The reactor is cooled by liquid D_2O and will operate at a heat output of about 61.9 Mw, producing secondary steam at about 600 psi. The steam is throttled to a pressure of about 400 psi and is superheated to 725°F in an oil-fired superheater to match the inlet conditions of an existing turbine. The turbine will produce 19,070 kw (gross) for a net output of 17,170 kw. The reactor is of the pressure-tube type, employing the cold-tube concept, with internal thermal insulation in the form of stagnant layers of D_2O. The reactor design is distinguished by the employment of a U-tube arrangement of its pressure tubes. The pressure tubes are hung in the D_2O tank and are arranged in pairs, with the bottom ends of each of the two tubes in a pair connected by a U bend. Both legs of the resulting U tube contain fuel assemblies, and coolant D_2O enters the top of one leg of the U and leaves at the top of the opposite leg. Thus the coolant makes a double pass through the reactor, the number of inlet and outlet connections is only half the number required for a straight-through design, and all inlet and outlet connections are located at the top of the reactor. Refueling, which requires reactor shutdown, is carried out with a shielded cask at the top of the reactor. Control rods are actuated from below. Inlet and outlet connections to the U tubes are made through individual connector tubes which are collected into inlet and outlet headers. The fuel assemblies are full core length and consist of 19-rod bundles, the rods consisting of UO_2 pellets canned in Zircaloy tubes having a 0.500-in. outside diameter. The rods are spaced in the bundle by spirally wound spacer wires.

The U-tube concept of the Carolinas-Virginia reactor has certain obvious advantages. It also places certain restrictions on other features of the design. For example, refueling must always be from the top of the reactor. In a very large reactor, the pressure drop associated with the two-pass arrangement could lead to some performance restrictions. Whether considerations of these types are important is not clear at the moment from the published literature.

The Plutonium Recycle Test Reactor (PRTR) under construction at Hanford is also a high-temperature D_2O-cooled and -moderated reactor. Although this reactor is being built primarily for studies of plutonium recycle and will not produce electric power, it may nevertheless give useful information on some of the problems of D_2O reactors. This reactor is described in reference 13, which was reviewed in the June 1960 issue of *Power Reactor Technology*, Vol. 3, No. 3, page 53.

Some of the major characteristics of the D_2O reactors now under construction in the United States and Canada are listed in Table XI-7.

Outside the United States and Canada, D_2O-cooled pressure-vessel reactors are under construction, for power generation and district heating,[14,15] in Sweden; and the boiling-D_2O reactor,[16] a pressure-vessel type, has recently gone into operation at Halden, Norway.

Other Coolants

For D_2O-moderated reactors, the coolants other than D_2O which have received most at-

Table XI-7 DESCRIPTION OF D_2O-MODERATED AND -COOLED POWER REACTORS AUTHORIZED FOR CONSTRUCTION[8]

	HWCTR	NPD-2	CVTR	PRTR
Designer	Du Pont	AECL	Westinghouse	General Electric
Forecast startup date	1961	1961	1962	1960
Site	Savannah River	Ontario, Canada	Parr, S. C.	Hanford
Objective	Test	Demonstration	Demonstration	Pu recycle study
Description:				
Category	Enriched U	Natural U	Enriched U	Pu and natural U
Reactor design	Pressure vessel	Pressure tube	Pressure tube	Pressure tube
Moderator temp., °F	~475	<200	<200	<200
Coolant	Liquid D_2O*	Liquid D_2O	Liquid D_2O	Liquid D_2O
Coolant circulation	Forced	Forced	Forced	Forced
Fuel material	†	UO_2	UO_2	Pu-Al + UO_2
Fuel shape	†	Rods	Rods	Rods or tubes
Fuel cladding	†	Zircaloy	Zircaloy	Zircaloy
Refueling plan	Batch	On-power	Batch	Batch
Plant steam cycle	None	Indirect	Indirect	Indirect
Steam condition		Saturated	Superheated‡	Saturated
Design parameters:				
Power, Mw(e) (net)	None	19.3	17.0	None
Thermal power, Mw	61	88.9	61.9	70
Reactor pressure, psig	1500	1070	1500	1050
Coolant discharge temp., °F	545 max.	530	555	530
Equivalent core diameter, ft	3.3	11.1	6.1	6.5
Core height, ft	9.4	12.6	8	7.3
Maximum heat flux, Btu/(hr)(sq ft)	†	158,000	343,000	330,000 (rods) 400,000 (tubes)
Design exposure (average), Mwd/metric ton of U		5400	3150§	5000

*Reactor includes facilities for cooling one fuel assembly by forced flow of boiling D_2O.

†Lattice includes 12 test positions for irradiation of fuel specimens of either uranium metal or uranium oxide at typical power-reactor conditions. Reactivity is provided by Zircaloy-clad fuel tubes of 9.3 wt.% U^{235} (fully enriched) in zirconium matrix.

‡Fossil-fueled superheater.

§Stated in reference 12 as 12,400 Mwd/metric ton—Editor's Note.

tention are CO_2 and organic liquids, although steam cooling and cooling by H_2O sprays have also been under active consideration recently (see reference 17, reviewed in the December 1960 issue of *Power Reactor Technology*, Vol. 4, No. 1).*

The gas-cooled reactors are represented† by the Florida gas-cooled reactor in the United States and by the French reactor, EL4, which is under development by the Commissariat à l'Energie Atomique in France. These reactors have in common the use of the following: D_2O as moderator, CO_2 as coolant, a cold pressure-tube design with internal thermal insulation, and uranium oxide fuel in beryllium jackets. Both reactors are presently in the developmental stage.

The Florida reactor[20] is a 50-Mw(e) prototype under design by the General Nuclear Engi- Corporation and the American Electric Power Service Corporation for the Florida West Coast Nuclear Group. Research and development are sponsored by the East Central Nuclear Group and the AEC. It is a prototype of a reactor which in a large size would be capable of operation on natural uranium. The reactor is arranged vertically, with the Zircaloy pressure tubes in contact with the relatively cool moderator and with thermal insulation provided inside the tubes by stagnant layers of CO_2. The moderator

*A recent Canadian study has found the steam-cooled concept to be less attractive than the D_2O cooled, as exemplified by CANDU (reference 18).

†A gas-cooled D_2O reactor of the pressure-vessel type, to be built in Bohunice, Czechoslovakia, was discussed at the 1958 Geneva Conference. The most recent mention of this reactor which has come to our attention is an item[19] in July 1959, noting that the pressure vessel had been built in the USSR.

Table XI-8 CHARACTERISTICS OF THE FLORIDA GAS-COOLED PLANT[20]

General

Reactor type	Gas-cooled, D_2O-moderated pressure tube
Thermal power (including heat loss), Mw(t)	159.7
Station net electrical rating, Mw(e)	50.5
Net efficiency, %	31.6
Net heat rate, Btu/kw-hr	10,805
Steam conditions at turbine:	
Pressure, psig	1450
Temp., °F	950
Containment enclosure	Cylindrical steel enclosure around reactor, primary systems, and steam generators

Fuel and Core

Fuel material	Slightly enriched UO_2 of 95 per cent theoretical density, in cored cylindrical pellet form
Initial enrichment, wt.% U^{235}	1.171
Fuel pellet, OD, in.	0.500
Fuel pellet core:	
Diameter, in.	0.200
Material	Beryllium oxide
Cladding and structural material	Beryllium
Cladding thickness, in.	0.038 + 12 fins
No. of fuel rods per bundle	19
Length of fuel bundle, ft	3
No. of bundles per pressure tube	4
Pressure tubes:	
Number	218
Centerline pitch, in.	8 × 9.5 (base and height of isosceles triangle)
Material	Zircaloy-2
Inside diameter, in.	5.01
Wall thickness, in.	0.093
Insulation material	Stagnant-CO_2-gas annuli plus metal radiation barriers
Equivalent core diameter, ft	12.1
Core height or length, ft	12.0
Reflector thickness, in.	12
Total UO_2 load, short tons	16.28
Exposure, Mwd/metric ton of U	11,023

Reactor Heat Transfer

Average heat flux from fuel surface, Btu/(hr)(sq ft)	87,000
Coolant flow velocity, ft/sec:	
Average in reactor	64
Maximum in reactor	100
Maximum cladding surface temperature (including all hot-spot factors), °F	1300
Maximum UO_2 fuel temperature (including all hot-spot factors), °F	3100
Mw/ton of U	11.1
Mw/ton of D_2O in core and reflector, hot operating	3.24

Control Rods

Number	18
Shape	Tubular
Size, in.	4.55 OD × 0.25 wall
Material (neutron absorbing)	B_4C
Control capacity, % k_{eff}	13.4

Moderator System

Total weight in system, tons	54.5
Operating pressure, psig	50
Average temp., °F	232.5

CO_2 Coolant System

Gas	CO_2
Pressure, psig	500 at blower suction
Reactor inlet temp., °F	550
Reactor outlet temp., °F	1050
No. of blowers	2 half size
Type	Centrifugal, single-stage, overhung impeller, single shaft seal
Capacity (including cleanup flow, per unit), lb/hr	2,000,000

Turbine-Generator Unit

Rating, kw	58,000
Shell arrangement	Single casing, single flow
Throttle pressure, psig	1450
Throttle temp., °F	950
Exhaust pressure, in. Hg abs.	2.5
Steam flow, lb/hr	392,900

is operated at a temperature of 232.5°F and at a pressure of 50 psig to allow utilization of its heat for feed-water heating. The CO_2 coolant, at a pressure of 500 psi, flows upward through the pressure tubes. On-power refueling is to be provided by a refueling machine that operates on the cooler inlet ends of the pressure tubes at the bottom of the reactor. Vertical control rods are actuated from above and are installed in pressure tubes similar to the fuel pressure tubes. Fuel assemblies consist of 3-ft-long bundles of 19 rod type elements. The elements

are made up of annular (cored) UO_2 pellets, 0.500 in. in diameter, canned in finned beryllium tubes. The long-pitch helical fins act also as spacers for the elements. The reactor core is 12 ft long, containing four of the 3-ft fuel bundles in each pressure tube, and is approximately 11 ft in diameter. Other characteristics of the reactor are given in Table XI-8.

The Canadian General Electric Company, Ltd., has been active in the development of the organic-cooled D_2O-moderated reactor,[21] but interest in this reactor type is widespread.[22] The definitive work on organic-cooled reactors has, of course, been done in the United States, primarily by Atomics International, where most emphasis has been placed on reactors that use organics as both coolant and moderator. It is generally recognized, however, that one of the attractive possibilities in the use of organics with other moderators, such as D_2O, is that the radiolytic decomposition rate of the organic will be reduced, simply because much of the energy of radiation will be absorbed by other materials in the reactor.

The Canadian General Electric Company is designing an organic-cooled deuterium-moderated reactor experiment (OCDRE) for Atomic Energy of Canada, Ltd. (AECL); the reactor would produce 35.1 Mw(t).[23] The decision to build the reactor will be based on the outcome of the conceptual design and development programs now in progress and on the results of economic studies. If AECL decides to proceed with the building of the reactor, it will be installed at the Whiteshell reactor development site near Winnepeg and will be scheduled for criticality in 1964.

The OCDRE is a calandria design, employing a calandria 9 ft high by 11 ft in diameter, with vertical tubes. It is fueled primarily with natural UO_2, but spikes of 1.4 per cent enriched UO_2 are used to supplement reactivity. Santowax OM-70 is the coolant, flowing in fuel-coolant tubes within the calandria tubes. There is considerable interest in the possibility of other coolants. The fuel assemblies are 4.76 ft long (half core height) and are made up of bundles of 22 rod type elements. The elements consist of UO_2 pellets canned in tubes of type M-257 sintered aluminum powder. The tubes have low, spiral fins. Although the organic coolant absorbs some neutrons, it is expected[21] that large organic-cooled D_2O-moderated reactors will have acceptably long reactivity lifetime (in the range 8000 Mwd/metric ton) with natural-uranium oxide fuel.

References

1. Nuclear Canada Issue, *Nucleonics*, 18(10): (October 1960).
2. W. B. Lewis, Competitive Nuclear Power for Canada, *Nucleonics*, 18(10): 54–59 (October 1960).
3. I. N. MacKay, The Canadian NPD-2 Nuclear Power Station, *Proceedings of the Second United Nations International Conference on the Peaceful Uses of Atomic Energy, Geneva, 1958*, Vol. 8, p. 313, United Nations, New York, 1958.
4. National Power Programmes—A World Survey, *Nuclear Power*, 4(33): 107 (January 1959).
5. Sargent & Lundy Engineers, Evaluation and Design: Heavy-Water Moderated Power Reactor Plants, USAEC Report TID-8529, June 30, 1960.
6. A. J. Mooradian and J. A. L. Robertson, CANDU Fueling Costs—Breaking the 1-Mill/kwh Barrier, *Nucleonics*, 18(10): 60–122 (October 1960).
7. E. I. du Pont de Nemours & Co., Engineering Dept., Heavy-Water-Moderated Power Reactors Engineering and Economic Evaluations, Volume I. Summary Report, USAEC Report DP-510, June 1960.
8. D. F. Babcock et al., Heavy-Water-Moderated Power Reactors, USAEC Report DP-480, E. I. du Pont de Nemours & Co., Nuclear Development Corp. of America, and Sargent & Lundy Engineers, March 1960.
9. Sargent & Lundy Engineers, Evaluation and Design: Heavy-Water Moderated Power Reactor Plants, USAEC Report TID-8530, Apr. 28, 1960.
10. Nuclear Development Corp. of America and Sargent & Lundy Engineers, Design Evaluation and Comparison of 200-Mw(e) Boiling D_2O Pressure Tube Indirect and Direct Cycle Power Reactor Plants, USAEC Report NDA-2131-6, June 1960.
11. Sargent & Lundy and Nuclear Development Corp. of America, Heavy-Water Moderated Power Reactor Plant Design Study, Section IV (Addendum I), USAEC Report TID-8503(Pt. 1), June 1959.
12. Westinghouse Electric Corp. and Stone and Webster Engineering Corp., Carolinas-Virginia Tube Reactor, Reference Design II, USAEC Report CVNA-40, Dec. 16, 1959.
13. N. G. Wittenbrock et al., eds., Plutonium Recycle Test Reactor Final Safeguards Analysis, USAEC Report HW-61236, Hanford Atomic Products Operation, Oct. 1, 1959.
14. P. H. Margen et al., R3—A Natural Uranium, Heavy Water Reactor for Combined Electricity Production and District Heating, *Proceedings of the Second United Nations International Conference on the Peaceful Uses of Atomic Energy, Geneva, 1958*, Vol. 8, p. 220, United Nations, New York, 1958.
15. I. Wivstad and C. Mileikowsky, Adam—A 75 Mw

Nuclear Energy Plant for House Heating Purposes, *Proceedings of the Second United Nations International Conference on the Peaceful Uses of Atomic Energy, Geneva, 1958*, Vol. 8, p. 238, United Nations, New York, 1958.

16. N. Hidle and O. Dahl, The Halden Boiling Heavy Water Reactor, *Proceedings of the Second United Nations International Conference on the Peaceful Uses of Atomic Energy, Geneva, 1958*, Vol. 9, p. 255, United Nations, New York, 1958.
17. J. G. Collier and P. M. C. Lacey, The Spray Cooled Reactor, *Nuclear Power*, 5(52): 68–73 (August 1960).
18. Atomic Energy of Canada, Ltd., Partial Economic Study of Steam-Cooled Heavy Water Moderated Reactors, Canadian Report CRNE-925(AECL-1018), April 1960.
19. Worldview, *Nuclear Power*, 4(39): 68 (July 1959).
20. General Nuclear Engineering Corp., Gas-Cooled Reactor Project, Progress Report No. 7, USAEC Report GNEC-141, Sept. 15, 1960.
21. M. J. McNelly, A Heavy-Water Moderated Power Reactor Employing an Organic Coolant, *Proceedings of the Second United Nations International Conference on the Peaceful Uses of Atomic Energy, Geneva, 1958*, Vol. 9, p. 79, United Nations, New York, 1958.
22. W. Hälg and Th. Schaub, Diphenyl Cooled, Heavy Water Moderated, Natural Uranium Reactor Prototype, *Proceedings of the Second United Nations International Conference on the Peaceful Uses of Atomic Energy, Geneva, 1958*, Vol. 9, p. 88, United Nations, New York, 1958.
23. I. MacKay, Organic-Cooled Deuterium-Moderated Reactors, *Nucleonics*, 18(10): 78–80 (October 1960).

Section XII

SUPERCRITICAL-WATER REACTOR

At the request of the AEC, the Argonne National Laboratory has made an evaluation of the status of the technology of supercritical-water reactors.[1] The objective of the survey was to determine whether sufficient technology exists to make possible a realistic economic analysis.

The survey drew upon three sources for data: the aircraft nuclear propulsion (ANP) supercritical-water-reactor project conducted by Pratt & Whitney, a maritime evaluation made by Westinghouse Atomic Power Department (WAPD), and a conceptual supercritical-water-reactor design prepared by Hanford Atomic Products Operation (HAPO).

The Pratt & Whitney project was the only one which conducted experiments resulting in specific design information; the other two were design studies. Only the HAPO study dealt with the design of a central power station. The others were directed toward propulsion type plants.

Supercritical-water technology and its application to central power station design has been advanced by some of the more recently designed fossil-fuel plants, in which the utilization of a supercritical-water cycle has resulted from the desire for higher plant thermal efficiencies. An example is the No. 6 generating unit of the Philo plant of the Ohio Power Company which operates at 4500 psig, with 1150°F steam and with an efficiency of 46 per cent. Another supercritical-steam plant (the Eddystone station) is now under construction at Philadelphia. Consequently, plant components for supercritical-steam plants will be available for operation at turbine throttle pressures up to 5000 psig and at temperatures up to 1200°F.

A basic decision to be made in the design of a supercritical-water reactor is the choice between the direct and indirect cycles. Of the three studies reviewed in reference 1, two investigated the direct cycle and one the indirect cycle.

Direct Cycle

The work done by Pratt & Whitney, up to the time it was terminated, served to establish considerable background in component development, materials investigation, corrosion work, and heat transfer for the direct-cycle reactor. These areas of study were the major contribution to civilian reactor technology, since the reactor — because of its compactness and high power density — would not be suitable for a central-station power plant. The reactor parameters used for this study are given in Table XII-1.

Table XII-1 ANP SUPERCRITICAL-WATER-REACTOR PARAMETERS[1]

Reactor inlet temp., °F	450
Reactor exit temp., °F	1000
Pressure, psi	5000
Flow rate, lb/sec	430
Average water density, g/cm^3	0.4
Reactor power, Mw	410

At the request of the AEC, HAPO originated a concept for a supercritical-water, direct-cycle-reactor central power station,[2] based upon the Philo supercritical-pressure steam-plant conditions. The reactor, cooled by H_2O at 5000 psi, is moderated by cool D_2O. The full-core-length fuel elements consist of relatively massive columns of UO_2, penetrated axially by Inconel X coolant tubes which serve to confine the high-pressure coolant as well as to separate it from the fuel. Twelve tubes are provided in each fuel element, and groups of two are connected in series at the bottom.

Thus coolant enters the element at the top, flows downward through six of the tubes, returns upward through the remaining six tubes, and leaves the element at the top. This return-flow arrangement allows installation of the elements in zirconium thimbles, which hang into the D_2O moderator tank from the top. A complete fuel element consists of the UO_2 column with its coolant tubes, a surrounding layer of granular ZrO_2 for thermal insulation, and an outer zirconium can. When the element is installed in its thimble, it is insulated further from the thimble wall by a helium-filled gas space. The internal pressure-tube arrangement is reminiscent of the Russian fuel elements for the water-cooled (and steam-cooled) graphite-moderated reactors,[3,4] although these elements employed metallic fuel, as reviewed in the December 1958 issue of *Power Reactor Technology*, Vol. 2, No. 1, pages 35 to 37. The multiple-tube oxide elements of the supercritical-water concept obviously present development problems, which are discussed in the reference.[2]

The coolant flow sequence is a complex one, involving four complete passes through the reactor per cycle (each pass consists of the downward and upward flow through a fuel element). The coolant initially enters the reactor at a temperature of 525°F and is heated, in two passes through the reactor, to 1150°F. It then flows through a heat exchanger to provide reheat for the steam cycle. A third pass through the reactor brings its temperature back up to 1150°F, and it is then passed through a second reheat exchanger. After a fourth reactor pass, to bring its temperature up to 1150°F again, the steam enters the high-pressure turbine. In its expansion cycle the steam flows through the following: the high-pressure turbine, a reheater, a reheat turbine, a second reheater, a second reheat turbine, and, finally, the low-pressure turbine.

Table XII-2 DESIGN CHARACTERISTICS OF SUPERCRITICAL-WATER REACTOR[2]

General	
Gross reactor thermal power, Mw	300
Gross electrical output, Mw	130
Gross cycle efficiency, %	43.3
Net electrical output, Mw	125
Reactor operating pressure, psig	5000
Temperature of steam leaving reactor, °F	1150
Pressure of steam at turbine, psig	4500
Flow, lb/hr	675,000
Power to primary coolant, Mw	282
Power to moderator, Mw	18
Fuel Elements	
Diameter of canned fuel, in.	4.04
Fuel cladding material	Zr
Cladding thickness, in.	0.020
Diameter of coolant channels in UO_2, in.	0.415
No. of coolant channels in UO_2	12
Coolant tube material	Inconel X
Coolant tube thickness, in.	0.020
Maximum diameter of UO_2, in.	3
Mean diameter of UO_2, in.	2.85
Insulation thickness, in.	0.50
Insulation	60 vol.% ZrO 40 vol.% argon, 20.4 lb/ft
Weight of UO_2	
Reactor Core	
Control method	D_2O moderator level; 30-50 vertical shims
Active height, ft	13
Effective diameter, ft	15
Thermal power, Mw	300
Maximum UO_2 temp., °F	4000
Maximum UO_2 surface temp., °F	3650
Maximum heat flux, Btu/(hr)(sq ft)	578,000
Maximum Zr can temp., °F	800
Radial maximum-to-average flux, unflattened	1.83
Vertical maximum-to-average flux, unflattened	1.352
Reactor Cooling	
Cooling	Light H_2O
Coolant inlet temp., °F:	
First pass	525
Second pass	811
Third pass	940
Fourth pass	930
Coolant outlet temp., °F:	
First pass	811
Second pass	1150
Third pass	1150
Fourth pass	1150
Total coolant flow rate, gal/min	12,100
Coolant-system design pressure, psig	5800
Moderator Coolant	
Coolant	D_2O
Total D_2O inventory, lb	118,000
Total D_2O inventory, gal	14,500
Flow, gal/min	3120
Coolant inlet temp., °F	160
Coolant outlet temp., °F	200

This appears to be the most uninhibited handling proposed to date for reactor-heated steam.

The reference[2] contains power cost estimates, arrived at by scaling the costs for the Plutonium Recycle Test Reactor (PRTR). For a plant having a net output of 125 Mw(e), the cost estimates range from 6.9 to 8.1 mills/kw-hr, depending on assumptions as to fuel fabrication costs. The main characteristics of the 125-Mw(e) plant are listed in Table XII-2.

Indirect Cycle

Reference 1 also summarizes a study of a supercritical-water reactor for marine propulsion; the study was performed by WAPD under contract to the AEC Maritime Reactors Branch. Although three cycles were considered (direct, indirect, and throttling direct), the indirect cycle was chosen to avoid the possible problems of radioactive deposition in the turbine system. Furthermore, the coolant inlet temperature was held at 860°F, which is above the critical temperature, to avoid the possibility of instabilities in flow, heat transfer, or reactivity in the region of the critical temperature. Table XII-3 lists the characteristics of a supercritical-water-reactor system using an indirect cycle.

Table XII-3 DESIGN PARAMETERS FOR INDIRECT-CYCLE SUPERCRITICAL POWER REACTOR[1]

Reactor thermal power, Mw	70
Electrical output, kw	21,237
Steam pressure (at turbine), psia	865
Steam temperature (at turbine), °F	900
Coolant pressure, psia	4000
Core diameter, in.	41.6
Core height, in.	60
Coolant flow rate, lb/hr	1.55×10^6

The estimated costs for the reference design plant were compared with those for a pressurized-water plant of the same electrical output. The comparative power costs for the supercritical-water and the pressurized-water plants were 18.99 and 13.55 mills/kw-hr, respectively.

Status of Supercritical-Water Technology

A comprehensive review of the supercritical-water technology was made by Westinghouse in 1957. These results are summarized and referenced in reference 1. The more important information is discussed briefly below.

Heat Transfer and Fluid Flow

There is very little experimental information on heat-transfer coefficients for supercritical water. McAdams[5] et al. have presented results for a pressure of 3500 psia. Pratt & Whitney (see reference 1) has extended the range of data to cover pressures from 4000 to 8000 psi and temperatures from 400 to 1000°F. The correlations of these data were based on properties considered to be functions of the wall and bulk temperatures. The normal type of dimensionless group correlation could not be used because of insufficient data concerning the properties of supercritical water. A recent report,[6] which describes the thermal conductivity and dynamic viscosity of water in the critical region, should help to remedy this insufficiency. Dickinson and Welch[7] recommended the following recipes for use in heat-transfer calculations (quoted from reference 1):

1. For design purposes, it is satisfactory to use the conventional formula for pipe flow: $Nu = 0.023Re^{0.8}\ Pr^{0.4}$, at surface temperatures below 600°F. Properties would be evaluated at the bulk temperature.
2. In the range from 800 to 1100°F, a constant Stanton number of 0.00189 can be used. The specific heat should be evaluated at the surface temperature.
3. In the range from 660 to 800°F, coefficients are high, owing to an apparent boiling-like phenomenon, and it is probably safest to assign some constant value to the coefficient in this temperature range, depending on the mass velocity and the pressure.

This "boiling-like" phenomenon is discussed in reference 1; the phenomenon is characterized by loud whistling noises and evidences of vibration.

Water Chemistry

Supercritical-water reactors for direct-cycle use apparently are characterized by very high water-purity requirements to avoid troublesome deposition problems. As an example of specifications on water purity for "conventional" supercritical-water plants, the No. 6 unit of the Philo plant calls for a 500-ppb maximum of feed-water-dissolved solids. In the Eddystone

No. 1 unit, 50 ppb is the allowable maximum. These can be contrasted to conventional reactor water-purity specifications of about 1 ppm. Although some data are available from the operation of the Philo plant, reference 1 concludes that:

> The major gap in supercritical water technology pertaining to a reactor system is the lack of information on the magnitude of the problems of deposition of radioactivity in the external system and of the buildup of internal crud under irradiation.

Power Cycles

The major attraction of the supercritical-water power plants is the possibility of high efficiency. The Philo plant, for example, employs seven stages of feed-water heating and two stages of reheat and operates at an over-all efficiency of 46.7 per cent. To attain comparable efficiencies, a supercritical-water nuclear plant probably must operate on the direct cycle, and such operation is recommended in reference 1 as the most promising. The reference estimates that a power reactor delivering coolant to a supercritical-water turbine at 4500 psia and 1150°F with no reheat and with no regenerative heating can attain an over-all efficiency of 37.2 per cent. The addition of seven stages of feed-water heating increases this to 44 per cent.

Materials and Components

The supercritical reactor requires fuel elements that can operate at temperatures in excess of 1000°F and at pressures above 3000 psia. Low-cross-section materials for this service are not at hand, and, as in the case of steam-cooled reactors and superheater reactors, the stainless steels and the nickel alloys appear to be the least absorptive practical materials that can be counted on with any certainty. The internal pressure-tube arrangement of the fuel element in the Hanford design study is directed toward minimizing the loss of neutrons to the absorptive structural material in a pressure-tube design.

Types 347 and 316 stainless steels are materials approved by the ASME Boiler Code which appear to be usable for the portions of the plant outside the reactor core. The main steam piping for the Philo plant is of type 347 stainless steel; whereas the Eddystone plant will employ piping of type 316 stainless, made by the forged and bored process.

Development work relative to components for supercritical-water power plants has been aided by the construction of the fossil-fired units. The operating conditions of plants that are operating or are under construction are given in Table XII-4. The supercritical-water turbines for these plants utilize several stages of feed-water heating and double reheat. The latter feature has not been used in nuclear power stations to date, at least not in this country. Reference 1 indicates that pressure vessels for supercritical-water power reactors can be constructed up to an inside diameter of 6 ft, with currently available materials and conventional techniques, and that very much larger vessels are probably beyond present technology.

Table XII-4 FOSSIL-FIRED SUPERCRITICAL PLANTS

Name	Coolant conditions	Power, Mw(e)
Breed and P. Sporn	3500 psi, 1050°F	450
Eddystone No. 2	3500 psi, 1050°F	325
Avon No. 8	3500 psi, 1100°F	250
Philo No. 6	4500 psi, 1150°F	125
Eddystone No. 1	5000 psi, 1150°F	325

References

1. J. F. Marchaterre and M. Petrick, Review of the Status of Supercritical Water Reactor Technology, USAEC Report ANL-6202, Argonne National Laboratory, August 1960.
2. Hanford Atomic Products Operation, Supercritical Pressure Power Reactor, USAEC Report HW-59684, Mar. 18, 1959.
3. N. A. Dollezhal et al., Experience with First USSR Atomic Power Station, *Proceedings of the Second United Nations International Conference on the Peaceful Uses of Atomic Energy, Geneva, 1958*, Vol. 8, p. 86, United Nations, New York, 1958.
4. N. A. Dollezhal et al., Uranium-Graphite Reactor with Superheated Steam, *Proceedings of the Second United Nations International Conference on the Peaceful Uses of Atomic Energy, Geneva, 1958*, Vol. 8, p. 398, United Nations, New York, 1958.
5. W. H. McAdams et al., Heat Transfer to Superheated Steam of High Pressures, *Trans. ASME*, 72: 421–428 (1950).
6. C. A. Fritsch and R. J. Grosh, A Description of Thermal Conductivity and Dynamic Viscosity of Water in the Critical Region, USAEC Report ANL-6238, Argonne National Laboratory, October 1960.
7. N. L. Dickinson and C. P. Welch, Heat Transfer to Supercritical Water, *Trans. ASME*, 80: 746–752 (April 1958).

Section XIII

ORGANIC-MODERATED REACTORS: PIQUA AUXILIARY SYSTEMS

Four reports describing the development of prototype systems that apply to the Piqua OMR have recently been issued. These reports are concerned with the coolant purification system, the coolant degasification system, the waste-gas-disposal system, and the high-boiler (HB) handling system.

Coolant Purification[1]

The coolant-purification-system prototype, described in reference 1, is necessary to remove the HB material which forms from radiolysis of the organic coolant. The design of the Piqua prototype is based on removing 86 lb of HB per hour; this allows a capacity safety factor since it is anticipated that the Piqua OMR will produce 58 lb of HB per hour.

The prototype system flow sheet is shown in Fig. XIII-1, the schematic drawing of the system. The heart of the system is the flash still wherein the HB is removed; the prototype system is designed around a full-size still. The first section of the reference contains a discussion and collection of the physical and thermodynamic properties of the organic coolant, Santowax OMP, and its degradation product, HB. These data are, of course, necessary before design of the still and associated equipment can be accomplished.

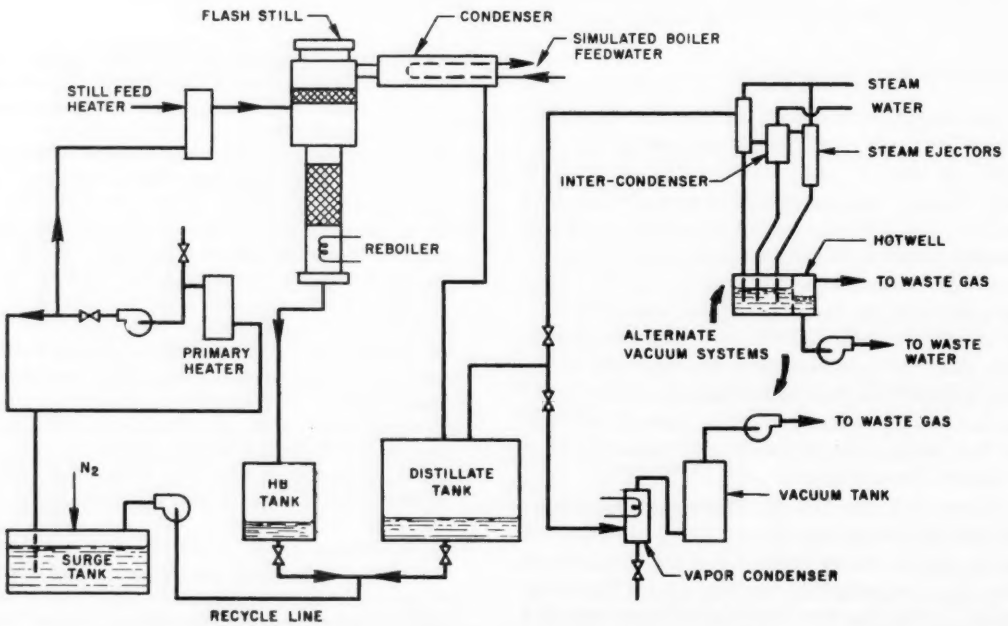

Fig. XIII-1 Schematic diagram of purification-system flow.[1]

After being heated to about 700°F in the primary-system heater and still-supply heater, the feed is introduced into the still wherein it is flashed at a rate of 2 gal/min. The overhead is processed in a deentrainment section of the still consisting of centrifugal flow inducers, flow reversal, and a Yorkmesh stainless-steel wire screen. The still pressure is between 0.5 and 1.0 psia. The overhead is then condensed in a shell-and-tube heat exchanger. In the Piqua installation, boiler feed water will be utilized in this condenser; but in the prototype operation, pressurized water at a temperature of about 300°F is used to simulate the feedwater stream. The distillate is then stored in a receiver.

The bottom section of the still is utilized for stripping. This section is composed of 4.5 ft of Raschig rings packed in an 8-in. steel pipe. After leaving the reboiler, the stripped bottoms are introduced into a hold tank. For operational purposes the overhead and bottoms are recombined and recycled as the feed stream. In the actual plant, however, the product will be recycled to the reactor system, and the bottoms will be stored.

Detailed calculations of the various stream flow rates and compositions were made and compared to the experimental performance of the purification system. These calculations were within about 5 per cent of the experimental performance, when allowances for nonadiabatic operation were included in the calculations.

High-Boiler Handling[2]

The construction and operation of a full-sized Piqua OMR HB-handling system are described in reference 2. In the Piqua plant the HB removed by the purification equipment will be stored for a period of six months in a 22,000-gal compartmented tank, at a temperature between 400 and 450°F to keep the material in the molten state. The HB material is unusual in that it has time-dependent physical properties. The viscosity, density, and molecular weight of the substance taken from the Organic Moderated Reactor Experiment (OMRE) are shown in Fig. XIII-2. At the end of six months, for example, the viscosity will have increased to about 60 centipoises.

The prototype HB-burning system is shown in Fig. XIII-3. The boiler is a return-tube unit designed to produce 285-psig saturated steam. The HB filter employed is a sintered-metal unit; the gas prefilter is a Mikro Pulsaire Model 9-6 dacron-bag dust collector, whereas the absolute filter is a Cambridge glass-asbestos cloth filter.

Four runs were made on the equipment, utilizing HB obtained from the OMRE. A summary of the conditions of the runs is given in Table XIII-1. The large amount of excess air required indicates that the burner nozzle design did not provide for sufficient atomization of the HB, and unstable and erratic performance of the burner was experienced. This nonsteady performance led to difficulties in ascertaining the quantitative decontamination factors of the dust-removal equipment; also the flow capabilities of the filter system were exceeded by the amount of excess air required, and this resulted in bypassing a portion of the boiler waste gas around each filter. The dust loading and activity data at various points in the system are given in Tables XIII-2 and XIII-3. The data are stated to be only an "...indication of the cleanup possible with the equipment... ."

Because of the difficulties experienced with the HB burner in the prototype boiler, other burning equipment designed specifically for combustion of asphaltic waste material was studied. A promising candidate was found in a Vortex burner, which had been used to dispose of heavy industrial combustible wastes. This burner was successfully used to burn Montar-9,

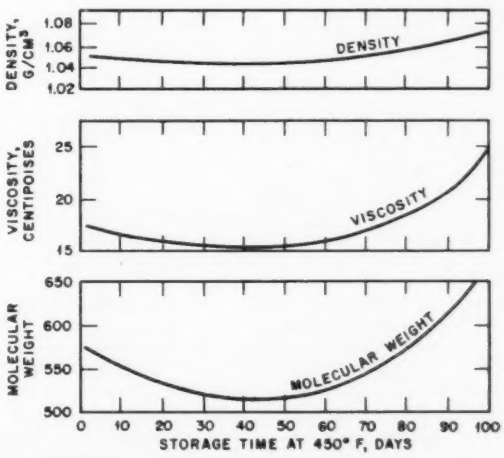

Fig. XIII-2 OMRE physical properties during storage.[2]

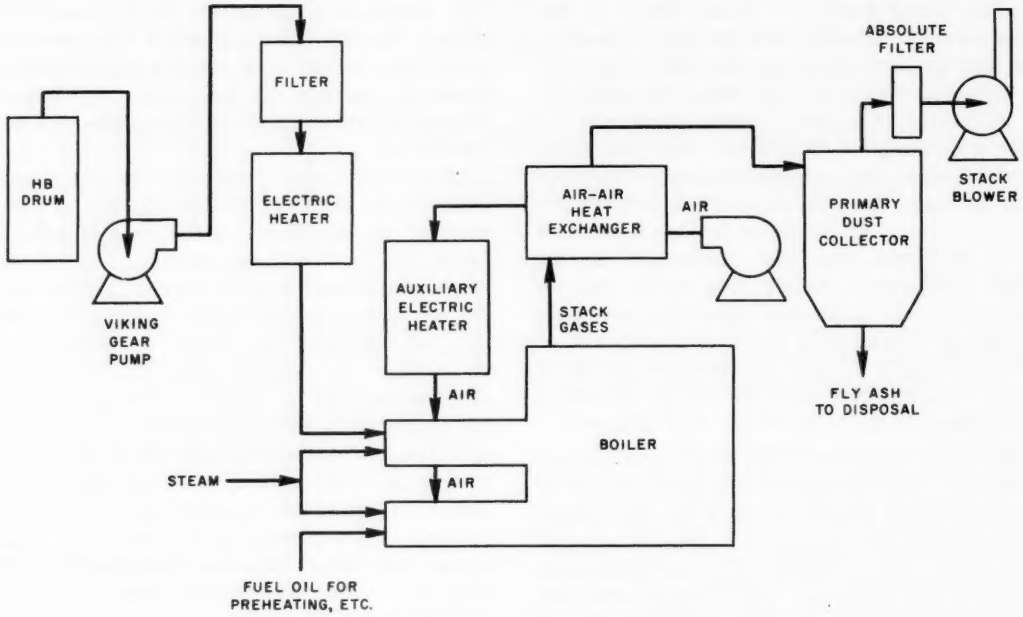

Fig. XIII-3 Schematic diagram of HB-burner prototype.[2]

Table XIII-1 COMBUSTION CONDITIONS FOR HB-BURNING PROTOTYPE[2]

	Run No.			
	1	2	3	4
HB flow, lb/hr	50	45	26	37
Air flow, scfm	380	335	330	315
Atomizing steam flow, lb/hr	35	26.6	29	27
Air temp., °F	375	400	370	414
HB temp., °F	400	400	400	390
Orsat analysis:				
CO_2, %	6.0	5.3		
CO, %	0.6	0.0		
O_2, %	13.2	14.6		
Excess air required, %	161	220	285	220

Table XIII-2 DUST LOADING DATA FOR EXHAUST GAS FROM HB-BURNING PROTOTYPE[2]

Sample location	Dust loading, grains/cu ft
Primary collector inlet	0.0143
Primary collector outlet	0.0033
Absolute filter inlet*	0.0109
Absolute filter outlet	0.0027

*A portion of this stream bypassed the primary collector.

a substance that is quite similar to HB. This burner has been specified for the Piqua OMR. The Viking gear pump used to supply the HB burner was found to be excessively worn, and it was recommended that additional study be directed toward finding a satisfactory pump.

Degasification System[3]

During operation of an OMR, various gases are liberated in the coolant stream from radiolytic and pyrolytic decomposition. In addition, varying amounts of water may be present due to inleakage and other sources. In order to preserve the moderating characteristics of the organic and to eliminate corrosion problems, it is necessary to provide for the removal of the gases and water vapor.

The design criteria for the Piqua plant allow a normal water concentration in the organic of 200 ppm. The degasification system is based on the fact that the solubility of gases in liquids, in general, decreases as the pressure decreases. The system consists of a charge tank, a vacuum degasification tank, condensers and freeze traps, and various pumps, along with necessary pres-

Table XIII-3 ACTIVITY DATA* FOR EXHAUST GAS FROM HB-BURNING PROTOTYPE[2]

Filter paper location	Gas through filter, cu ft	Activity, counts/min	Activity minus background, counts/min	Particulate activity per cu ft of gas, counts/min
		Run 1		
Background		25.6 ± 2.26		
Primary collector inlet	1.6 ± 0.032	77.2 ± 3.92	51.60 ± 4.52	32.3 ± 2.90
Primary collector outlet	1.8 ± 0.036	33.6 ± 2.58	8.0 ± 3.42	4.45 ± 1.9
Absolute filter inlet†	1.7 ± 0.034	111 ± 4.72	85.40 ± 5.24	50.2 ± 3.30
Absolute filter outlet	4.98 ± 0.099	33.4 ± 2.58	7.80 ± 3.42	1.57 ± 0.68
		Run 2		
Background		35 ± 2.64		
Primary collector inlet	1.42 ± 0.028	123 ± 4.96	88 ± 5.62	62 ± 4.14
Primary collector outlet	15.0 ± 0.30	41 ± 2.86	6 ± 3.9	0.4 ± 0.259
Absolute filter inlet†	2.56 ± 0.051	140 ± 5.3	105 ± 5.91	41 ± 2.44
Absolute filter outlet	2.56 ± 0.051	36 ± 2.68	1 ± 3.76	0.39 ± 1.46

* Estimated data ± standard deviation.

† A portion of this stream bypassed the primary collector.

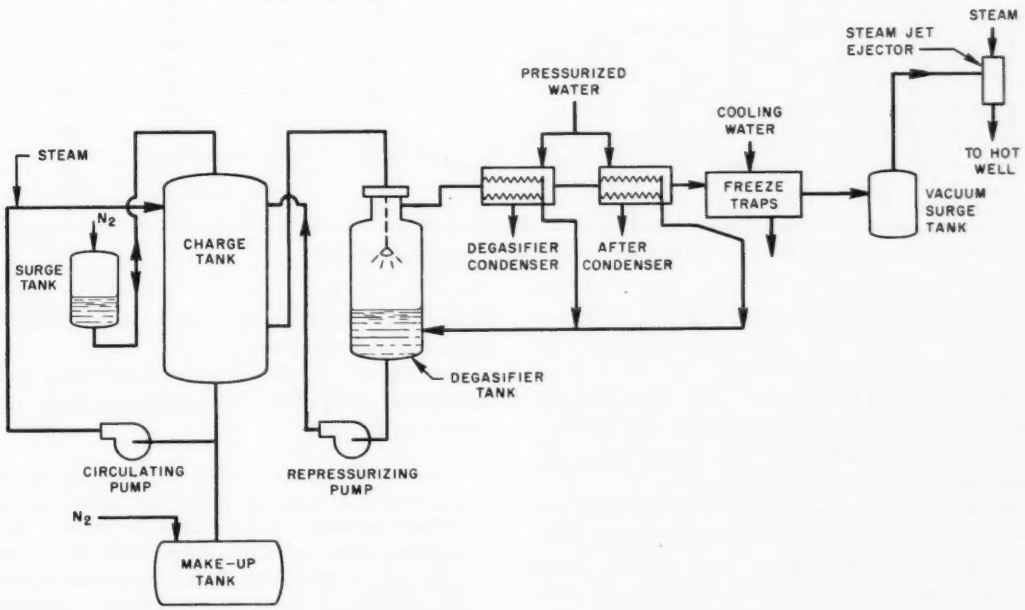

Fig. XIII-4 Schematic diagram of degasification-system prototype.[3]

sure-, flow-, and temperature-measurement-and-control instrumentation. Figure XIII-4 is a schematic drawing of the Piqua degasification system prototype. The prototype was constructed to one-quarter scale, since the extrapolation to full size was believed acceptable. Santowax OMP was utilized in the prototype operations, and water was added via the steam

Table XIII-4 RESULTS OF DEGASIFICATION TESTS*[3]

Run no.	Time, hr	Steam injection rate, lb/hr	Service loop water concentration, ppm	Degasifier return water concentration, ppm	Degasifier feed rate, gal/min	Degasifier pressure, psia	Main loop temp., °F	Degasifier condenser temp., °F	After-condenser temp., °F
1	4.75	2.0	210	157	12	3.00	533	410	322
	5.75	2.0	223	294	8	2.80	547	454	330
	9.50	2.0	201	214	8	3.30	545	454	333
2	4.50	2.0	203	279	8	4.50	572	429	309
	6.25	2.0	243	195	8	4.20	568	454	314
	9.75	2.0	223	193	8	4.00	568	449	323
	12.75	2.0	244	255	8	3.75	567	410	317
3	1.08	2.0	170	217	8	4.50	585	414	314
4	7.50	2.0	331	268	8	2.92	557	452	323
	9.00	2.0	193	223	8	3.12	559	452	318
5	1.00	1.5	170	258	8	3.51	579	451	312
	5.00	1.5	185	215	8	3.53	565	451	309
	9.25	1.5	158	120	8	3.25	564	453	309
	11.25	1.5	235	152	8	3.00	562	452	311
	13.00	1.5	366	188	8	3.00	560	452	315
6	0.75	1.5	280	144	8	3.40	567	452	330
	8.67	1.5	229	188	8	3.30	567	453	318
7	1.00	0.0	259	170	8	3.00	568	445	315
	4.00	0.0	237	181	8	2.80	564	440	305
	11.83	1.5	171	149	8	3.38	568	447	330
8	4.50	1.7	410	323	8	3.50	567	451	320
	10.00	1.8	188	170	8	3.50	570	446	325
	12.75	1.8	199	160	8	3.50	568	450	322
	23.00	1.8	312	200	8	3.50	571	451	318
	27.75	1.7	200	160	8	3.50	574	450	303
	33.50	1.8	172	266	8	3.50	561	450	324
	35.00	1.8	243	143	8	3.50	561	445	326
9	47.25	1.8	186	262	25	4.00	557	456	323
	48.75	1.8	163	197	25	4.00	558	444	323
	51.17	1.8	185	332	25	4.00	556	452	317

*All tests were made using a full-cone nozzle (Spraying Systems Co. Model 2H17).

line to provide for controlled addition of "contaminant" during the prototype testing. The charge tank, circulating pump, and surge tank were designated the service loop, whereas the degasification train consisted of the degasification tank, the condensers and freeze traps, a repressurizing pump, and the ejector.

Table XIII-4 is a summary of the degasification tests accomplished on the prototype unit. The water analyses were done by the Karl Fischer method. Table XIII-4 indicates that during some runs more water was present in the degassed stream of organic than in the feed stream; it is stated that this condition probably resulted from sampling difficulties. Continuous water-analysis instrumentation was included in the prototype but proved unsatisfactory for this application. Comparison between the continuous instrument readings and the Fischer analysis revealed no correlation.

The report contains several interesting comments on equipment performance. These are quoted as follows:[3]

> Numerous difficulties were encountered with organic material freezing in stagnant lines. Such locations included pressure taps for orifice flowmeters, condenser drain lines, transmitter lead lines, and sample taps. In all cases the problem was resolved by shortening the lines to a minimum and by being particularly careful with the application of steam tracing (in conjunction with Thermon[*]). This experience was very costly because

*Thermal conductive heat-transfer cement manufactured by Thermon Manufacturing Company, Houston, Tex.

the degasifier feed and repressurizing pump discharge flowmeters were inoperative during two-thirds of the program.

Major problems were encountered with respect to the condenser train. In summary, these resolved to be due to the following:

1. The shells of both the degasifier condenser and after-condenser were insufficiently steam traced. At times the walls provided more cooling than was desired by the entire condenser.

2. Each condenser shell was five feet in length and was provided with a single drainage line located at the center. This was only a ½ inch line, and it was partially covered by one of the condenser tubes; consequently, condensate collected and became subcooled.

These problems were corrected by retracing the shells, by relocating the drains to the ends of each shell, and by tilting the shells approximately 5 degrees to improve drainage. Concurrent with these lengthy modifications, further changes were made to eliminate the possible problem of an insufficient pressure head to Fischer-Porter flowmeters in the condenser drain lines by elevating the entire condensing system six feet. A collection tank was installed at the discharge of each condenser to prevent accumulation of condensate around cooling tubes. Additional baffling was also provided for each condenser. These modifications resulted in satisfactory operation of the condensing train.

On several occasions the circulating pump seal leaked profusely as the temperature of the seal approached the melting point of the coolant (~ 310°F). This was troublesome and potentially dangerous. The first time this happened a faulty seal was presumed and the unit was removed; however, no damage was evident. On other occasions leaking was stopped by draining the pump housing, refilling, and restarting within a few minutes. The trouble may have been caused by solid organic particles holding the seal faces apart.

Table XIII-5 ESTIMATED WASTE GASES FROM PIQUA OMR SYSTEMS[4]

Gas source	Composition	Vol.%	Rate, scfh	Radioactivity
Degasifier system	Hydrogen	63	20	C^{14}, H^3, S^{35}
	Methane	11		(Does not include fission gases)
	Ethane and ethylene	18		
	Propane and propylene	6		
	Other	2		
Purification system	Same as degasifier system		0.03	Same as degasifier system
HB-burning system	Carbon dioxide	14	15,400	C^{14}, H^3, S^{35}, P^{32}
	Nitrogen	79		Fe^{59}, Co^{60}, Cl^{36}
	Oxygen	7		Mn^{54}

The prototype degasification plant was also utilized for another test. In the Piqua OMR the degasification tank acts as a surge tank to allow for the expansion of the organic coolant during temperature fluctuations corresponding to reactor power changes. For prototype experiments the expansion of the coolant was simulated by admitting nitrogen to the surge tank, since it was not possible to provide enough heat to cause significant density changes in reasonably short periods of time. The pressure-control instrumentation demonstrated that it could follow pressure changes satisfactorily.

Waste-Gas Disposal[4]

The gaseous waste products from the Piqua OMR are given in Table XIII-5. In addition, the gases discharged from the steam jets used to pull a vacuum on the purification and degasifier systems contain diphenyl and terphenyl, and these materials are to be removed before discharge.

Bench-scale experimentation was conducted to study the following processes: adsorption of organic vapors with activated carbon or silica gel; water scrubbing of organic vapors; filtration of polyphenyl dusts and aerosols in gas streams; water extraction of radioactivity from organic coolant; and removal of organic coolant and terphenyls from water by centrifuging. The Piqua OMR waste-gas-treatment prototype was designed to full scale; not included, however, were tanks and equipment for the storage and decay of fission gases, since the prototype was in an exposed location. The necessity of treating organic-laden vapors required inclusion of a water-treatment system as part of the waste-gas system. The prototype flow diagram is shown in Fig. XIII-5. The steam ejectors shown are the same ones in Fig. XIII-1. The alternate vacuum system shown in Fig. XIII-1 has not been reproduced in Fig. XIII-5, but in the prototype this pump's discharge is piped into

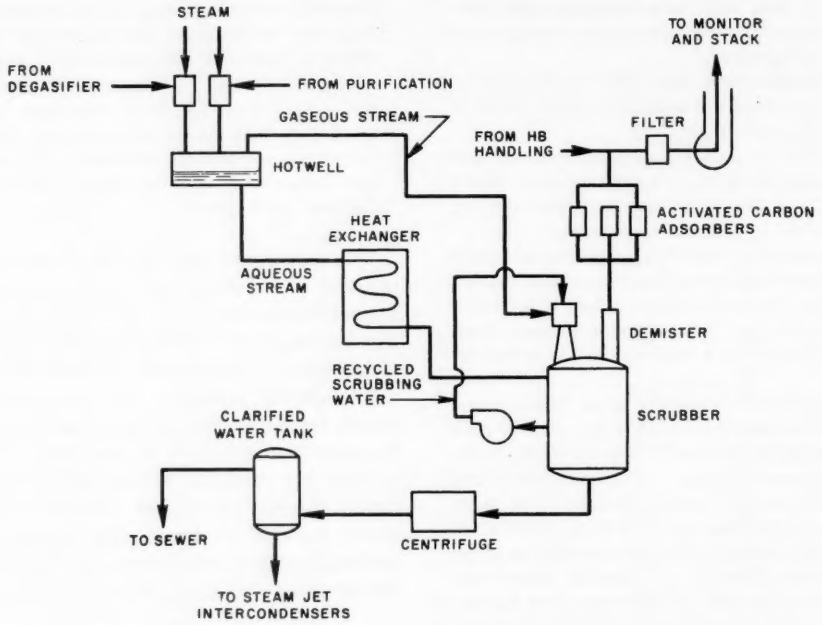

Fig. XIII-5 Schematic diagram of gas-treatment-system prototype.[4]

the gas piping between the activated carbon adsorbers and the absolute filter. The filters shown in Fig. XIII-5 are the primary dust collector and the absolute filter used in the HB prototype (Fig. XIII-3). The entire system was constructed of mild steel, utilizing welded fittings in the gas system and threaded fittings in the water system.

The initial operation of the waste-gas-treatment prototype was as a service unit to the other Piqua prototypes, since the gas-treatment prototype furnished a source of vacuum and filtered and monitored the stack effluent. Difficulty was experienced in monitoring the radioactivity of the stack gases at levels near the maximum permissible concentration. The circulating-water stream in the scrubber was found to contain a stable emulsion that could not be broken by settling or centrifugal clarification. The source of the emulsion was traced to the mechanical vacuum pump oil which had found its way into the scrubber. Development work established that a diatomaceous earth filter successfully broke the emulsion.

References

1. W. N. Bley and R. W. Burkhardt, Piqua OMR Purification System Development, USAEC Report NAA-SR-5073, Atomics International, Nov. 1, 1960.
2. R. R. Stiens, Piqua OMR High Boiler Handling, USAEC Report NAA-SR-4791, Atomics International, Aug. 30, 1960.
3. G. W. Corporales and P. R. Benson, Operation of the Piqua OMR Degasification System Prototype, USAEC Report NAA-SR-4894, Aug. 30, 1960.
4. H. M. Gilroy and J. H. Wilson, Piqua OMR Waste Gas Disposal, USAEC Report NAA-SR-4576, Atomics International, July 15, 1960.

LEGAL NOTICE

This document was prepared under the sponsorship of the U. S. Atomic Energy Commission. Neither the United States, nor the Commission, nor any person acting on behalf of the Commission:

A. Makes any warranty or representation, expressed or implied, with respect to the accuracy, completeness, or usefulness of the information contained in this report, or that the use of any information, apparatus, method, or process disclosed in this report may not infringe privately owned rights; or

B. Assumes any liabilities with respect to the use of, or for damages resulting from the use of any information, apparatus, method, or process disclosed in this report.

As used in the above, "person acting on behalf of the Commission" includes any employee or contractor of the Commission, or employee of such contractor, to the extent that such employee or contractor of the Commission, or employee of such contractor prepares, disseminates, or provides access to, any information pursuant to his employment or contract with the Commission, or his employment with such contractor.

NUCLEAR SCIENCE ABSTRACTS

The U. S. Atomic Energy Commission, Office of Technical Information, publishes *Nuclear Science Abstracts (NSA)*, a semimonthly journal containing abstracts of the literature of nuclear science and engineering.

NSA covers (1) research reports of the U. S. Atomic Energy Commission and its contractors; (2) research reports of government agencies, universities, and industrial research organizations on a world-wide basis; and (3) translations, patents, books, and articles appearing in technical and scientific journals.

Complete indexes covering subject, author, source, and report number are included in each issue. These are cumulated quarterly, semiannually, and annually providing a detailed and convenient key to the literature.

Availability of *NSA*

SALE *NSA* is available on subscription from the Superintendent of Documents, U. S. Government Printing Office, Washington 25, D. C., at $18.00 per year for the semimonthly abstract issues and $15.00 per year for the four cumulated-index issues. Subscriptions are postpaid within the United States, Canada, Mexico, and all Central and South American countries, except Argentina, Brazil, British and French Guiana, Surinam, and British Honduras. Subscribers in these Central and South American countries, and in all other countries throughout the world, should remit $22.50 per year for subscriptions to semimonthly abstract issues and $17.50 per year for the four cumulated-index issues.

EXCHANGE *NSA* is also available on an exchange basis to universities, research institutions, industrial firms, and publishers of scientific information. Inquiries should be directed to the Office of Technical Information Extension, U. S. Atomic Energy Commission, P. O. Box 62, Oak Ridge, Tennessee.

TECHNICAL PROGRESS REVIEWS may be purchased from Superintendent of Documents, U. S. Government Printing Office, Washington 25, D. C. for $2.00 per year for each subscription or for $0.55 per issue. The use of the coupon below will facilitate the handling of your order.

POSTAGE AND REMITTANCE: Postpaid within the United States, Canada, Mexico, and all Central and South American countries except as hereinafter noted. Add $0.50 per year, or $0.15 per single issue, for postage to all other countries, including Argentina, Brazil, British and French Guiana, Surinam, and British Honduras. Payment should be by check, money order, or document coupons, and MUST accompany order. Remittances from foreign countries should be made by international money order, or draft on an American bank, payable to the Superintendent of Documents, or by UNESCO book coupons.

order form

SUPERINTENDENT OF DOCUMENTS
U. S. GOVERNMENT PRINTING OFFICE
WASHINGTON 25, D. C.

Enclosed:
document coupons ☐ check ☐ money order ☐

Charge to Superintendent of Documents No._____

Please send a one-year subscription to

☐ REACTOR CORE MATERIALS
☐ POWER REACTOR TECHNOLOGY
☐ NUCLEAR SAFETY
☐ REACTOR FUEL PROCESSING

(Each subscription $2.00 a year; $0.55 per issue.)

SUPERINTENDENT OF DOCUMENTS
U. S. GOVERNMENT PRINTING OFFICE
WASHINGTON 25, D. C.

(Print clearly)

Name_____

Street_____

City_____ Zone____ State_____